STUDY OF VIBRATION CHARACTERISTICS OF DIFFERENT MATERIALS BY SINE SWEEP TEST

A Dissertation

Submitted in partial fulfillment of the requirement for the award of

Degree of

MASTER OF ENGINEERING

IN

CAD/CAM & ROBOTICS

Submitted By

ANKUSH JALHOTRA

Roll No. 800981003

UNDER THE GUIDANCE OF

Dr. S.P. NIGAM

Professor
Mechanical Engineering Department
Thapar University, Patiala
&
Dr. NAVEEN KWATRA

Associate Professor
Civil Engineering Department
Thapar University, Patiala

MECHANICAL ENGINEERING DEPARTMENT
THAPAR UNIVERSITY
PATIALA-147004, INDIA

CERTIFICATE

I hereby declare that the work which is being presented in the dissertation work entitled, "**STUDY OF VIBRATION CHARACTERISTICS OF DIFFERENT MATERIALS BY SINE SWEEP TEST**", in the partial fulfillment of the requirements for the award of degree of **Master of Engineering in Mechanical Engineering in CAD/CAM & ROBOTICS** submitted in the Mechanical Engineering Department, Thapar University Patiala, is an authentic record of my own work carried out under the supervision of **Dr. S.P. Nigam and Dr. Naveen Kwatra**. The matter presented in this thesis has not been submitted for the award of any other degree of this or any other university.

Date:- 15-07-2011

Place:- Patiala

Ankush Jalhotra

ANKUSH JALHOTRA

Roll No. 800981003

.....

This is to certify that the above statement made by the candidate is correct and true to the best of our knowledge

Dr. S.P. NIGAM
Visiting Professor
Mechanical Engineering Department
Thapar University, Patiala

Dr. NAVEEN KWATRA
Associate Professor
Civil Engineering Department
Thapar University, Patiala

.....

Countersigned by

(Dr. AJAY BATISH)
Professor & Head
Mechanical Engineering Department
Thapar University, Patiala

(Dr. S.K. MOHAPATRA)
Dean
Academic Affairs
Thapar University, Patiala

ACKNOWLEDGEMENT

I would like to express a deep sense of gratitude and thank profusely my guide **Dr. S.P NIGAM** for his sincere & invaluable guidance, suggestions and attitude, which inspired me to submit the thesis report in the present form. His dynamism and diligent enthusiasm has been highly instrumental in keeping my spirits high. His flawless and forthright suggestions blended with an innate intelligent application have crowned my tasks with success.

I express my special thanks to **Dr. NAVEEN KWATRA,** Associate Professor for his ever helping attitude during the course of work. I am also thankful to Dr. Ajay Batish, Professor& Head, Department of Mechanical Engineering for his encouragement and inspiration for execution of the thesis work.

I am deeply indebted to my parents for their inspiration and ever encouraging moral support, which enabled me to pursue my studies.

I am also very thankful to the entire faculty and staff especially Dr. V.P. Agrawal of mechanical engineering department for their intellectual support and cooperation.

I take this opportunity to thank all my friends especially Gurpreet Singh and Pulkit Bajaj for their help and moral support.

Dated: 15-07-2011

Ankush Jalhotra

ANKUSH JALHOTRA

Roll No. 800981003

ABSTRACT

Estimating damping in structures made of different materials (steel, brass, aluminium) and processes still remains as one of the biggest challenges. All materials possess certain amount of internal damping, which is manifested as dissipation of energy from the system. This energy in a vibratory system is either dissipated into heat or radiated away from the system. Material damping or internal damping contributes to about 10-15 % of total system damping. The main objective of this thesis is to estimate the damping ratio, natural frequency of aluminium, brass, and steel by forced vibration analysis experimentally and verify theoretically. Cantilever beams of required size and shape are prepared for experimental purpose and the damping ratio is investigated. Damping ratio is determined by sweep sine test using half power bandwidth method. Forced vibration tests also confirmed the damping ratios obtained by sweep sine method. It is observed that damping ratio is higher for steel than brass than aluminium.

This thesis presents results of an experimental forced vibration analysis of beams made with different materials such as Steel, Brass, and Aluminum. The beams were excited using an electodynamic shaker excitation technique over the frequency range 5-50 Hz. Frequency response functions (FRFs) were obtained using OROS vibration analyzer. The FRFs were processed using NV Solutions analysis package to identify natural frequencies and Damping ratio of the cantilever specimens for each material.

CONTENTS

LIST OF FIGURES

CONTENTS **PAGE NO**

LIST OF TABLES

CONTENTS **PAGE NO**

NOMENCLATURE

SYMBOLS	DESCRIPTIONS
ω_n	Natural Frequency(rad /s)
ω_o	Natural Frequency(rad /s)
f_n	Natural frequency(Hz)
ζ	Damping ratio
C	Damping coefficient
C_c	Critical damping coefficient
E	Modulus of elasticity
I	Moment of inertia
ρ	Mass density
A	Cross-sectional area
Φ_n	Characteristic function

CHAPTER 1

INTRODUCTION

INTRODUCTION

Vibrations give a significant effect in many aspects of our life. For example, any unbalance in machines with rotating parts such as fans, ventilators, centrifugal separators, washing machines, lathes, centrifugal pumps, rotary presses, and turbines can cause vibrations. For these machines, vibrations are generally undesirable. Buildings and structures can experience vibrations due to operating machinery; passing vehicular, air, and rail traffic or natural phenomena such as earthquakes and winds.

Vibrations is evident everywhere and in many cases greatly affects the nature of engineering designs. Vibration can be harmful and should be avoided or it can be extremely useful and desired. For examples, structural vibration testing and analysis contributes to progress in many industries, including aerospace, auto-making, manufacturing, wood and paper production, power generation, defense, consumer electronics, telecommunications and transportation. The most common application is identification and suppression of unwanted vibration to improve product quality. The term vibration describes repetitive motion that can be measured and observed in a structure. Unwanted vibration can cause fatigue or degrade the performance of a structure. Therefore it is desirable to eliminate or reduce the effects of vibration.

In addition, the science and engineering of vibration involve two broad categories of applications; there is elimination or suppression of undesirable vibrations and generation of the necessary forms and quantities of useful vibrations. Undesirable and harmful types of vibration include structural motions generated due to earthquakes and vibrations transmitted from machinery to its supporting structures caused by vibrations. Recent advances of vibration are quite significant and the corresponding applications are numerous. One can then visualize several practical applications where modeling, analysis, design, control, monitoring and testing relate to vibration are important. [19]

1.1 BACKGROUND

1.1.1 Vibration and damping

Excessive stresses and strains caused by vibrations are one of the major causes for failures of mechanical systems and structures. When the vibration excitation frequency is close to the resonant frequency of a lightly damped structure it can cause a catastrophic failure, because the vibration amplitude can become very large. One of the most famous examples is the collapse of the Tacoma narrows bridge, also known as the "galloping gertie' in 1940. Figure 1.1 shows the bridge undergoing twisted mode vibrations due to aerodynamic flutter.

Figure 1.1 shows the bridge undergoing twisted mode vibrations of the Tacoma narrows bridge

Damping is the energy dissipation properties of a material or system under cyclic stress. It is an effect that tends to reduce the amplitude of oscillations in an oscillatory system, particularly the harmonic oscillator.

Vibration damping plays an important role in machines and structures by improving performance and stability, reducing noise and increasing lifetime. Advances in and increased demands of motion control, vibration reduction, vibration isolation, and noise suppuration

require improvements in damping technology. Useful methods and accurate models are required to design, implement, and optimize damping treatments.

Vibration damping is often divided into two categories, active and passive.

Active damping:

Active damping treatments utilize sensors to measure the performance of the machine or structure, and a control algorithm calculates a corrective action which is supplied by an actuator.

Active damping refers to energy dissipation from the system by external means, such as controlled actuator, etc. Due to their lack of versatility, passive damping and cancellation strategies become ineffective when the dynamics of the system and/or the frequencies of the disturbance vary with time. Not to mention that active systems can potentially provide increased effectiveness in controlling vibration compared to passive approaches. And, some applications do not lend themselves to have large passive vibration control appendages, such as a tuned mass damper, attached to them. Active damping and cancellation control can address these two concerns. Due to remarkable advances in sensor, actuator, and more importantly computer technologies in recent years active systems have become cost effective solutions to most sound and vibration control problems.

Passive damping:

Passive treatments typically involve converting kinetic or strain energy into heat through methods such as constrained-layer damping, tuned mass dampers, viscous fluids, or passively shunted piezoelectric material. Passive treatments are typically not more complicated and more expansive than active treatments

Passive damping refers to energy dissipation within the structure by add-on damping devices such as isolator inserts, by structural joints and supports, or by structural member's internal damping. The most commonly applied vibration control techniques are based on the use of passive technologies. The majority of these applications are based on passive damping using viscoelastic materials for vibration control and sound absorbing materials. Although most

passive damping treatments are inexpensive to fabricate, their successful application require a thorough understanding of the vibration problem in hand and the properties of the damping materials. Viscous dampers (dashpots), tuned-mass dampers, dynamic absorbers, shunted piezoceramics dampers, and magnetic dampers are other mechanisms of passive vibration control. Passive sound and vibration control has its limitations such as: lack of versatility, large size and weight when used for low-frequency vibration control.

Material damping: Energy dissipation in a volume of macro-continuous media.

System damping: Energy dissipation in the total structure. In addition to damping due to materials, it also includes energy dissipation effects of joints, fasteners, and interfaces

1.2 FACTORS AFFECTING THE DAMPING CAPACITY

- Frequency and amplitude of excitation
- Kinematic co-efficient of friction at the interfaces
- Size and shape of the inserts, bolts, rivets, viscoelastic material etc.
- Intensity of interface pressure

1.3 TECHNIQUES ADAPTED TO IMPROVE THE DAMPING CAPACITY

- Use of constrained/unconstrained viscoelastic layers
- Fabrication of multilayered sandwich construction
- Insertion of special high elastic inserts in the parent structures
- Application of spaced damping techniques
- Fabricating layered and jointed structures with welded/riveted/bolted joint

1.4 VIBRATION PROBLEM AND EVOLUTION OF PASSIVE DAMPING

The damping of structural components and materials is often a significantly overlooked criterion for good mechanical design. The lack of damping in structural components has led to numerous mechanical failures over a seemingly infinite multitude of structures. For accounting the damping effects, lots of research and efforts have been done in this field to suppress vibration and to reduce the mechanical failures. Since it was discovered that

damping materials could be used as treatments in passive damping technology to structures to improve damping performance, there has been a flurry of ongoing research over the last few decades to either alter existing materials, or developing entirely new materials to improve the structural dynamics of components to which a damping material could be applied. The most common damping materials available on the current market are viscoelastic materials. Viscoelastic materials are generally polymers, which allow a wide range of different compositions resulting in different material properties and behavior. Thus, viscoelastic damping materials can be developed and tailored fairly efficiently for a specific application. [20]

1.5 VISCOELASTICITY

Viscoelastic materials encompass a broad range of materials, including, but not limited to, pressure sensitive adhesives, epoxies, rubbers, foams, thermoplastics, enamels and mastics. Their common characteristic is that their modulus is represented by a complex quantity, possessing both a stored and dissipative energy component. This complex modulus reveals the material's stiffness and damping properties as a function of temperature and frequency, and is usually represented by the SDOF (single degree of freedom) hysteretic model of Figure 1.2 and Equation 1.1. The hysteretic model is used instead of the classic viscous damping model because it is a better representation of the true behavior of viscoelastic materials in which the damping is proportional to strain and independent of rate.

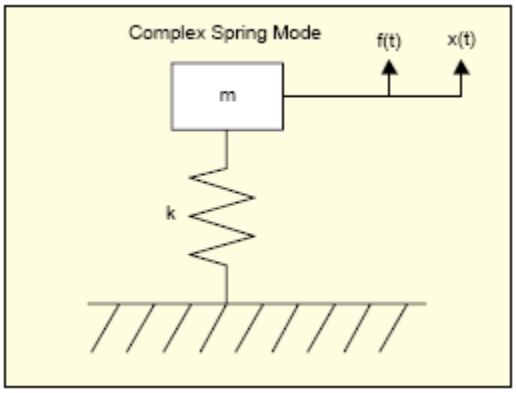

Figure 1.2 SDOF hysteretic model.

$$E(T,f) = E_1 + iE_2 = E_1(1 + i\eta) \quad (1.1)$$

where

E_1=young's storage modulus

E_2=loss modulus

η=loss factor=E_2/E_1

1.6 MEASURES OF DAMPING

Several techniques are used to quantify the level of damping in a structure:

1.6.1 Half-Power Bandwidth Method

For the SDOF structure defined by Equation 1.1, the structure will possess a classic compliance response as shown in Figure 1.3(a). The level of damping can be subjectively determined by noting the sharpness of the resonant peak at ω_o: the more rounded the shape, the more damping present in the structure. For a quantitative measure of damping, the half-power bandwidth method can be employed. As defined in Equation 1.3, the damping of the structure η can be determined from the ratio of $\Delta\omega$ to ω_o with $\Delta\omega$ determined from the half-power point down from the resonant peak value, *A*max (equal to the inverse of the amplification factor *Q*). On a decibel scale, this corresponds to a –3 dB drop from the peak. For that reason, this damping measurement technique is also referred to as the 3 dB method.

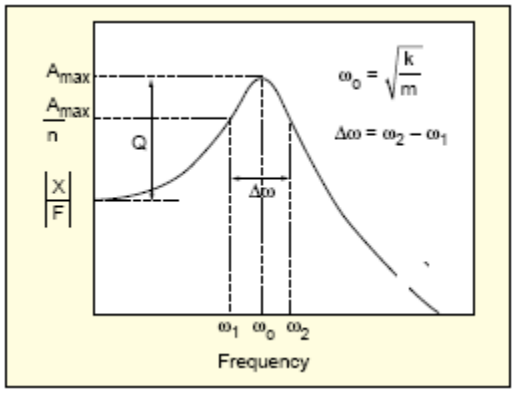

Figure 1.3(a) Compliance transfer function for a SDOF system.

$$m\ddot{X}(t) + k^{*}X(t) = F(t) \tag{1.2}$$

Where:

$$k^{*} = k(1 + \eta i)\ ;\ F(t) = F_{O}e^{i\omega t}$$

$$X(t) = e^{I\omega t}$$

$$\dot{X}(t) = i\omega X_{o}e^{i\omega}$$

$$\ddot{X}(t) = -\omega^{2}X_{o}e^{I\omega t}$$

$$\eta = C\frac{\Delta\omega}{\omega_{O}} \tag{1.3}$$

$$C = \frac{1}{\sqrt{n^{2}-1}}\ or\ \eta = \frac{\Delta\omega}{\omega_{O}}\ for\ \eta = \sqrt{2}(half - power)$$

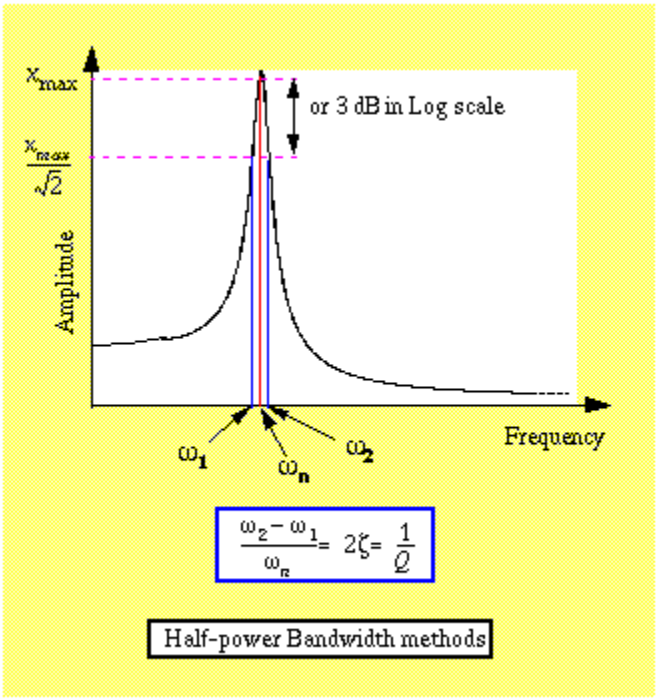

Figure 1.3(b) Frequency response function for a SDOF system.

To estimate damping ratio from frequency domain as shown in figure 1.3(b). In this method, FRF amplitude of the system is obtained first. Corresponding to each natural frequency, there

is a peak in FRF amplitude. 3 dB down from the peak there are two points corresponding to half power point, as shown in the figure below. The more the damping, the more the frequency range between this two point. Half-power bandwidth BD is defined as the ratio of the frequency range between the two half power points to the natural frequency at this mode.

1.6.2 Amplification Factor Method.

Another representation of damping for the SDOF system of Figure 1.2 is the amplification factor Q which is the ratio of the response amplitude at resonance ω_o to the static response at $\omega = 0$. The amplification factor relates to the hysteretic loss factor η through Equation 1.4.

$$Q = \sqrt{(1+\eta^2)/\eta} \tag{1.4}$$

1.6.3 Log Decrement Method.

Another measure of damping can be made from the transient response of the system in Figure 1.2. The log decrement method computes damping from the rate of decay of the system response in the time domain. Computing the damping by this method is illustrated in Figure 1.4(a) and 1.4(b) and is defined in Equation 1.5. Logarithmic decrement method is used to measure damping in time domain. In this method, the free vibration displacement amplitude history of a system to an impulse is measured and recorded. A typical free decay curve is shown as below. Logarithmic decrement is the natural logarithmic value of the ratio of two adjacent peak values of displacement in free decay vibration.

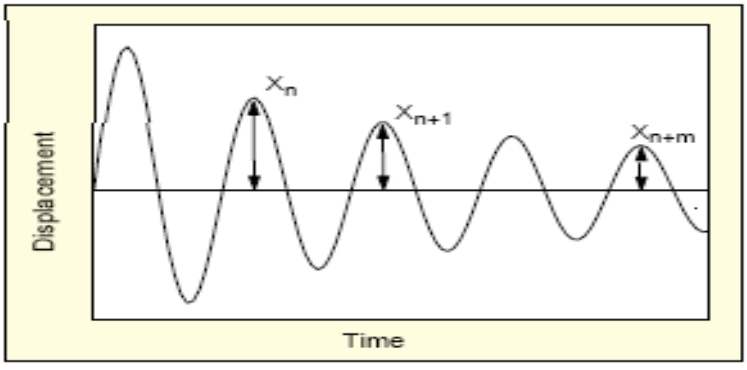

Figure 1.4(a) Transient response of a classically underdamped system.

$$\delta = \frac{1}{m} \ln \frac{X_n}{X_{n+m}} \tag{1.5}$$

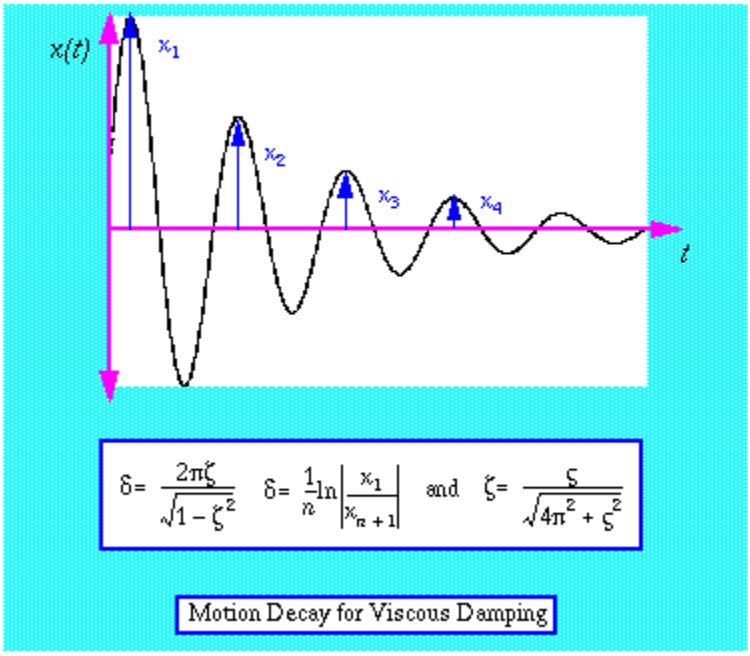

Figure 1.4(b) Motion decay for viscous damping

1.6.4 Hysteresis Loop Method.

Another estimate of damping can be achieved by calculating the energy loss per cycle of oscillation due to steady-state harmonic loading. Again assume the complex spring element of Figure 1.2 is subjected to the cyclic stress $s(t)$ resulting in a strain response of $e(t)$. By plotting the instantaneous stress versus strain for a given cycle of motion, the elliptically shaped hysteresis curve of Figure 1.5 is generated. The area captured within the hysteresis loop D is equal to the dissipated energy per cycle of harmonic motion. For reasonable levels of damping, the loop area can be used to calculate damping, as shown in Equation 1.6. [21]

$$\eta = D/(\pi \sigma_o \omega_o) \tag{1.6}$$

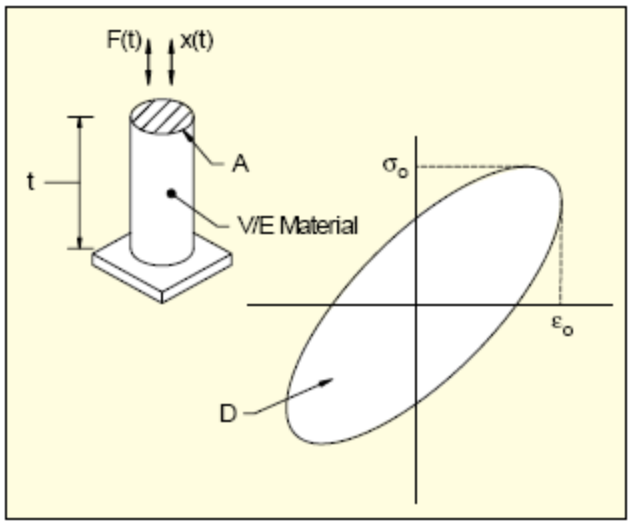

Figure 1.5 Hysteresis loop for force-excited SDOF system [21]

1.7 MODAL ANALYSIS

Modal analysis is a worldwide used methodology that allows fast and reliable identification of system dynamics in complex structures. In the last decades several methods have been developed in quest to improve accuracy of modal models extracted from test data and to enlarge the applicability of modal analysis in industrial context.

Structures vibrate in special shapes called mode shapes when excited at their resonant frequencies. A mode shape is the characteristics deformation shape defined by relative amplitudes of the extreme positions of vibration of a system at a single natural frequency. The modal parameters are the natural frequencies, damping ratios, and modal masses associated with each of the mode shapes. Under normal operating conditions, the structure will vibrate in a complex combination of all the mode shapes. Modal analysis refers to measuring and predicting the mode shapes and frequencies of a structure.

1.8 EXPERIMENTAL MODAL ANALYSIS

Experimental modal analysis is to identify the modal response of an existing structure to help to solve a vibration problem. Impact test or bump test is used in the experimental modal analysis. Impact testing is a fast and low cost way of finding the modes of machines and structures. Experimental modal analysis consists of exciting the structure with an impact

hammer, measuring the FRF between the excitation and many points on structure and then using software to visualize the mode shapes. Accelerometers measure the vibration levels at several points on the structure and a signal analyzer computes the FRF. The structures are divided into a grid pattern with enough points to cover the entire grid structures, or at least the area of interest. One FRF measurement is made for every measurement location on the structure. The number of measurements points is determined by size and complexity of the structure and the highest resonant frequency of interest.

Each FRF identifies the resonant frequencies of the structure and modal amplitudes of the measuring grid point associated with FRF. The modal amplitude indicates the ratio of vibration acceleration divided by force input. The objective of modal analysis is to understand the mode shapes by visualizing the deformed geometry. The FRF is a fundamental measurement that isolates the inherent dynamic properties of a mechanical. The process of determining modal parameters from experimental data involves several phases including:

- Modal Analysis Theory
- Experimental Modal Analysis Methods
- Modal Data Acquisition
- Modal Parameter Estimation
- Modal Data Presentation/Validation [17]

Experimental modal analysis is a supportive tool to the study of various vibration problems. In addition to verifying theoretical results, it helps to study the actual dynamic behavior of a structure away from idealization. Modal analysis is "the representation of the dynamic properties of an elastic structure in terms of its modes of vibration." The elastic structure tends to bend, twist and vibrate when subjected to an external dynamic force. The dynamic properties are also known as the modal parameters which are unique for the structure. The modal parameters are:

- Natural frequency
- Damping factor
- Mode shape

The physical appearance of the three modal parameters is expressed by the "way" the structure behaves dynamically. When a structure vibrates at a certain frequency, it will possess a unique shape of motion known as the mode shape. At the same time, it will be dissipating the energy, absorbed from the external force, at a rate known as the damping factor. The frequency at which the structure may vibrate is the natural frequency.

Mathematically, the modes of vibration are the solution of the eigen problem. The existence of the above mentioned parameters leads the designers to add other design criteria. It is the dynamic behavior of a structure when subjected to any force. The design codes and specifications will be affected drastically when vibration is involved. New restrictions will be added on the design in terms of mass, stiffness, boundary condition, geometry, type of external forces (in case of rotating machines) and locations to avoid the effect of earthquakes and excessive winds. The determination of the modal parameters is the key to solve the problem created such as noise, excessive vibration, failure of mechanical systems due to fatigue etc. The modal parameters are determined by two methods; sine test method and frequency response function method.

1.9 SINE TEST METHOD

The extraction of the modal parameters using this method is done for every mode independently. The structure is excited by a sinusoidal forcing function. The excitation frequency is adjusted until it matches with one of the natural frequencies of the structure (which is unknown).

This is observed when the structure is vibrating with maximum amplitude. At this stage, the structure is vibrating at a resonance frequency which is the natural frequency. The shape of the action is the mode shape which corresponds to the natural frequency.

During the motion, the structure absorbs an amount of energy from the sinusoidal force and it will be vibrating at constant maximum amplitude in a steady-state motion. When the force is removed, the energy is dissipated at a rate which is represented by the decay curve (Fig. 1.2). The rate of decay or the rate of dissipation of the energy is a representation of the ability of the structure to handling external forces.

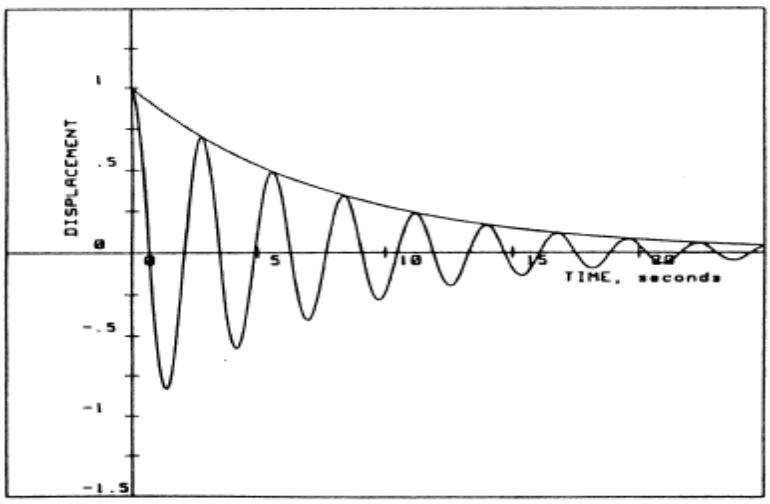

Fig. 1.6 Decay curve of a damped system

1.10 FREQUENCY RESPONSE FUNCTION METHOD

A dual channel signal analyzer (Fast Fourier Transform analyzer, FFT) is used to obtain the frequency response function (FRF). The frequency response function is another property of a dynamic system. It is the ratio of the response to the force applied on the structure. Mathematically it is the Fourier transform x(t) of the output divided by the Fourier transform of the input. The frequency response function is unique regardless of what type of force is used to excite the structure. To produce the FRF by the FFT analyzer, the structure is excited at one point by a selected excitation frequency. The force generated is measured by a force transducer, and the response in terms of acceleration is measured at the same excitation point or any other selected point. The ratio of the output to the input is displayed as a function of frequency. To obtain the three modal parameters, the frequency response function has to be measured at a number of points which represent the structure physically. The structure may be excited at one point and the response measured at the others (impulse test) or vice versa (random test). [17-18]

1.11 OBJECTIVE OF THE PRESENT WORK

The objective of thesis is defined as follows:

- To study the transverse vibration (natural frequency & damping) of a beam using forced excitation technique.
- To study the vibration characteristics of a cantilever beams made with different material such as steel, brass and aluminum.
- To determine the first natural frequency of a cantilever beam using both theoretical and experimental techniques and to estimate the first mode's damping.

1.12 SCOPE

To achieve the above objectives, the scope of this work for the project generally involves the following:

a) To build up the experiment test rig for testing.
b) To conduct vibration measurements to obtain the natural frequency and damping value at first mode.
c) To compare the different damping materials based on experimental results.

The subject of vibration has been of interest to engineers for both academic and practical purposes. The cases of failure of structures and machines due to dynamic loads motivate further research on how to reduce the detrimental effect of vibration. This effect may be expressed in terms of maximum vibration levels which cause fatigue failure to structures Subjected to cyclic loadings. Moreover, the vibration level, which usually results in high noise, causes discomfort to people in residential buildings or in transportation means.

Research work has been done to come up with methods to reduce the vibration amplitude such as shock absorbers, damping materials, tuned mass dampers, and impact dampers.

1.13 OUTLINE OF THESIS

CHAPTER 2 is a presentation of previous studies of material damping, forced vibration techniques to measure damping of materials. This includes theoretical and experimental investigations done by other investigators of impact hammers on single and multi-degree of freedom systems, as well vibration exciters.

CHAPTER 3 is a review of experimental procedure and methodology. Methods to find the modal parameters experimentally and theoretically are also presented throughout the chapter.

This chapter presents a description of the physical model (cantilever) and materials used in the experiment. The method of testing is also presented.

CHAPTER4 The experimental results and analysis are presented in details. The study of the results in terms of the parameters is also presented.

CHAPTER 2
LITERATURE REVIEW

A wealth of literature exists in the area of vibrations of beams but while going through the literature regarding material damping of cantilever beams it has been figured out that still a lot of work has to be done regarding it. Usually whenever study of various materials has been done the focus of researchers has been damping, mode shapes, resonant frequency, etc. but material damping has been one area that has been paid much attention. Some important literatures are shown below:

1. **R. D. Adams [1]** determined the specific damping capacity of a wide range of engineering metals at direct cyclic stresses up to the fatigue limit. A recently damping apparatus was used in which the specimen vibrated in its fundamental free-free longitudinal mode, driven by magnetostrictive vibrator. The energy dissipation was determined from the rate rise of temperature. The energy dissipation was determined the rate of rise of temperature at different sections of the specimen. Below the cyclic stress sensitivity limit, δ_L, the damping of ferromagnetic materials was principally due to the magnetomechanical.

   The magnetomechanical damping mechanism is non-damaging and usually causes a peak in the damping-stress relationship. Suppressing the magneto mechanical effect by applying a saturating magnetic field showed that the damping of plain carbon steels was virtually independent of stress provided δ_L was not exceeded. Above this stress, the damping increased rapidly owing to micro plastic strain and was a function of stress history. Re-testing at lower amplitudes showed that the effective value of δ_L was considerably less than that for virgin material. Ageing at room temperature allowed some recovery.

   A specific damping capacity of 26 % was recorded for Sandston, a commercial high-damping manganese/copper alloy. This was exceeded only by a coarse flake graphite cast iron and annealed nickel (magnetomechanical). The damping of cast irons is due to the shape of the graphite inclusions rather than to the quantity of free graphite in the steel matrix. The aluminium and copper alloys gave the lowest

values of damping, but all were markedly stress-dependent except Duralumin. Brasses with a small free lead content had considerably higher damping than otherwise identical but lead-free materials.

2. **J M. Lee and K. G. McConnell [2]** employed various laboratory techniques which require relatively simple instrumentation in order to ensure a valid damping measurement based on a proposed mathematical model from which cross correlation of the data may be obtained. Measurements were made (utilizing an accelerometer, strain gages, and a sound-level meter) under forced (3-dB frequency band or amplification factor Q) and free-vibration conditions at the fundamental and higher axial modes. Analysis (based on the viscous and complex-moduli theories) of the material damping of an aluminum alloy 2024-3-4 in longitudinal vibrations shows good cross correlation between theories and experimental methods. These methods were extended to damping measurements of yellow brass and commercial steel. A multiple regression analysis was employed in the damping data reduction and was found to be useful in eliminating the data scatter. A sound-level meter was used as a non-contacting test method which proved useful even though its use does have drawbacks.

3. **R.F. Gibson and R. Plunkett [3]** described a technique for measuring material damping in specimens under forced flexural vibration. Although the method was developed for testing fiber-reinforced composite materials, it could be used for any structural material. The test specimen is a double-cantilever beam clamped at its midpoint and excited in resonant flexural vibration by an electromagnetic shaker. Under steady state conditions, material damping is defined in terms of the ratio of input energy to strain energy stored in the specimen. If external losses are negligible, the input energy must equal the energy dissipated in the specimen. Input energy and strain energy are found from measured specimen dimensions, resonant frequency, input acceleration and bending strain. Problems associated with minimization of external energy losses in the apparatus and verification of measurements was discussed. Measured damping of aluminum-alloy calibration

specimens shows good agreement with calculated thermo elastic damping. Examples of measured damping showing amplitude and frequency dependence in fiber-reinforced plastic materials are presented.

4. **Y. Kume and F. Hashimoto [4]** describe a method for estimating material damping in a cantilever beam. This method shows that the damping can be calculated in terms of the stress distribution functions for each mode of vibration and the damping stress function. The stress distribution function is determined by the deformation in the cantilever beam as given by the solution for undamped forced vibration. The function obtained by Lazan is employed as the damping stress function. This approach gives the damping of the beam when incorporated in machine structures undergoing vibrations. By using this approach one theoretically derives the relationship between the loss factor and the maximum stress amplitude in each mode of vibration

5. **Edward F. Crawley and Marthinus C. Van Schoor [5]** were measured the material damping in beam-like specimens of aluminum and metal matrix composites. A unique apparatus to determine damping by free decay while the specimens are in free fall in a vacuum was used. The specimens tested include 2024-T3 and 6061-T4 aluminum, and unidirectional graphite/metal matrix specimens with P55 and P100 fibers and 6061 Aluminum and AZ91C Magnesium as matrix materials. Tests were conducted to determine the dependence of damping on frequency and stress level. For the aluminum specimens, the material damping followed the Zener model at very low stress levels. Below the Zener relaxation frequency, a strong dependence of damping on stress was found for even moderate stress levels. Damping for the aluminum matrix materials was slightly above that predicted by the Zener model for a homogeneous bar of the matrix aluminum. For the magnesium matrix specimens, damping significantly above the Zener prediction for the homogeneous matrix material was observed.

6. **Marek Pietrzakowski [6]** investigated experimentally as well numerically active damping effects of cantilever beam transverse vibrations. The control system under consideration consists of collocated piezoceramic sensor and actuator patches, which are coupled with velocity feedback. Experimental results of free and forced vibrations confirmed the effectiveness of the control circuit with the analog derivative controller for suppression of low frequency beam motion. The numerical simulation is perforrmed to verify the theoretical models of the tested mechanical system. The analysis is based on the simplified pure bending interaction between the perfectly bonded piezoactuator and the beam which has constant equivalent stiffness or is locally stiffed by the piezoaceramic patches .The applied dynamic coupling modeling includes the effect of actuator tangential inertial forces and the bonding laver with a finite shearing stiffness. The results of the simulation are in a good agreement with experiment taking in the simplified model of the system .Considering the bonding layer and the actuator longitudinal movement decreases the active damping effectiveness even for a relatively stiff glue layer.

7. **A. Salzmann, S. Fragomeni, Y. C. Loo [7]** discussed an overview of the free-vibration damping analysis technique commonly employed by laboratories to determine the amount of material damping contained by a concrete specimen. From laboratory investigations the difficulties associated with a technique often employed for the extraction of damping from the free-vibration decay curve are identified. Extensive free-vibration tests undertaken on a wide variety of concrete beams indicate that for the traditional logdec technique, damping is to be extracted from the optimal peak ratio (An/A1) region of the free-vibration decay curve. An analysis of the effect of experimental test variables; hammers weight and hammers excitation position, on the calculation of damping is undertaken. The results show that neither test variable produces measurable impact on the calculation of damping.

8. **Jean-Luc Wojtowicki, Luc Jaouenb, Raymond Panneton [8]** studied the Oberst method that is widely used for the measurement of the mechanical properties of viscoelastic damping materials. The application of this method, as described in the ASTM E756 standard, gives good results as long as the experimental set-up does not interfere with the system under test. The main difficulty is to avoid adding damping and mass to the beam owing to the excitation and response measurement. In this concern, a method is proposed to skirt those problems. The classical cantilever Oberst beam is replaced by a double sized free-free beam excited in its center. The analysis is based on a frequency response function measured between the imposed velocity at the center (measured with an accelerometer) and an arbitrary point on the beam (measured with a laser vibrometer). The composite beam (base beam + material) properties are first extracted from the measurement by an optimization algorithm. Young's modulus and structural damping coefficient of the material under test can be deduced using classical formulations of the ASTM E756 standard for typical materials or using a finite element model for more complex cases. An application to a thick and soft viscoelastic material is presented; the results are shown to be consistent with Kramers–Kronig relations.
9. **R.F. Gibson and R. Plunkett [9]** describe a technique for measuring material damping in specimens under forced flexural vibration. Although the method was developed for testing fiber-reinforced composite materials, it could be used for any structural material. The test specimen is a double-cantilever beam clamped at its midpoint and excited in resonant flexural vibration by an electromagnetic shaker. Under steady state conditions, material damping is defined in terms of the ratio of input energy to strain energy stored in the specimen. If external losses are negligible, the input energy must equal the energy dissipated in the specimen. Input energy and strain energy are found from measured specimen dimensions, resonant frequency, input acceleration and bending strain. Problems associated with minimization of external energy losses in the apparatus and verification of measurements was discussed. Measured damping of aluminum-alloy calibration specimens shows good agreement with calculated thermo elastic damping.

Examples of measured damping showing amplitude and frequency dependence in fiber-reinforced plastic materials are presented.

10. **Richard S. Norek [10]** presented the solution of the equation of motion for transverse harmonic vibrations of a uniform beam made out of isotropic material with structural damping according to the Voight-Kelvin hypothesis, and also under the Euler-Bernoulli assumption that the plane sections of the beam remain plain during bending. Two solutions of the equation for a cantilever beam were presented; one for a harmonically varying concentrated load at the free end of the beam and another for a harmonically varying uniformly distributed load along the beam. The results included natural frequencies and maximum amplitudes during resonances. The loads were selected in a special way; that the work of the distributed load during static deflection of the beam was equal to the corresponding work under the concentrated load. The results showed that the corresponding resonant frequencies did not differ appreciably between the two cases. However, the corresponding maximum amplitudes varied considerably for higher modes. A discussion of the results included also examples from the industry on the inadequacy of the Euler-Bernoulli assumption for turbine blades.

11. **D. Ravi Prasad et al [11]** Modal analysis is a process of describing a structure in terms of its natural characteristics which are the frequency, damping and mode shapes - its dynamic properties. The change of modal characteristics directly provides an indication of structural condition based on changes in frequencies and mode shapes of vibration. This paper presents results of an experimental modal analysis of beams made with different materials such as Steel, Brass, copper and Aluminum. The beams were excited using an impact hammer excitation technique over the frequency range of interest, 0–2000 Hz. Frequency response functions (FRFs) were obtained using vibration analyzer. The FRFs were processed using NV Solutions modal analysis package to identify natural frequencies, Damping and the corresponding mode shapes of the beams.

12. **M. Chiba [12]** conducted Experimental studies to clarify the influence of horizontal harmonic excitations on the dynamic stability of a slender cantilever beam under vertical harmonic excitation. Three kinds of aluminum test beams with rectangular cross section have been used. The test beam being clamped at one end and free at the other end, was vertically stood, and was harmonically excited to both vertical and horizontal directions simultaneously. The direction of the horizontal excitation was taken parallel to one of the beam side faces, i.e. two directions were considered as X and Y directions which have the largest and smallest flexural rigidity, respectively. By varying the horizontal excitation amplitude, keeping the amplitude of excitation in the vertical direction, the influence of the horizontal excitation has been investigated on the principal instability regions in which unstable vibration of the fundamental vibration mode occurs. The excitation frequency in the vertical excitation was taken around twice the fundamental natural frequency 2fY1 in smallest rigidity direction, while that in the horizontal direction was taken around both the fundamental natural frequency fY1 and twice of it 2fY1. Obtained experimental results present useful fundamental data for aseismatic design of structures under earthquake containing both vertical and horizontal excitation components.

13. **Umashankar K. S. et al [13]** estimated the damping ratio of aluminium manufactured through powder metallurgy (P/M) process and compare it with the commercially available Cast aluminium. Aluminium powder is compacted, sintered and then it is extruded to the required geometry. Cantilever beams of required size and shape are prepared for experimental purpose and the damping ratio is investigated. Damping ratio is determined by sweep sine test using half power bandwidth method. Free vibration tests also confirmed the damping ratios obtained by sweep sine method. It is observed that damping ratio is higher for sintered aluminium than cast aluminium which may be attributed to increased porosity
14. **David M. Beams [14]** determined the natural frequencies of the first three vibrational modes of a cantilever beam using the swept-sine technique. The swept-

sine technique applies a sinusoidal excitation to the system under test and measures the system's response as the frequency of the stimulus is swept across a specified frequency range. A mechanical variable (e.g., displacement, acceleration) that varies sinusoidally is the stimulus in mechanical systems; a sinusoidally-varying voltage or current is the excitation in an electrical system. In this case, a cantilever beam (a beam clamped at one end and free at the other) constitutes the mechanical system that will be subjected to a sinusoidal displacement.

15. **Fabio Lo Castro and Paolo Bisegna [15]** discussed forced damping vibration strategies that have a paramount relevance in all those cases where surface vibrations represent disturbances. Knowing that surfaces show different resonant modes of vibration related to their geometry we have selected a cantilever beam that has only one principal resonant frequency. Therefore we have developed a circuit that, using the opposite phase signals technique, reduces the oscillation time of the cantilever beam. Different sensors as accelerometer, piezoelectric, infrared proximity detector have been used to read out the vibration of the cantilever.

16. **Shibabrat Naik, Wrik Mallik [16]** studied of substantial importance in compliant structures, nowadays, are the dynamic parameters such as the modal frequencies and damping constant of their components. These parameters are the essential technical information required in engineering analysis and design. In addition, this information is needed for numerical simulations and finite element modeling to predict the response of the structures to a variety of dynamic loadings. In this work, experimental modal testing of a cantilever beam has been performed to obtain the mode shapes, modal frequencies and the damping parameters. A Fast Fourier Transform Analyzer, PULSE lab shop was used to obtain the Frequency Response Functions and subsequent extraction of modal data was performed using ME'scope. These modal parameters were then checked using finite element analysis software, ANSYS which were found to comply with the experimental results. The range of applications for modal data is vast and includes checking modal frequencies, forming qualitative descriptions of the mode shapes-as an aid to understanding dynamic structural behavior for trouble-shooting, verifying and

improving analytical models. It is with this objective that the experimental method was standardized and thus the mathematical model can be updated further.

The experimental methods include obtaining the FRF plots from a cantilever beam and then using the ME'scope to obtain the various parts of the FRF plots like the magnitude, phase, real, imaginary. Then the modal data was analyzed to obtain different parameters which were further compared with the model developed in ANSYS.

Summary of literature

From the literature review, it is seen impact hammer and shaker testing are usually applied to help solve some vibration problem in the research. It is because these tools are economical tool to investigate the vibration behavior of uncomplicated structures. It is proven that using impact hammer method is more convenient to analyze the natural frequency and mode shapes of single or more than one degree of freedom or more than one degree of freedom model. The technique to obtain the natural frequencies, damping ratio and mode shapes is through the FFT spectrum. Simply stated, modal analysis is the process of characterizing the dynamic properties of an elastic structure by identifying the mode of vibrations. That is, each mode has a specific natural frequency and damping factor which can be identified from practically any point of the structure.

CHAPTER 3

GENERAL PROCEDURE AND EXPERIMENTAL SETUP

Vibration testing is the process of applying a controlled amount of vibration to a test specimen, usually for the purposes of establishing reliability or testing to destruction. In practice the test article is securely mounted on a shaker table or actuator, which may be operated by electro dynamic or hydraulic force; typically hydraulic force is used at very low frequencies because of the large displacements involved, and electro-dynamic force is used where higher frequencies are involved.

An electro-dynamic shaker is a linear motor: a moving coil in a fixed magnetic field that is the same principle used in the construction of a loud-speaker. The magnetic field is generated either by permanent magnets or a DC current in a field coil. Some type of signal source is necessary to drive the amplifier, and an accelerometer is needed to measure the vibration response of the test article. Accelerometers are referred to as Integrated, meaning they have a built-in amplifier and need a current source for power, or Charge type, requiring an external charge-converter to make a usable signal from their output. If the test article is large, then the response may vary across its surface and multiple accelerometers may be used and the outputs averaged. The overall response curve is usually very non-uniform due to the response curves of the amplifier and shaker, and mechanical resonances of the shaker, test article, and mounting fixtures. To cure this, a controller is used to servo the actual measured response to the desired response curve. The signal source usually attempts to simulate the real-world environment that the test article will operate in. Two methodologies are commonly used: Swept-sine and Random testing. In the Swept-sine approach the frequency is swept back and forth with amplitudes corresponding to the desired test levels.

In Random testing the frequency spectrum of a noise source is shaped to represent the environment that the article will operate in. An additional test approach is Classical shock testing where the article is subjected to one or more high level shock pulses; this is similar to a one time drop-test that might occur in shipping. In all three approaches the test level can be increased until destruction occurs, thus establishing the safety margins.

3.1 SHAKER DETAIL

The shaker used in the present testing was electro-dynamic shaker. The MEV series of vibrators is having derive coil connected rigidly to the moving platform and positioned in the magnetic field .When an AC flows in the derive coil it gives rise to a force by converting an electric current into mechanical force that moves the Platform

A modem armature suspension system is having four heavy duty rolling struts and a central linear bearing assembly, which provide an armature with excellent cross –axial restraint. The use of rolling strut design makes it easily convertible to long stroke application required for half sine bump tests while maintaining all dynamic qualities of the vibration exciter i.e. low distortion, high cross –axial stiffness and the ability to work with off center loading.

An air cooling nit is coupled with the exciter for cooling of drive coil, field coil and flexure to ensure continuous performance. This is achieved by a centrifugal blower, which sucks hot air from the vibrator through a flexible hosepipe. The sufficient numbers of reinforcing stainless steel inserts are provided on the vibration platform for specimen fitment. [26]

(a)Power amplifier (b) Exciter

Figure 3.1 Electro-dynamic shaker system.

Model	MEV 0400
Peak sine force	400Kgf
Frequency range	1 Hz to 1000 Hz
Maximum payload	50 Kg
Armature resonance	Above 1 KHz
Maximum displacement	25mm (pk-pk)
Maximum velocity	1.5 meter/sec(normal)
Maximum acceleration at max. speed	4 'g'
Moving armature suspension	rolling strut/link arm type
Shaker rotation	90degree through trunion arrangement
Hole pattern	M8/M10 SS inserts at a regular pitch
Drive power	thru a solid state power amplifier (class 'D' switch mode amplifier) amplifier)
Cooling method	Forced air extraction with suitable interlocks and protection
Protection	Over temperature with field interlock , over travel, cooling interlock
Duty	Continuous
Slip table & vibrator mounting arrangement	On a common frame to avoid slip table misalignment (combo base)
Shaker mounting	On isolation foundation

Table 3.1 Specifications of electrodynamic shaker [22]

(a) accelerometer

(b) OROS Analyzer
Figure 3.2 Measurement equipment used in vibration test

3.2 DESCRIPTION OF SPECIMENS (CANTILEVER BEAM)

Flexural member	Beam	Beam	Beam
Material	Aluminum	Brass	Steel
Length	500 mm	500 mm	500 mm
Width	25.4 mm	25.4 mm	25.4 mm
Depth	6,10 mm	6,10 mm	6,10 mm
Boundary condition	Cantilever	Cantilever	Cantilever
Mass density	2700 kg/m^3	7037kg/m^3	7850kg/m^3
Modulus of elasticity	70 GPa	103.4GPa	200GPa

Table 3.2 Geometric and material properties for the test specimens

3.3 DETERMINATION OF THEORETICAL NATURAL FREQUENCY

A uniform beam in vibration is assumed to be governed by Euler's equation:

$$EI\frac{\partial^4 y}{\partial x^4} + \rho A\frac{\partial^2 y}{\partial t^2} = 0 \quad (3.1)$$

where E is the modulus of elasticity, I is the moment of inertia, and ρA is the density times the cross-sectional area or mass per unit length. The deflection curve must be approximated by a function in the form of:

$$y(x,t) = \phi_n(x)e^{i\omega_n t} \quad (3.2)$$

which is then substituted into equation 3.2

$$\frac{\partial^4 \phi_n(x)}{\partial x^4} - \beta_n^4 \phi_n(x) = 0 \quad (3.3)$$

where ϕ_n = the characteristic function describing the deflection of the *n*th mode

$$\beta_n^4 = \frac{\rho A \omega_n^4}{EI}$$

Equation 3.3 can be solved for ω_n using the ϕ_n approximation and applying the appropriate boundary conditions. For a clamped -free beam, the boundary conditions are as follows:

Description	Boundary Conditions
Clamped(Fixed)	y=0 $\frac{\partial y}{\partial x} = 0$
Free	$\frac{\partial^2 y}{\partial x^2} = 0$ $\frac{\partial}{\partial x}\left(EI\ \frac{\partial^2 Y}{\partial X^2}\right)$ =0

Thus, the natural frequency, ω_n, can be determined from the following equation:

$$\omega_n = (\beta_n L)^2 \sqrt{\frac{EI}{\rho A L^4}}$$

where L is the length of the beam and the values for $(\beta_n L)^2$ are as follows:[27]

n	$\beta_n L$	$(\beta_n l)^2$
1	1.8751	3.5160
2	4.6941	22.0345
3	7.8548	61.6972

3.4 INSTRUMENT SETUP

The instruments used in the testing are shown in Fig. 3.1 and Fig. 3.2. The experimental vibration system consists of three main components; (i) electro-dynamic shaker (ii) accelerometer (iii) power amplifier and data acquisition system. The electro-dynamic shaker is used to provide a source of excitation to the test specimen. The accelerometer is used to convert the mechanical motion of the structure into an electrical signal. The charge amplifier is used to match the characteristics of the transducer to the input electronics of the digital data acquisition system (OROS). Software called NVGATE is then used to execute signal processing and analysis.

3.5 EXPERIMENTAL PROCEDURE AND TEST METHODOLOGY

Forced vibration is conducted on the test specimens to obtain its dynamic characteristics including natural frequencies and damping ratios. The beam is clamped on the combo base slip of 400 Kgf electro-dynamic shaker that provides an external (i.e., transverse to the axis of the beam) sinusoidal excitation at the base of the beam. The excitation is applied at the root of the test specimen (vertically mounted, slender, uniform cross-section, steel, brass, aluminum(6063) cantilever beam on the combo base slip has dimensions 500 mm 25.4 mm × 10 mm and 500 mm x25.4 mm x 6 mm)by using an electro-dynamic shaker .

During forced vibration, the dynamic responses of the beam are measured through tri-axial piezoelectric accelerometers with nominal sensitivity of 10.33mV/g as shown in Figure 3.1. For this test, the location of accelerometer at free end is carried out in order to extract the modal parameters. The layout of the sensors on the test specimen is depicted in Figure 3.4. The vertically mounted accelerometer at free end is used primarily for measuring the response in terms of acceleration. A data acquisition system is used to store the record data and transfer measured data to the PC for data post-processing. Frequency response functions (FRFs) were obtained using OROS vibration analyzer. The FRFs were processed using NV GATE Solutions modal analysis packages to identify natural frequencies, damping and the corresponding mode shapes of the beams.

Figure 3.3 Beam mounted on combo base slip table of electro-dynamic shaker

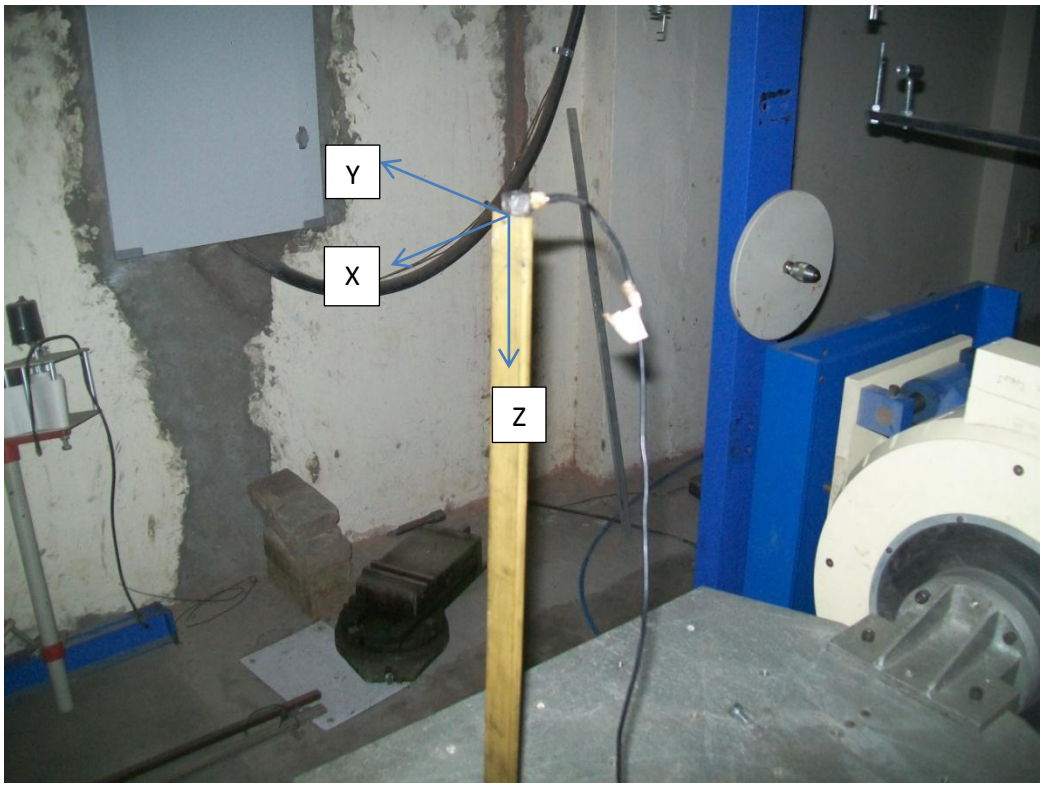

Figure 3.4 Accelerometer mounted at the free end of the beam

3.5.1 Measurement procedure

1. A beam of a particular material (steel, brass, aluminum), dimensions (*L*, *w*, *d*) was used as the cantilever beam
2. The fixed end was made by clamping the beam on the combo base slip table of electro-dynamic shaker with M8 threaded bolts.
3. The connections of the FFT analyzer, laptop, transducers and exciter along with the requisite power connections were made.
4. Placed tri-axial accelerometer at the free end of the cantilever beam, to measure the forced vibration response (acceleration).
5. Ensured the connection of the exciter with the controller and the level of input power.
6. Connected another accelerometer on the combo slip table of electro-dynamic shaker to measure the input response. Make a proper connection of accelerometer with data acquisition system (OROS Analyzer) and with computer to capture the vibration data.

7. During setting of the swept-sine parameter make sure that in the vibration measurement software the time duration should be greater than the total time of excitation.
8. Started the experiment by giving force signal to the exciter and allow the beam to forced vibrate.
9. The FFT analyzer and the accelerometer are interfaced to convert the time domain data to frequency domain.
10. Recorded all the data obtained from the transducer in the form of variation of the vibration response with time.
11. Repeated the experiments to check the repeatability of the experimentation (i.e., vibration data).
12. Repeated the whole experiment for different material.
13. Recorded the whole set of data in a data base for further processing and analysis.

3.6 PROCEDURE FOR SINE SWEEP TEST OF A CANTILEVER BEAM

By applying a constant excitation force and sweeping the frequency of excitation one can measure the resulting vibration and calculate the frequency response function, and hence characterize the system. The name sweep sine arises due to the fact that the system is allowed to respond between 2 frequency limits, chosen in such a way that the suspected natural frequency may lie between these two frequency limits. At a particular instance of time, the input frequency becomes equal to the natural frequency of the system and the amplitude level increases significantly. This is the resonance peak and can be clearly distinguished in the response curve. As soon as the input frequency crosses the resonant frequency, system amplitude keeps on reducing. From analysis point of view, resonant frequency amplitude is very important. Here unlike impulse excitation technique, the structure is excited by a pure sine wave of fixed amplitude but varying frequency and the system response to this varying frequency is studied.

Use vibration equations to find the fundamental frequency of a cantilever beam and also obtain this frequency experimentally using an electrodynamic shaker table system, accelerometers and OROS analyzer.

3.7 MEASUREMENT OF NATURAL FREQUENCY IN FRFS SPECTRUM

The natural frequency is determined from frequency response functions. Frequency response functions (FRFs) were obtained using OROS vibration analyzer. The FRFs were processed using NV GATE Solutions modal analysis packages to identify natural frequency.

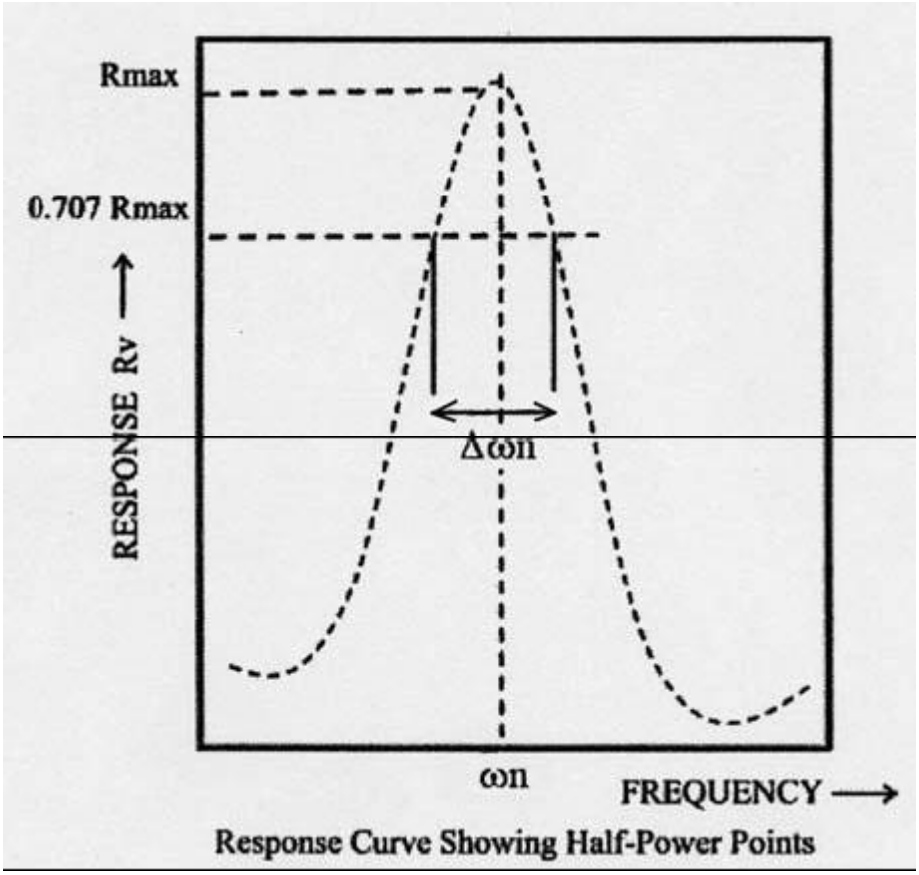

Figure 3.5 Natural Frequency Determination using Half-Power Method

3.8 CALCULATION OF DAMPING VALUE USING HALF-POWER METHOD

The damping value is calculated as:

$$\zeta = \frac{\omega_2 - \omega_1}{2\,\omega_n}$$

where ω_2 and ω_1 are the frequencies corresponding to the half-power points which are defined at which the response amplitude is 0.707 times the resonant response amplitude, and ω_n is the resonant frequency.

CHAPTER 4
RESULTS AND DISCUSSIONS

The objective of the present work is to compare the damping of different structural materials i.e. steel, aluminium and brass. In the present study the observations have been taken to calculate damping ratio for different materials of same length and width but different thickness by sine sweep test at different frequency ranges i.e. 5-50, 10-100(Hz).

Data for vibration characteristics has been taken for first mode i.e. fundamental mode at the free end of the cantilever set up. The graphs have been plotted between excitation frequency and amplitude (g) keeping excitation force (gain of shaker is equal to 4.6 Voltage and 3.2 Ampere) constant. All the data used in these graphs has been shown in Appendix A-E.

The natural frequencies and damping ratio are determined based on frequency response spectrum obtained by analyzing the acceleration signals from the beam as the response data. This output is subjected to Fast Fourier Transform (FFT) to get the frequency domain spectrum.

As frequency and damping are global properties and can be estimated from any frequency response measurement taken from the structure except from measurements at a point where the mode shape has zero amplitude.

The natural frequencies (only for fundamental mode) of the specimens are identified as the frequencies corresponding to peaks present in the FFT spectrum.

4.1 VIBRATION CHARACTERISTICS OF ALUMINIUM BEAM OF THICKNESS 6mm

The vibration characteristics (natural frequency & damping ratio) of aluminium beam of thickness 6mm have been determined by sine sweep test .Graphs for response (acceleration) with respect to constant excitation force for aluminium beam of thickness 6mm has been shown in figures 4.1 and 4.2 both in time domain as well as in frequency domain.

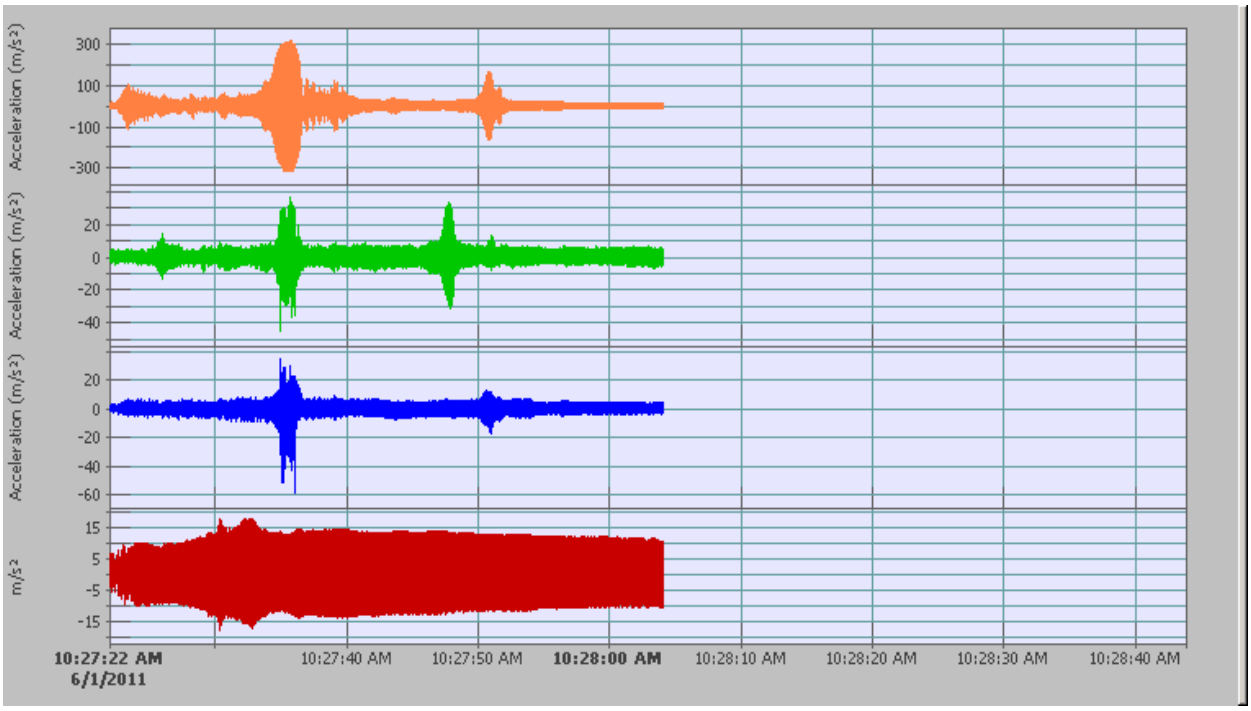

Figure 4.1 Time-response graph for aluminium beam of thickness 6 mm

Figure 4.1 shows acceleration data in the time domain, which is converted to the frequency domain via FFT (Fast Fourier Transform) so that the natural frequencies and damping can be identified.

The three colours i.e. orange, green and blue represents the acceleration data in x, y, and z directions respectively in the time domain plot reads from start to stop varying of frequency in the selected frequency range(5 Hz-50 Hz) in which the fundamental frequency lies.

It can be observed from figure 4.1that for constant excitation force, the maximum response (acceleration) occurred in x-direction as indicated by red spikes in the time domain plot.

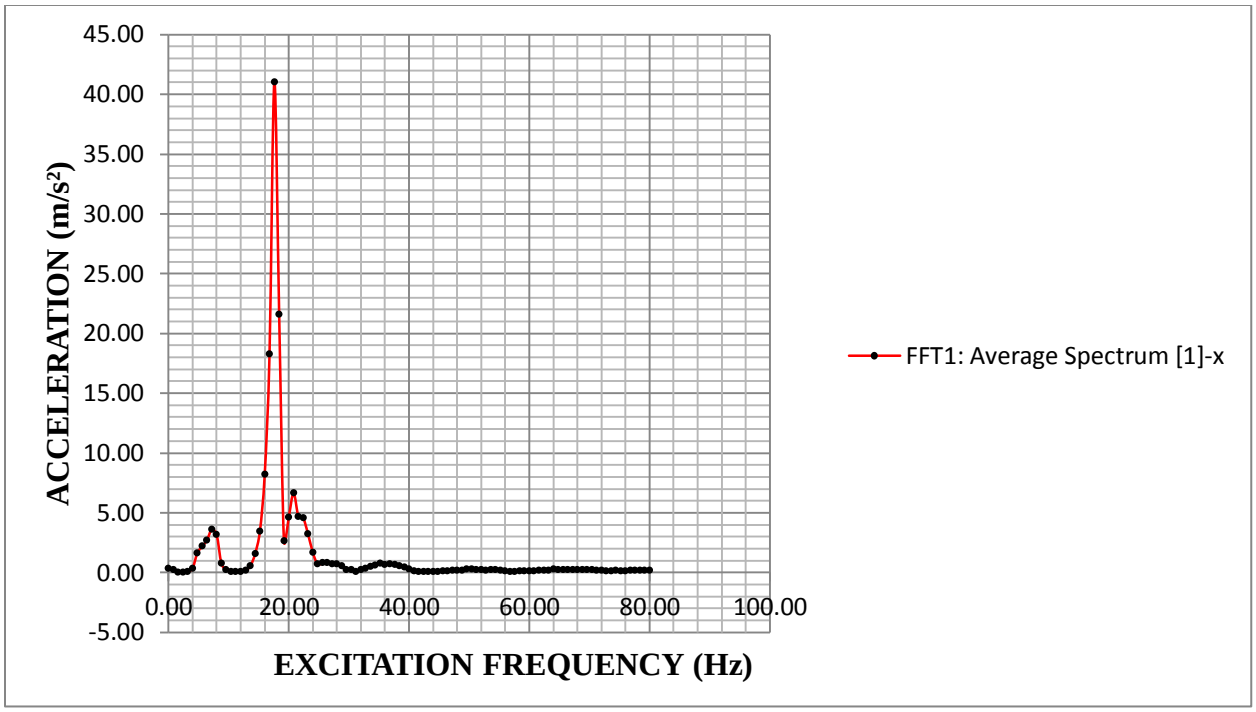

Figure 4.2 (a) Acceleration Vs excitation frequency graph for aluminium beam in x- direction (500mm X 25.4mm X 6mm)

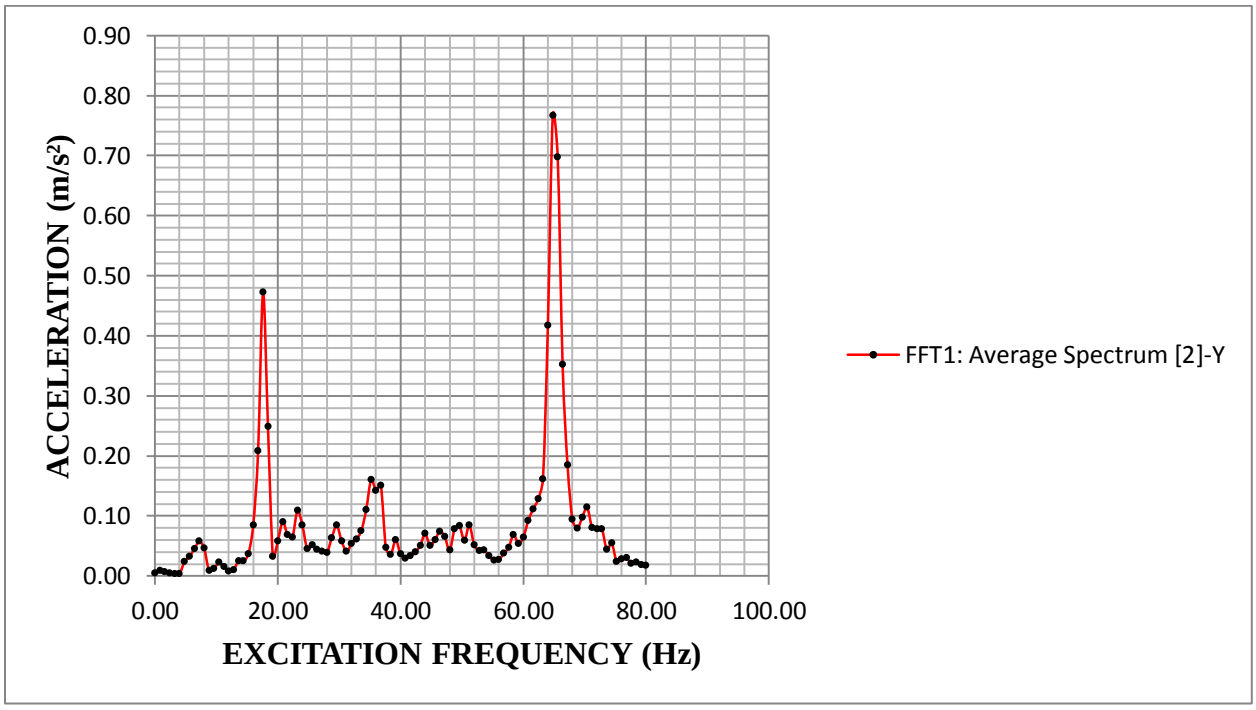

Figure 4.2 (b) Acceleration Vs excitation frequency graph for aluminium beam in y-direction (500mm X 25.4mm X 6mm)

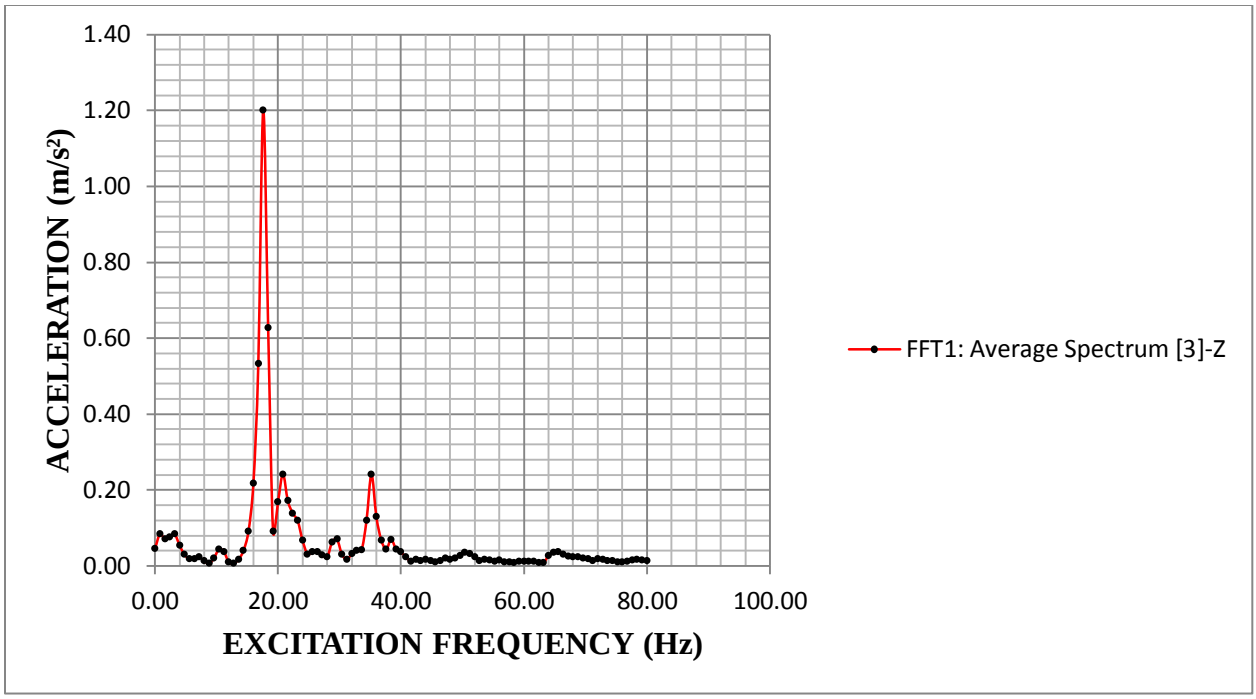

Figure 4.2 (c) Acceleration Vs excitation frequency graph for aluminium beam in z-direction (500mm X 25.4mm X 6mm)

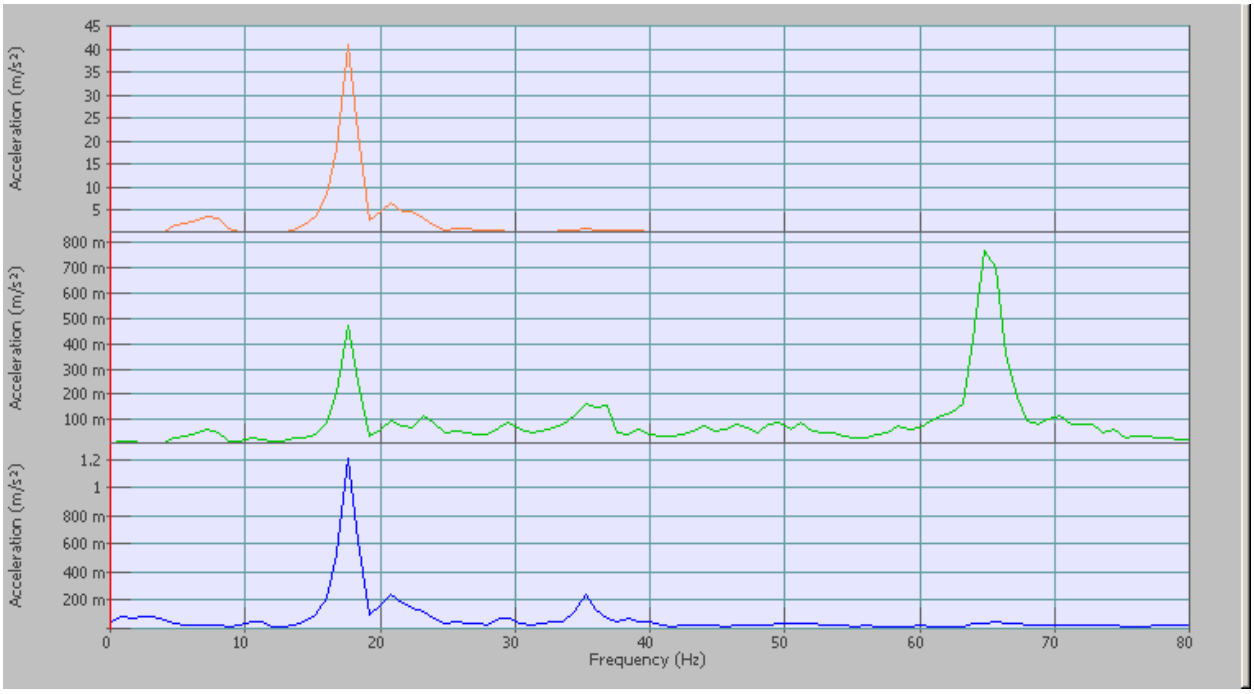

Figure 4.3 Average spectrums of FFT in x, y, and z directions for aluminum beam of thickness 6 mm

The processed FRFs (i.e. FFT) obtained using OROS analyzer for aluminium of beam length 500 mm through sweep sine test has been shown in the figures 4.2(a) to 4.2(c).

The graphs showing variations of the magnitude of response in terms of acceleration (g) with respect to excitation frequency for aluminium beam in three directions by analyzing the acceleration signals from orthogonally aligned tri axial accelerometer.
The peak value shows maximum amplitude in terms of acceleration corresponding to fundamental natural frequency i.e. resonant frequency.

From figure 4.2(a) the natural frequency which corresponds to the peak response can be seen to be 17.60 Hz. The half power points where the response amplitude is equal to 0.707 times the peak response can be identified as $\omega_{1=}$ 17.10 Hz and ω_2 =18.05 Hz.

From analysis point of view resonant frequency response amplitude is very important. Since the input force is constant during excitation, the output can be viewed as frequency response function .Hence output response can be considered for analysis of damping for first mode in x-direction only. As shown in figure 4.2 (a) for constant force, it is seen that the maximum amplitude occurs not at the resonant frequency i.e. at frequency of 19.58 Hz but a little towards its left i.e. at frequency of 17.60 Hz. At first mode, ω_p =17.60 Hz is the frequency corresponding to peak amplitude i.e. 41 m/s^2. Hence the damping ratio corresponding to natural frequency 17.60 Hz is 0.03039.

From figure 4.3, it has been observed from average spectrum of response that the maximum response occurs in the x-axis which is the dominant axis (i.e., transverse to the axis of beam) in which specimen vibrates (in the direction of moving shaker table) more as compared to other two axes.

4.2 VIBRATION CHARACTERISTICS OF ALUMINIUM BEAM OF THICKNESS 10mm

The vibration characteristics (natural frequency & damping ratio) of aluminium beam of thickness 10mm have been determined by sine sweep test .Graphs for response (acceleration) with respect to constant excitation force for aluminium beam of thickness 10mm has been shown in figures 4.4 and 4.5 both in time domain as well as in frequency domain

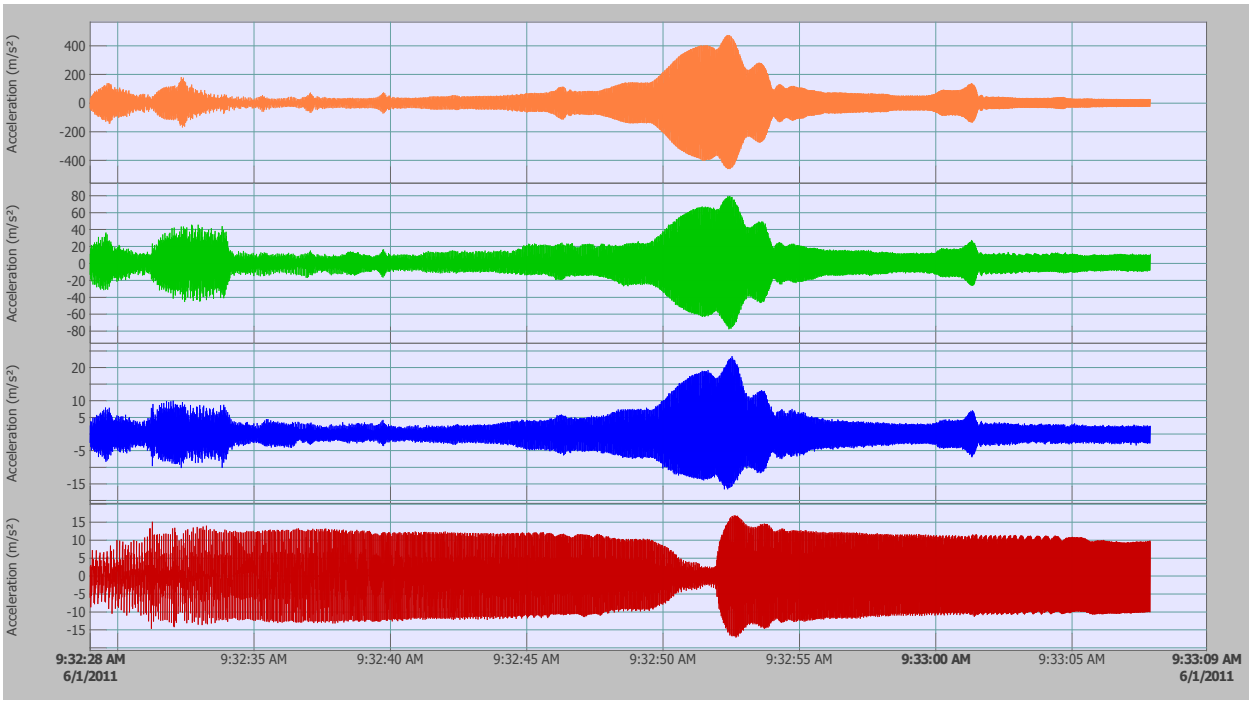

Figure 4.4 Time-response graph for aluminium beam of thickness 10 mm

Figure 4.4 shows the acceleration data in the time domain, which is converted to the frequency domain via FFT (Fast Fourier Transform) so that the natural frequencies and damping can be identified. The three colours i.e. orange, green and blue represents the acceleration data in x, y, and z direction respectively in the time domain plot reads from start to stop varying of frequency in the selected frequency range(5 Hz-50 Hz) in which the fundamental frequency lies.

It can be observed from figure 4.4 that for constant excitation force, the maximum response (acceleration) occurred in x-direction as indicated by red spikes in the time domain plot.

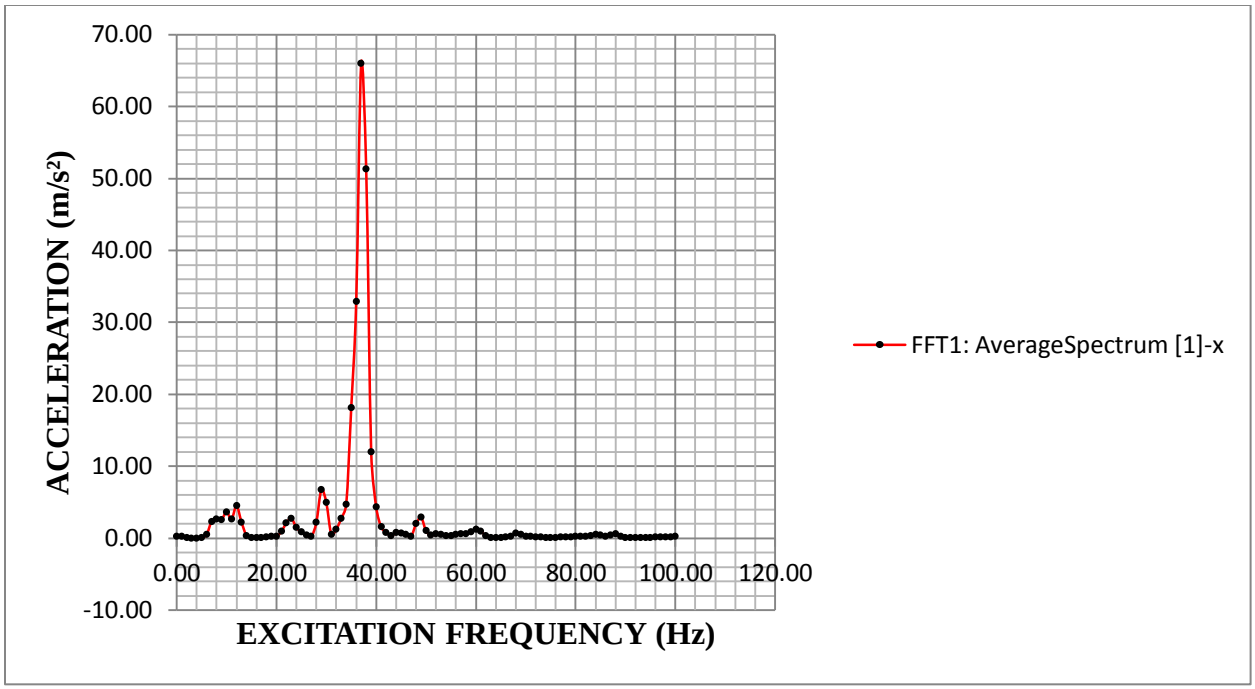

Figure 4.5 (a) Acceleration Vs excitation frequency graph for aluminium beam in x-direction (500mm X 25.4mm X 10mm)

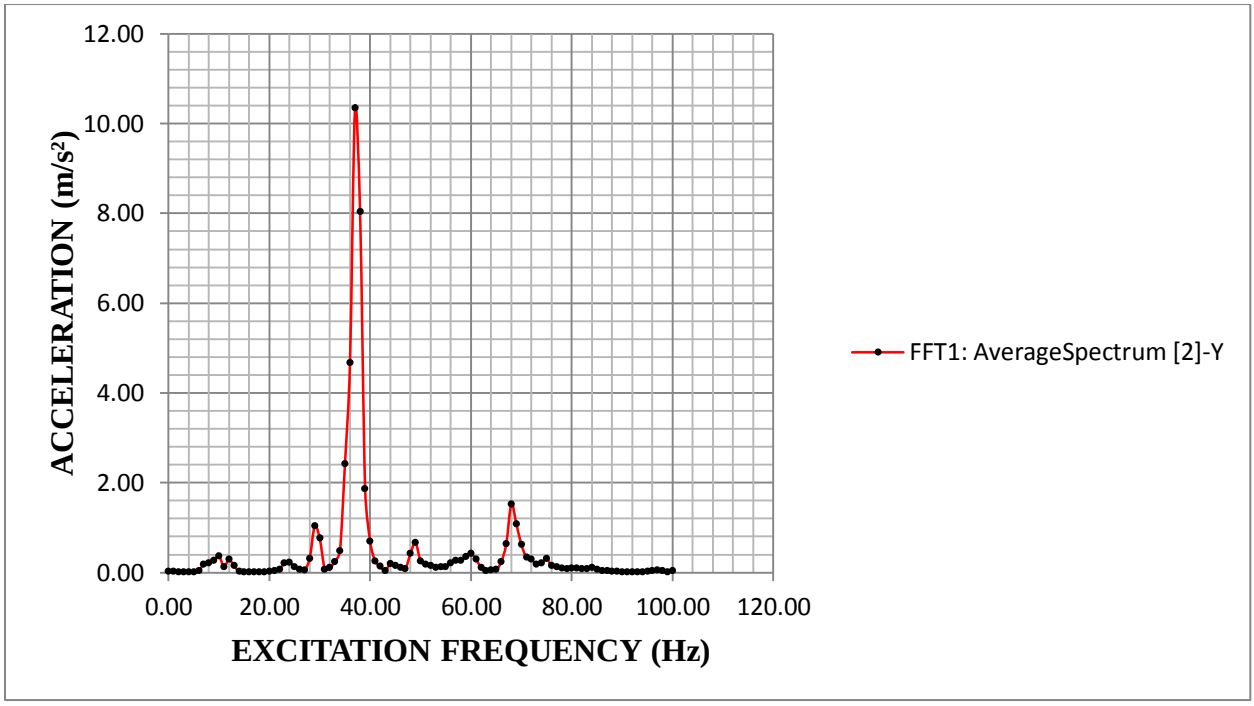

Figure 4.5 (b) Acceleration Vs excitation frequency graph for aluminium beam in y-direction (500mm X 25.4mm X 10mm)

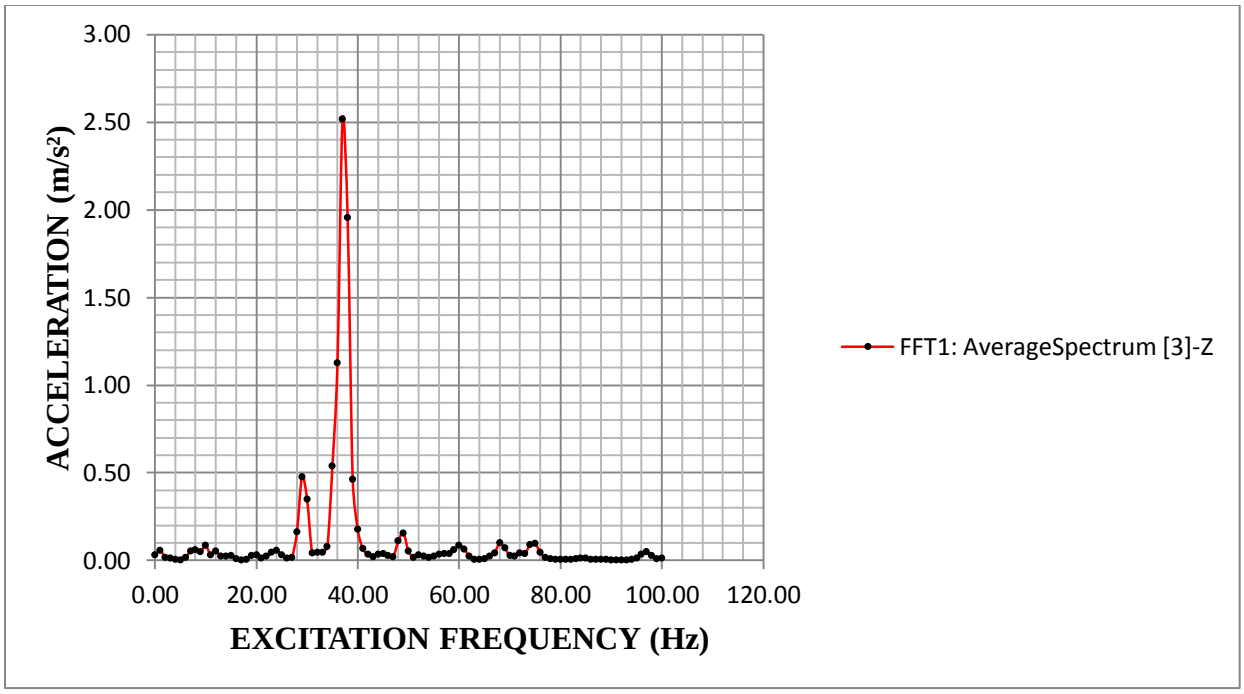

Figure 4.5 (c) Acceleration Vs excitation frequency graph for aluminium beam in z-direction (500mm X 25.4mm X 10mm)

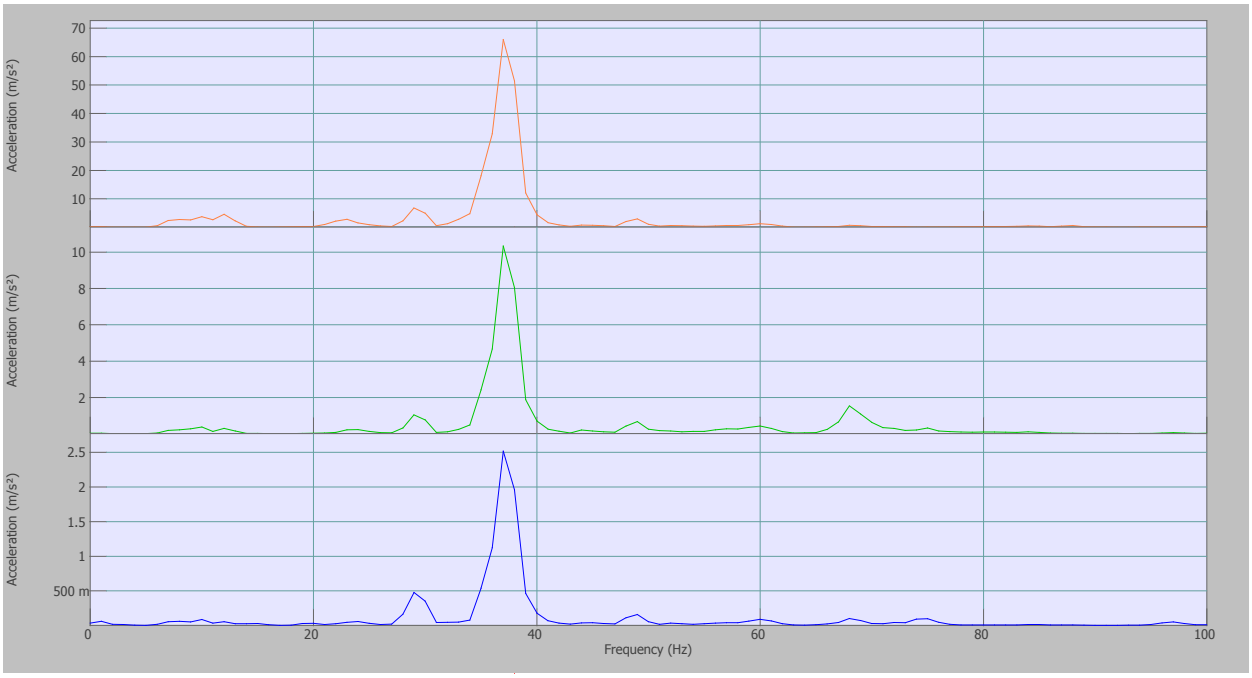

Figure 4.6 Average spectrums of FFT in x, y and z directions for aluminum beam of thickness 10 mm

The processed FRFs (i.e. FFT) obtained using OROS analyzer for aluminium of beam length 500 mm through sweep sine test has been shown in the figures 4.5 (a) to 4.5 (c) .

This shows variation of amplitude in terms of acceleration (g) with respect to excitation frequency for aluminium beam in three directions by analyzing the acceleration signals from orthogonally aligned tri axial accelerometer.

The peak value shows maximum amplitude in terms of acceleration corresponding to fundamental natural frequency i.e. resonant frequency.

From figure 4.5(a) the natural frequency which corresponds to the peak response can be seen to be 37 Hz. The half power points where the response amplitude is equal to 0.707 times the peak response can be identified as $\omega_{1=}$ 36.05 Hz and ω_2 =38.09 Hz.

From analysis point of view resonant frequency response amplitude is very important. Since the input force is constant during excitation, the output can be viewed as frequency response function. Hence output response can be considered for analysis of damping for first mode in x-direction only. As shown in figure 4.5 (a) for constant force, it is seen that the maximum amplitude occurs not at the resonant frequency i.e. at frequency of 32.90 Hz but a little towards its right i.e. at frequency of 37 Hz. At first mode, ω_p =37 Hz is the frequency corresponding to peak amplitude i.e.66m/s^2. Hence the damping ratio corresponding to natural frequency 37 Hz is 0.02756.

From figure 4.6, it was observed from average spectrum of response that the maximum response occurs in the x-axis which is the dominant axis (i.e., transverse to the axis of beam) in which specimen vibrates (in the direction of moving shaker table) more as compared in other two axes.

As seen from the experiments results for the vibration characteristics of aluminium beam of thicknesses 10 mm and 6mm , the natural frequency reduces in case of thickness 6 mm for the same span length and are in fair matching with theoretical. Hence the damping ratio in case of thickness 6 mm was found to be more as compared to thickness 10mm. The reason for higher damping could be the gap between frequency range of two half power points and

lower stiffness value i.e. 768.09N/m which in turn lower elastic modulus. Figure 4.7-4.8 shows the comparison of experimental natural frequencies and damping ratios for aluminium beam of different thickness (6mm and 10mm).

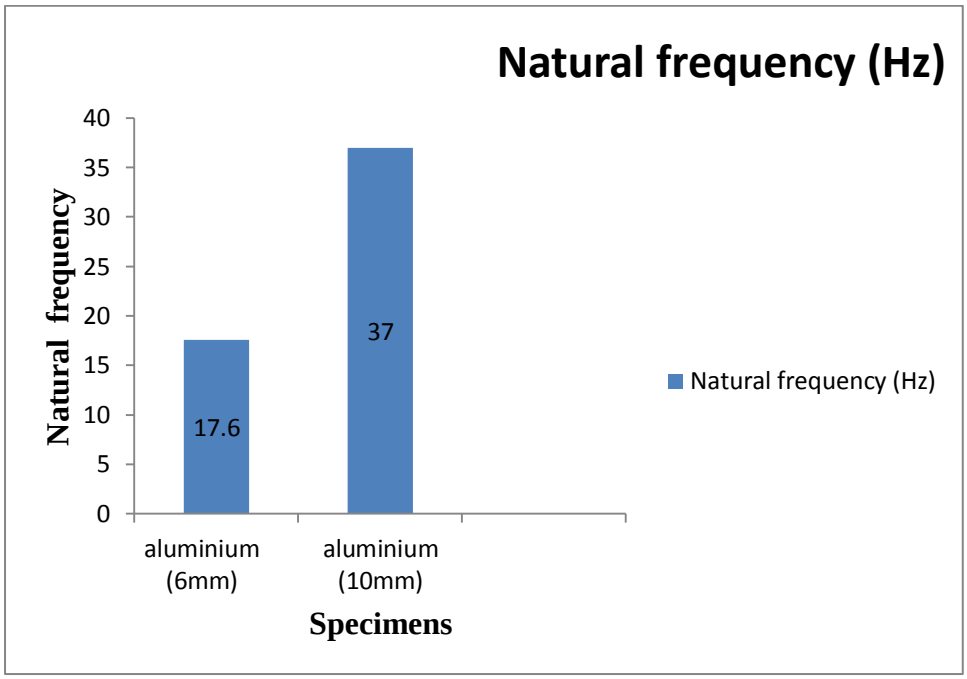

Figure 4.7 Comparison of natural frequencies for aluminium beam of thickness 6 and 10mm

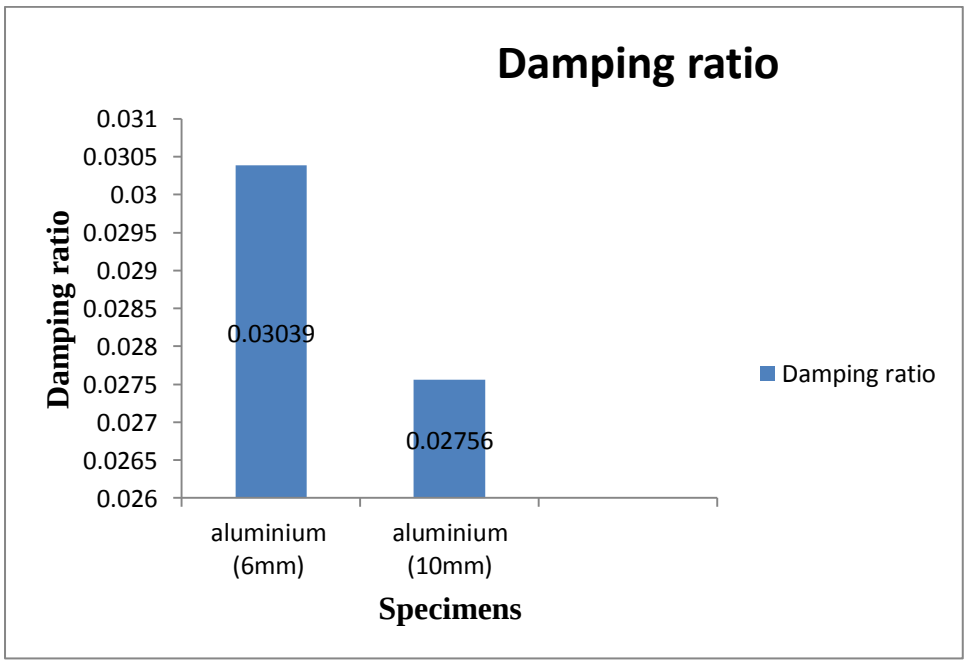

Figure 4.8 Comparison of damping ratios for aluminium beam of thickness 6 and 10mm

4.3 VIBRATION CHARACTERISTICS OF BRASS BEAM OF THICKNESS 6mm

The vibration characteristics (natural frequency & damping ratio) of brass beam of thickness 6 mm have been determined by sine sweep test. Graphs for response (acceleration) with respect to constant excitation force for brass beam of thickness 6mm have been shown in figure 4.9and 4.10 both in time domain as well as in frequency domain

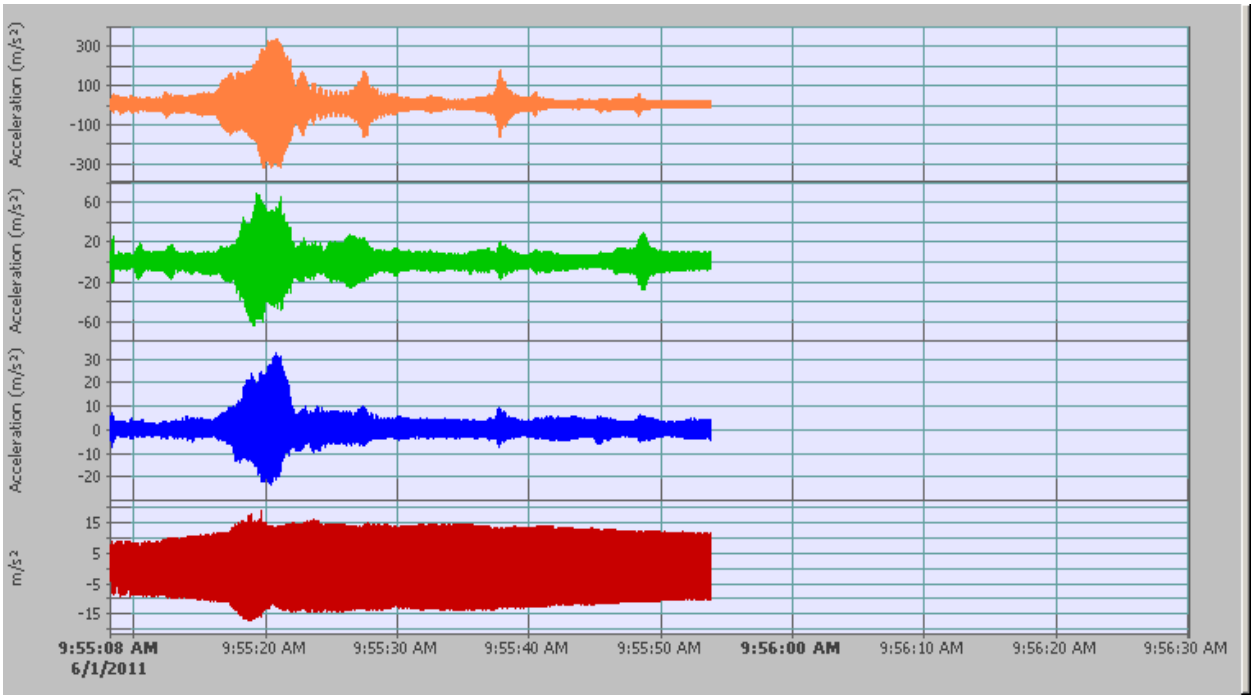

Figure 4.9 Time -response graph for brass beam of thickness 6 mm

Figure 4.9 shows that initial acceleration data is in the time domain, which is converted to the frequency domain via FFT (Fast Fourier Transform) so that the natural frequencies and damping can be identified.

The three colours i.e. orange, green and blue represents the acceleration data in x, y, and z direction respectively in the time domain plot reads from start to stop varying of frequency in the selected frequency range(5 Hz-50 Hz) in which the fundamental frequency lies.

It can be observed from figure 4.9 that for constant excitation force, the maximum response (acceleration) occurred in x-direction as indicated by red spikes in the time plot.

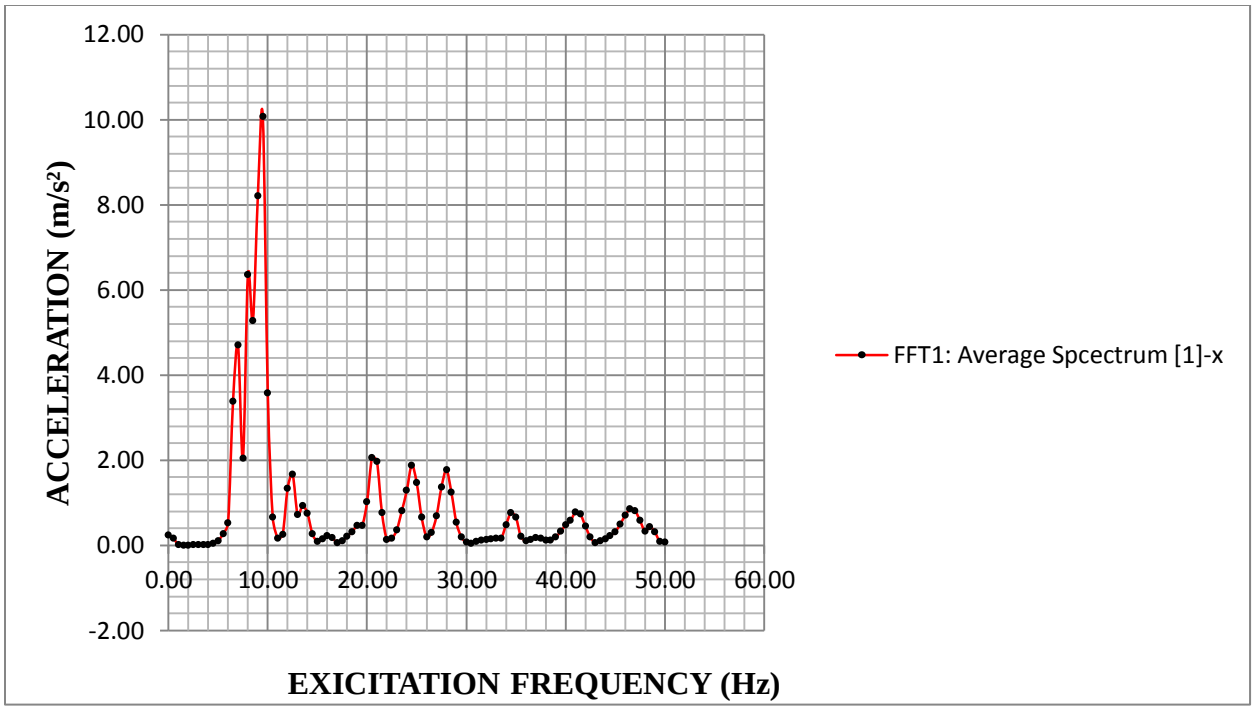

Figure 4.10(a) Acceleration Vs excitation frequency graph for brass beam (500mm X 25.4mm X 6mm)

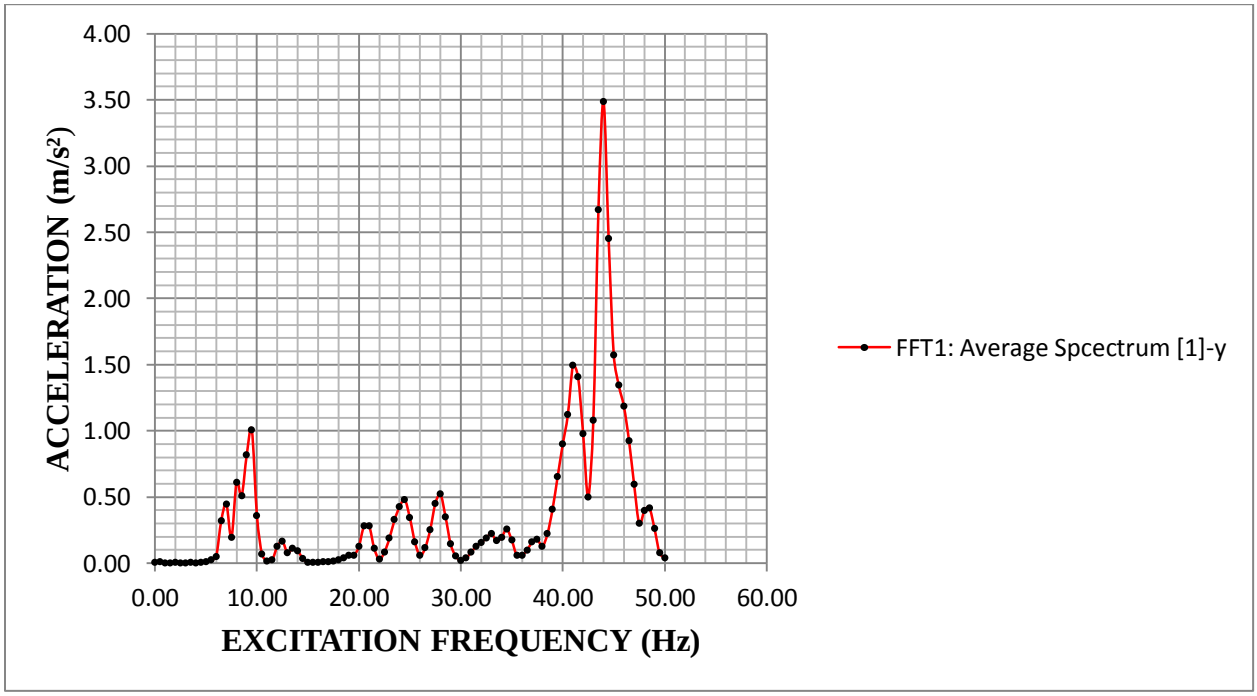

Figure 4.10 (b) Acceleration Vs excitation frequency graph for brass beam (500mm X 25.4mm X 6mm)

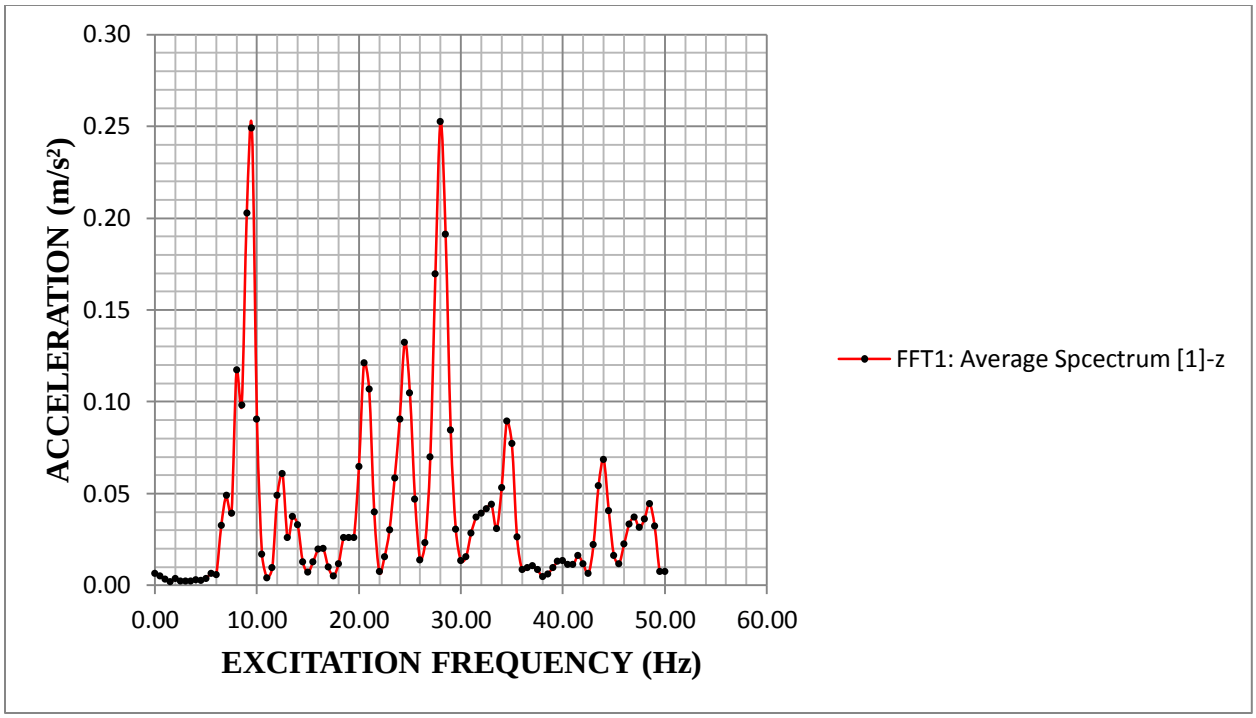

Figure 4.10(c) Acceleration Vs excitation frequency graph for brass beam (500mm X 25.4mm X 6mm)

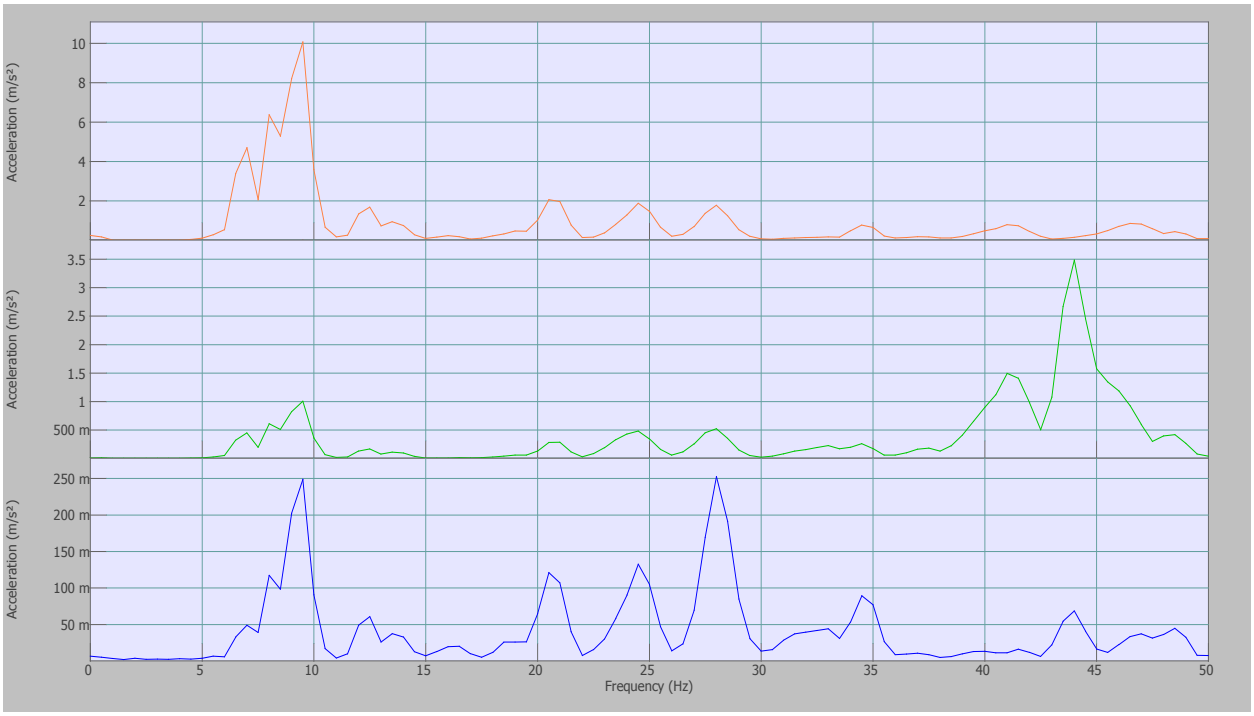

Figure 4.11 Average spectrum of FFT in x, y, z directions for brass beam of thickness 6 mm

The processed FRFs (i.e. FFT) obtained using OROS analyzer for brass of beam length 500 mm through sweep sine test has been shown in the figures 4.10(a) to 4.10(c)

This shows variation of amplitude in terms of acceleration (g) with respect to excitation frequency for brass beam in three directions by analyzing the acceleration signals from orthogonally aligned tri axial accelerometer.

The peak value shows maximum amplitude in terms of acceleration corresponding to fundamental natural frequency i.e. resonant frequency.

From figure 4.10(a) the natural frequency which corresponds to the peak response can be seen to be 9.5 Hz. The half power points where the response amplitude is equal to 0.707 times the peak response can be identified as $\omega_{1=}$ 8.45 Hz and ω_2 =9.80 Hz.

From analysis point of view resonant frequency response amplitude is very important. Since the input force is constant during excitation, the output can be viewed as frequency response function. Hence output response can be considered for analysis of damping for first mode in x-direction only. As shown in figure 4.10 (a) for constant force, it is seen that he maximum amplitude occurs not at the resonant frequency i.e. at frequency of 14.84 Hz but towards its left i.e. at frequency of 9.5 Hz. At first mode, ω_p =9.5 Hz is the frequency corresponding to peak amplitude i.e. 10.7 m/s^2. This shift increases with the increase in damping. Hence the damping ratio corresponding to natural frequency 9.5 Hz is 0.063157.
From figure 4.11 it has been observed from average spectrum of response that the maximum response occurs in the x-axis which is the dominant axis (i.e., transverse to the axis of beam) in which specimen vibrates (in the direction of moving shaker table) more as compared in other two axes.

4.4 VIBRATION CHARACTERISTICS OF BRASS BEAM OF THICKNESS 10mm

The vibration characteristics (natural frequency & damping ratio) of brass beam of thickness 10mm have been determined by sine sweep test .Graphs for response (acceleration) with respect to constant excitation force for brass beam of thickness 10mm has been shown in figures 4.12 and 4.13 both in time domain as well as in frequency domain.

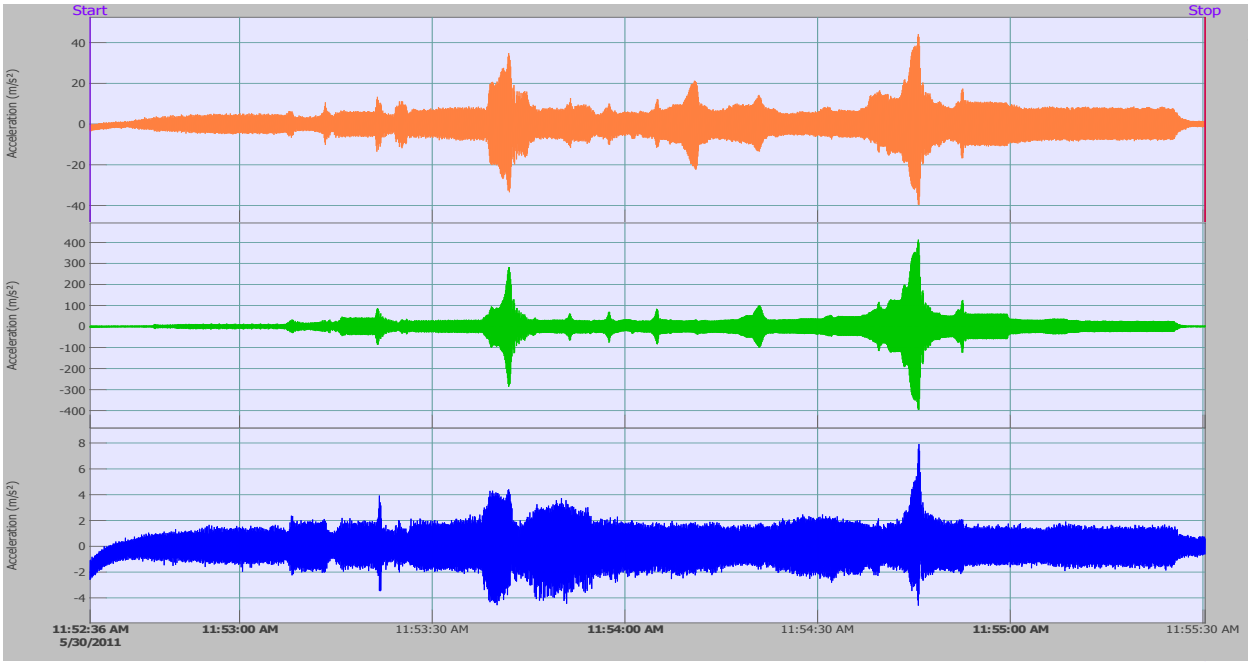

Figure 4.12 Time-response graph for brass beam of thickness 10 mm

Figure 4.12 shows the acceleration data in the time domain, which is converted to the frequency domain via FFT (Fast Fourier Transform) so that the natural frequencies and damping can be identified.

The three colours i.e. orange, green and blue represents the acceleration data in x, y, and z direction respectively in the time domain plot reads from start to stop varying of frequency in the selected frequency range(5 Hz-50 Hz) in which the fundamental frequency lies.

It can be observed from 4.12 that for constant excitation force the maximum response (acceleration) occurred in z-direction as indicated by blue spikes in the time domain plot.

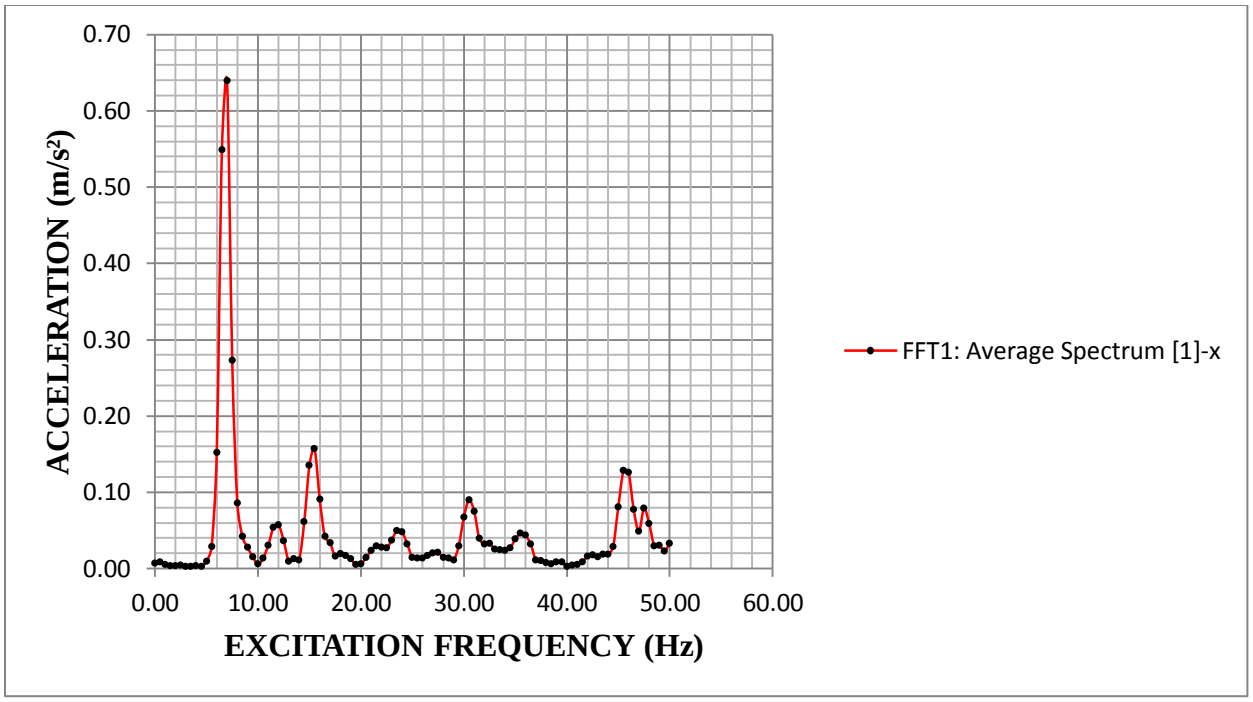

Figure 4.13 (a) Acceleration Vs excitation frequency graph for brass beam in x-direction (500mm X 25.4mm X 10mm)

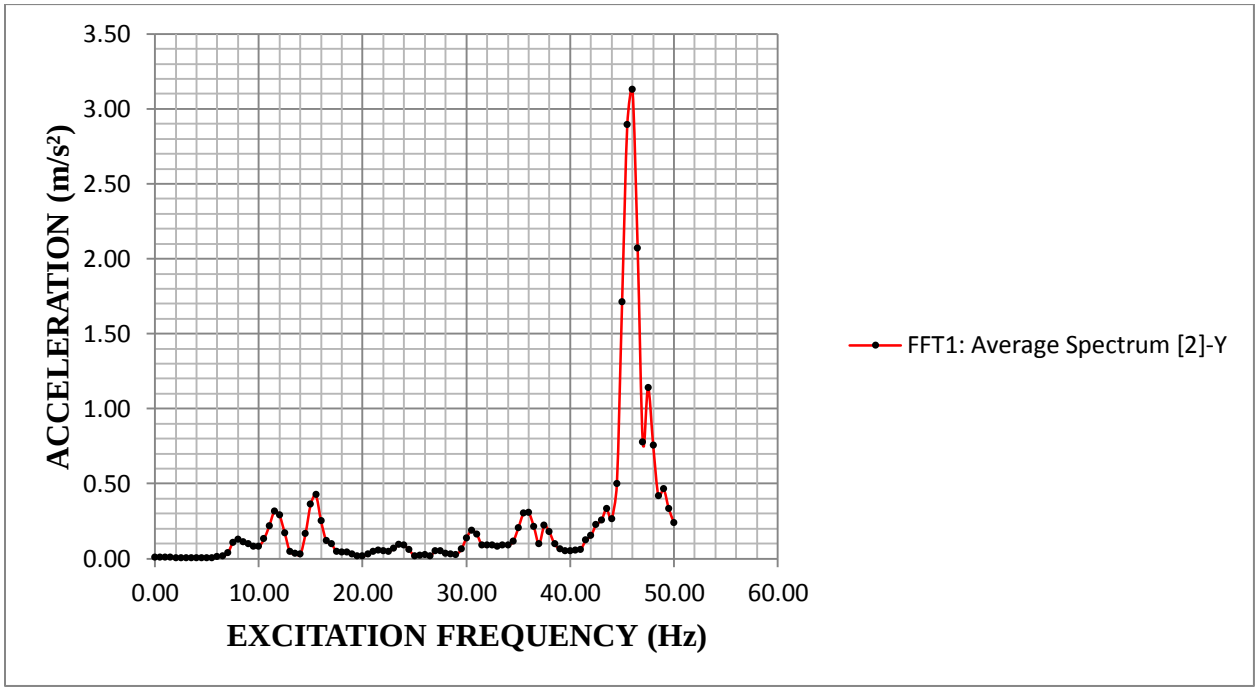

Figure 4.13 (b) Acceleration Vs excitation frequency graph for brass beam in y-direction (500mm X 25.4mm X 10mm)

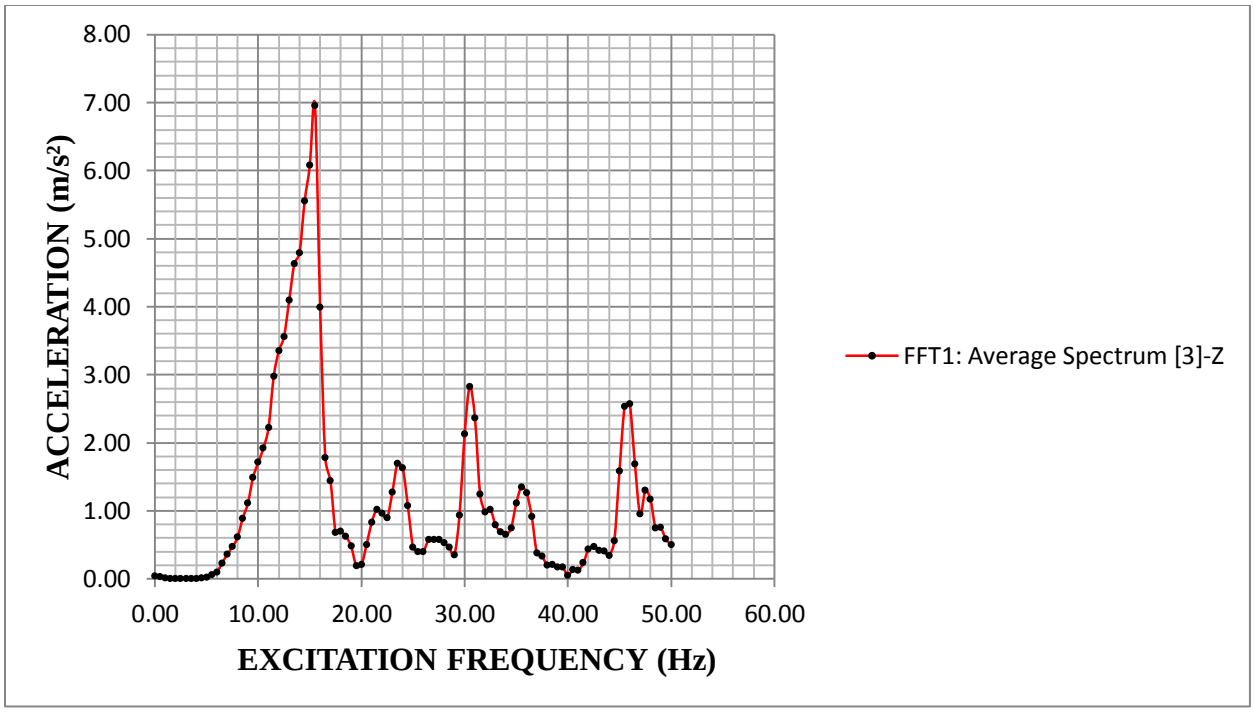

Figure 4.13 (c) Acceleration Vs excitation frequency graph for brass beam in z-direction (500mm X 25.4mm X 10mm)

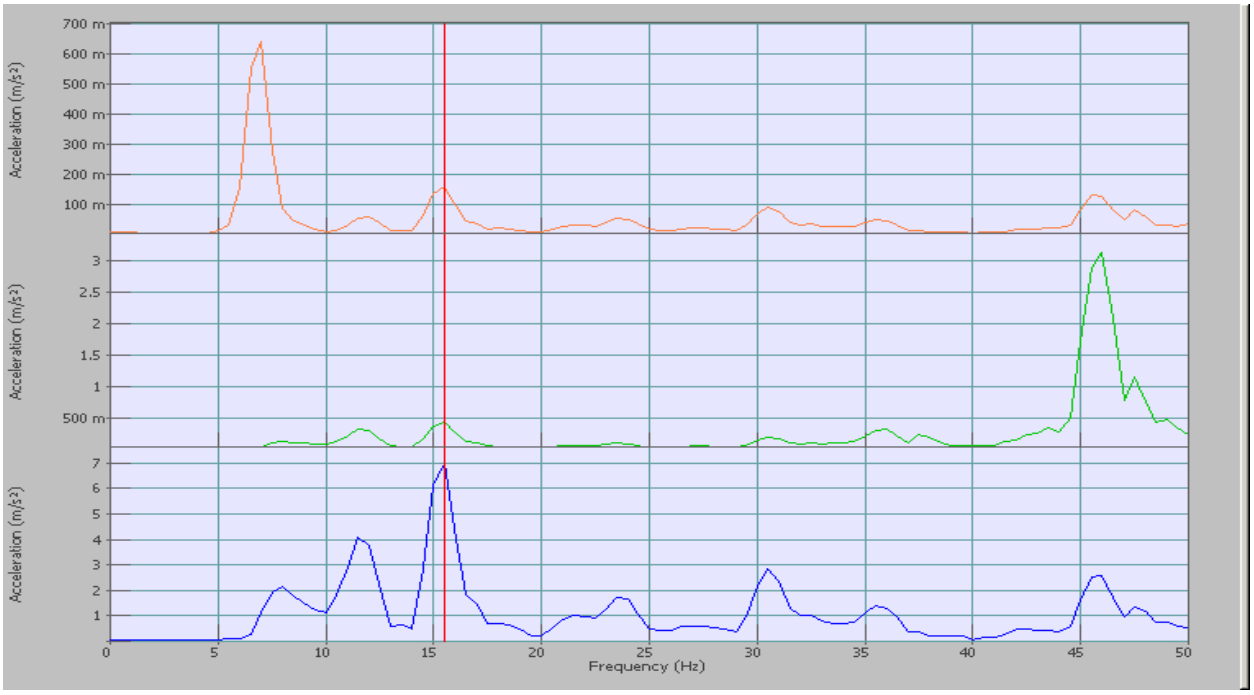

Figure 4.14 Average spectrum of FFT in x, y and z directions for brass beam of thickness 10 mm

The processed FRFs (i.e. FFT) obtained using OROS analyzer for brass of beam length 500 mm through sweep sine test has been shown in the figures 4.13(a) to 4.13(c).

This shows variation of amplitude in terms of acceleration (g) with respect to excitation frequency for brass beam in three directions by analyzing the acceleration signals from orthogonally aligned tri axial accelerometer.

The peak value shows maximum amplitude in terms of acceleration corresponding to fundamental natural frequency i.e. resonant frequency.

From figure 4.13(c) the natural frequency which corresponds to the peak response can be seen to be 15.50 Hz. The half power points where the response amplitude is equal to 0.707 times the peak response can be identified as $\omega_{1=}$ 14.30 Hz and ω_2 =15.80 Hz.

From analysis point of view resonant frequency response amplitude is very important. Since the input force is constant during excitation, the output can be viewed as frequency response function. Hence output response can be considered for analysis of damping for first mode in z-direction only. As shown in figure.4.13 (c) for constant force it is seen that the maximum amplitude occurs not at the resonant frequency i.e. at frequency of 24.83 Hz. but a little towards its left i.e. at frequency of 15.50 Hz. At first mode, ω_p =15.50 Hz is the frequency corresponding to peak amplitude i.e. 6.95 m/s^2. Hence the damping ratio corresponding to natural frequency 15.50 Hz is 0.032259.This shift increases with the increase in damping.

From figure 4.14, it has been observed from average spectrum of response that the maximum response occurs in the z-axis which is the dominant axis (i.e., transverse to the axis of beam) in which specimen vibrates more (in the direction of moving shaker table) as compared in other two axes.

As seen from the experiment results for the vibration characteristics of brass beam of thicknesses 10 mm and 6mm ,the natural frequency reduces in case of thickness 6 mm for the same span length and are in fair matching with theoretical. Hence the damping ratio in case of thickness 6 mm was found to be more as compared to thickness 10mm. The reason for higher damping could be the gap between the frequency range between half power points and lower stiffness value i.e. 1130.2 N/m.

Figure 4.15-4.16 shows the comparison of natural frequencies and damping ratios for brass beam of different thickness (6mm and 10mm).

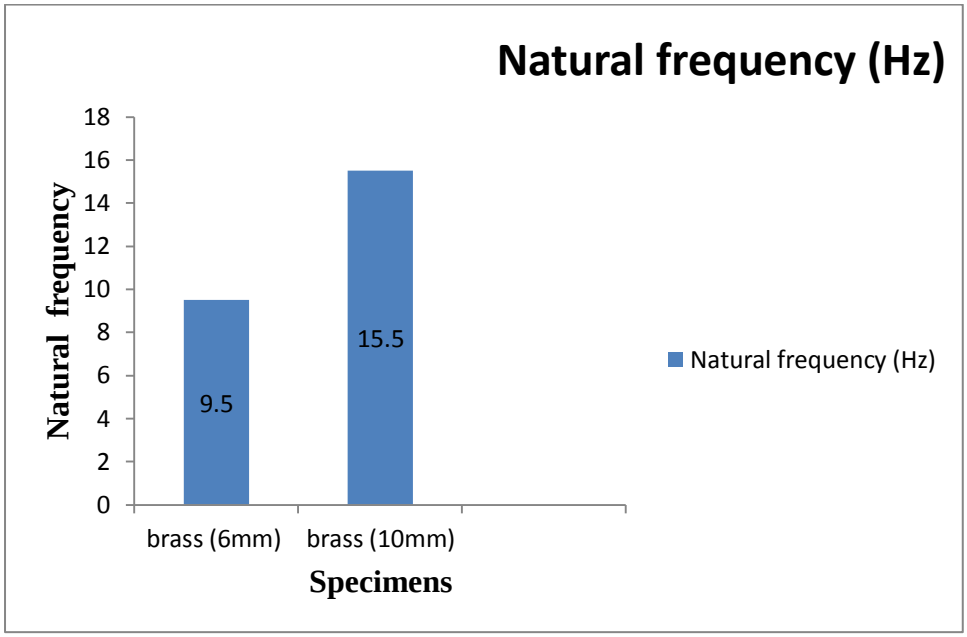

Figure 4.15 Comparison of natural frequencies for brass beam of thickness 6 and 10mm

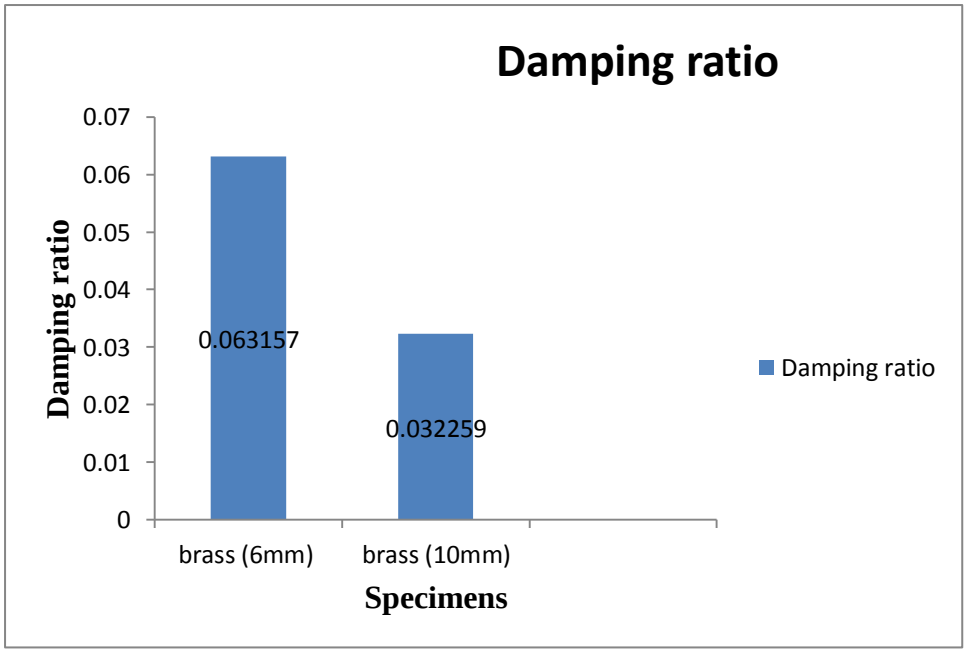

Figure 4.16 Comparison of damping ratios for brass beam of thickness 6 and 10mm

4.5 VIBRATION CHARACTERISTICS OF MILD STEEL BEAM OF THICKNESS 6mm

The vibration characteristics (natural frequency & damping ratio) of mild steel beam of thickness 6mm have been determined by sine sweep test .Graphs for response (acceleration) with respect to constant excitation force for mild steel beam of thickness 6mm has been shown in figures 4.17 and 4.18 both in time domain as well as in frequency domain.

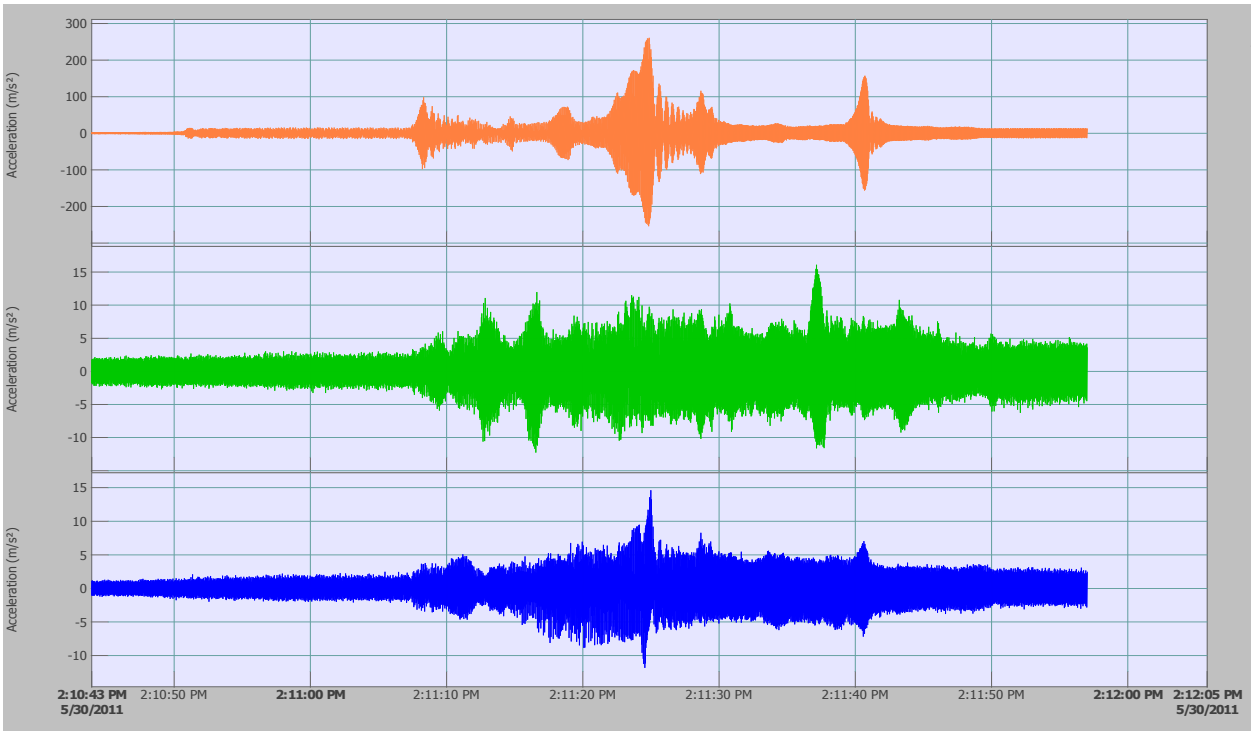

Figure 4.17 Time-response graph for mild steel beam of thickness 6 mm

Figure 4.17 shows acceleration data in the time domain, which is converted to the frequency domain via FFT (Fast Fourier Transform) so that the natural frequencies and damping can be identified.

The three colours i.e. orange, green and blue represents the acceleration data in x, y, and z direction respectively in the time domain plot reads from start to stop varying of frequency in the selected frequency range(5 Hz-50 Hz) in which the fundamental frequency lies.

It can be observed from figure 4.17 that for constant excitation force, the maximum response (acceleration) occurred in x-direction as indicated by red spikes in the time domain plot.

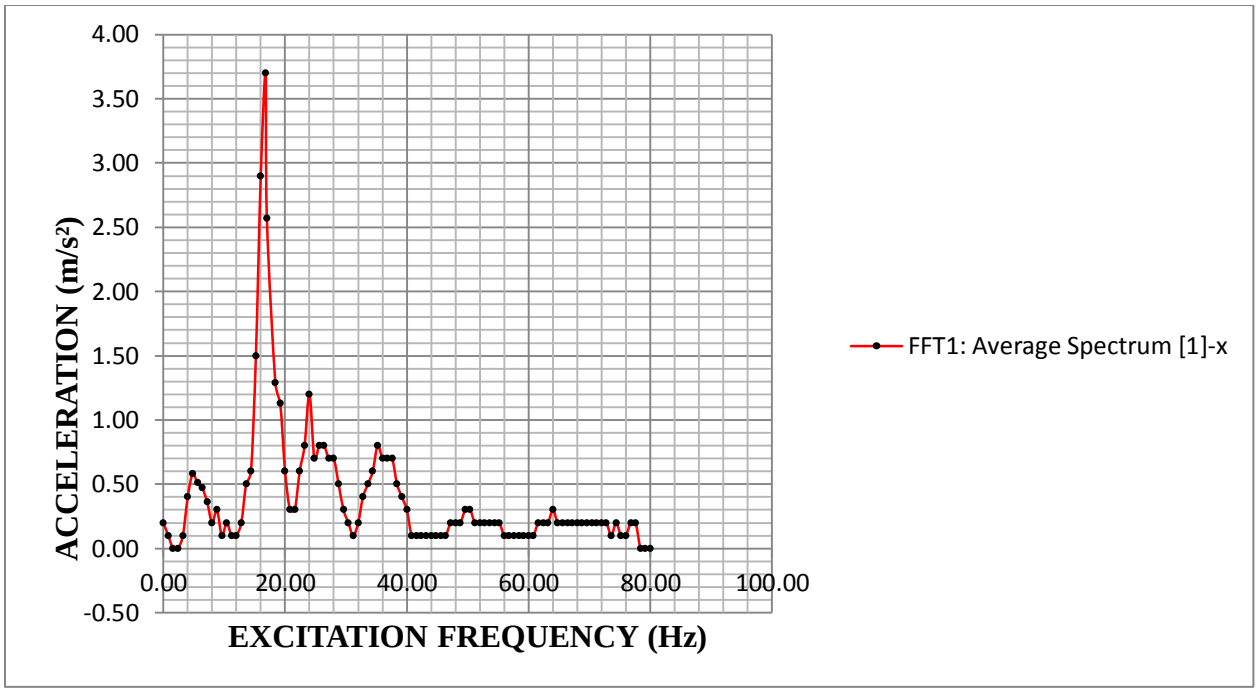

Figure 4.18 (a) Acceleration Vs excitation frequency graph for mild steel beam in x-direction (500mm X 25.4mm X 6mm)

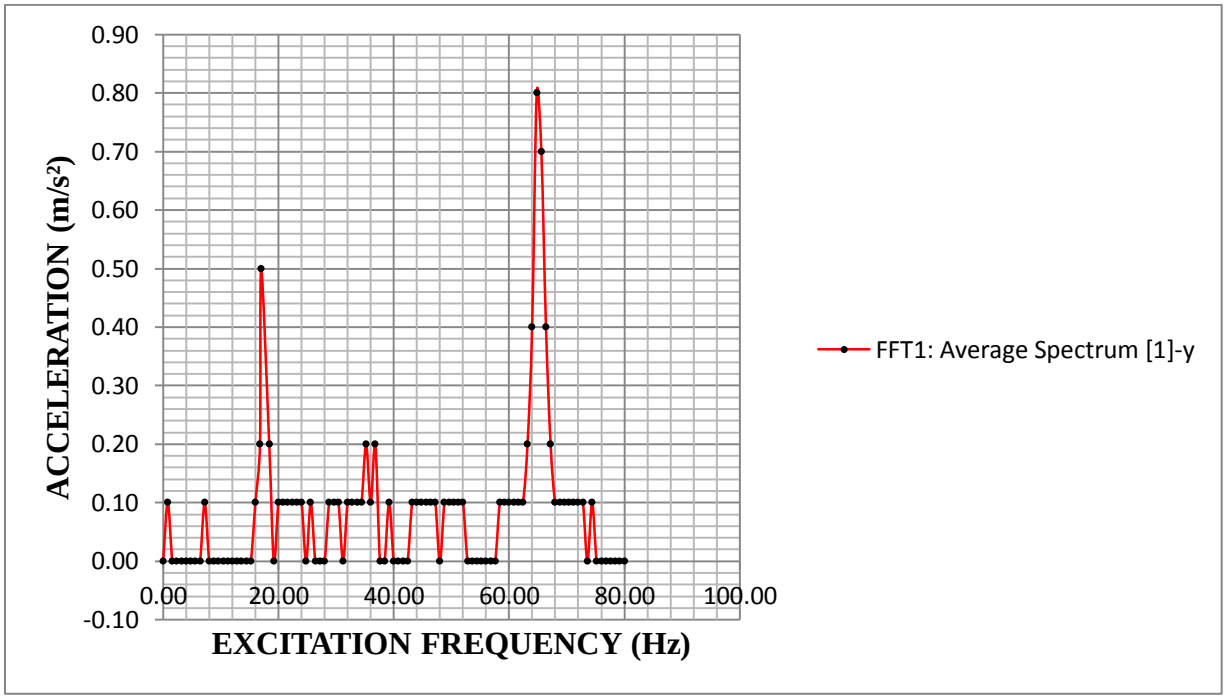

Figure 4.18 (b) Acceleration Vs excitation frequency graph for mild steel beam in y-direction (500mm X 25.4mm X 6mm)

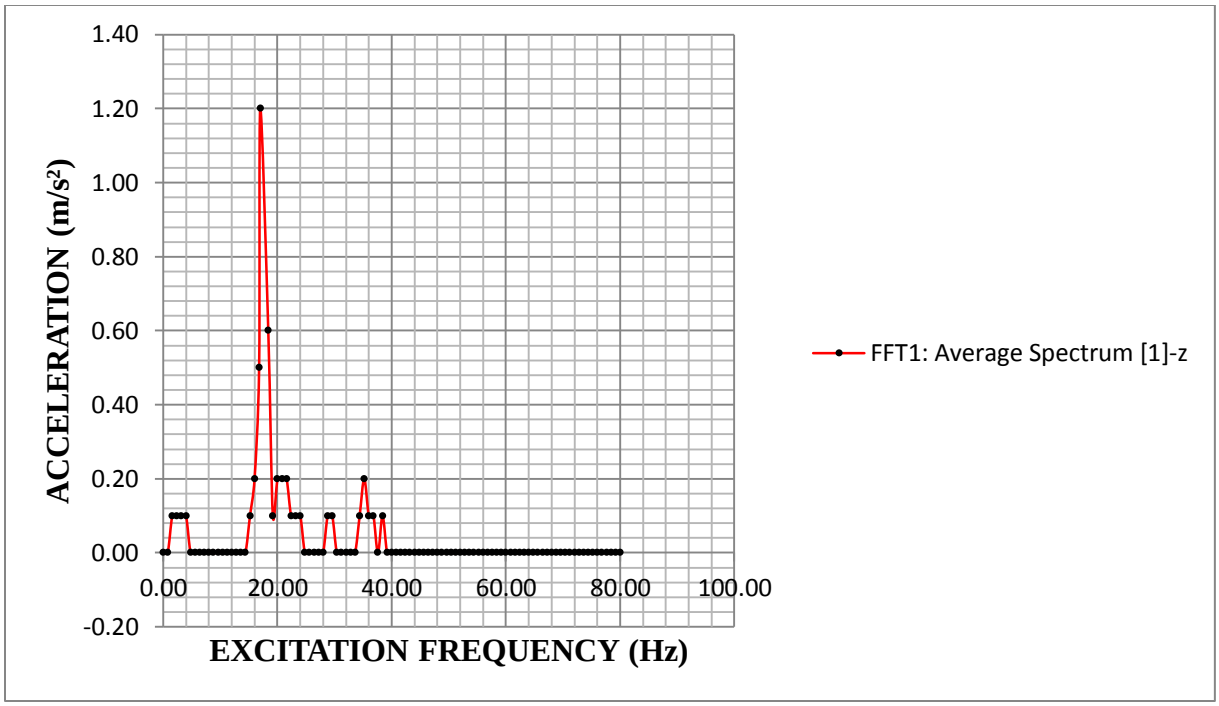

Figure 4.18 (c) Acceleration Vs excitation frequency graph for mild steel beam in z- direction (500mm X 25.4mm X 6mm)

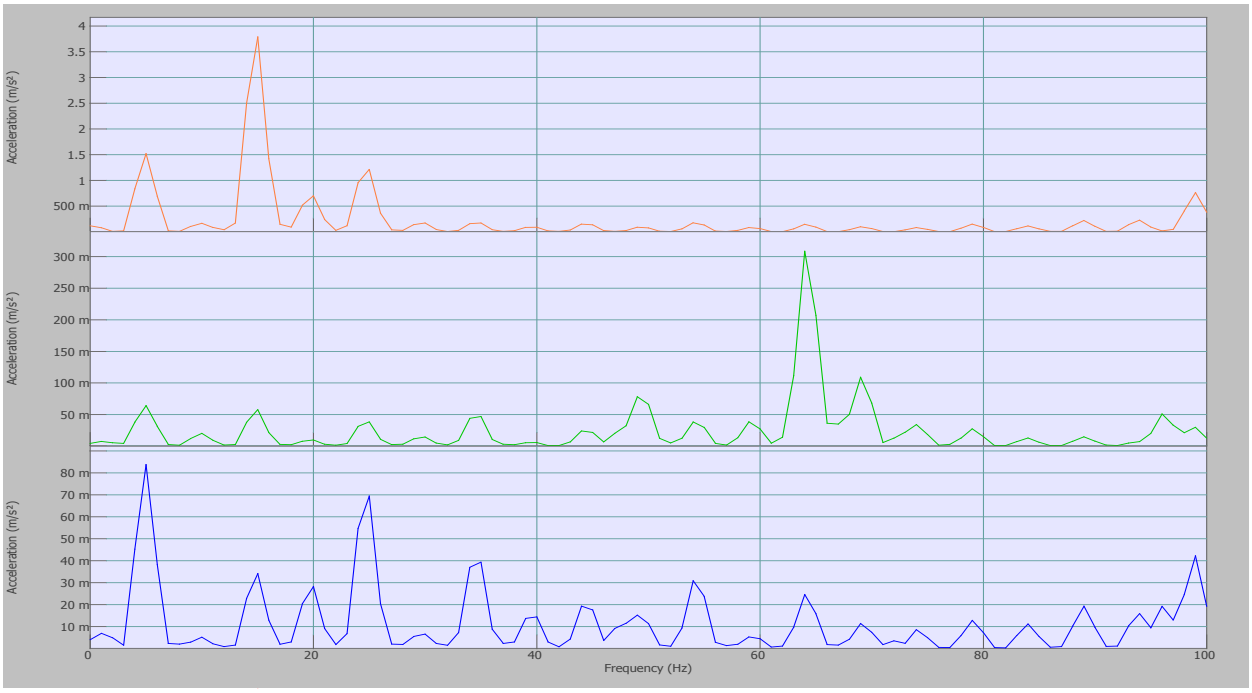

Figure 4.19 Average spectrum of FFT in x, y, z directions for mild steel beam of thickness 6mm

The processed FRFs (i.e. FFT) obtained using OROS analyzer for mild steel of beam length 500 mm through sweep sine test has been shown in the figures 4.18 (a) to 4.18 (c).

This shows variation of amplitude in terms of acceleration (g) with respect to excitation frequency for mild steel beam in three directions by analyzing the signals from orthogonally aligned tri axial accelerometer.
The peak value shows maximum amplitude in terms of acceleration corresponding to fundamental natural frequency i.e. resonant frequency.

From figure 4.18(a) the natural frequency which corresponds to the peak response can be seen to be 16.80 Hz. The half power points where the response amplitude is equal to 0.707 times the peak response can be identified as ω_1 = 15.30 Hz and ω_2 =17.70 Hz.

From analysis point of view resonant frequency response amplitude is very important. Since the input force is constant during excitation, the output can be viewed as frequency response function. Hence output response can be considered for analysis of damping for first mode in x-direction only. As shown in figure 4.18(a) for constant force, it is seen that he maximum amplitude occurs not at the resonant frequency i.e. at frequency of 20.06 Hz but a little towards its left i.e. at frequency of 16.80 Hz. At first mode, 16.80 Hz is the frequency corresponding to peak amplitude i.e. 3.7 m/s^2. Hence the damping ratio corresponding to natural frequency 16.80 Hz is 0.069047. This shift increases with the increase in damping.
From figure 4.19 it has been observed from average spectrum of response that the maximum response occurs in the x-axis which is the dominant axis (i.e., transverse to the axis of beam) in which specimen vibrates (in the direction of moving shaker table) more as compared to other two axes.

4.6 VIBRATION CHARACTERISTICS OF MILD STEEL BEAM OF THICKNESS 10mm

The vibration characteristics (natural frequency & damping ratio) of mild steel beam of thickness 10mm have been determined by sine sweep test .Graphs for response (acceleration) with respect to constant excitation force for mild steel beam of thickness 10mm has been shown in figures 4.20 and 4.21 both in time domain as well as in frequency domain.

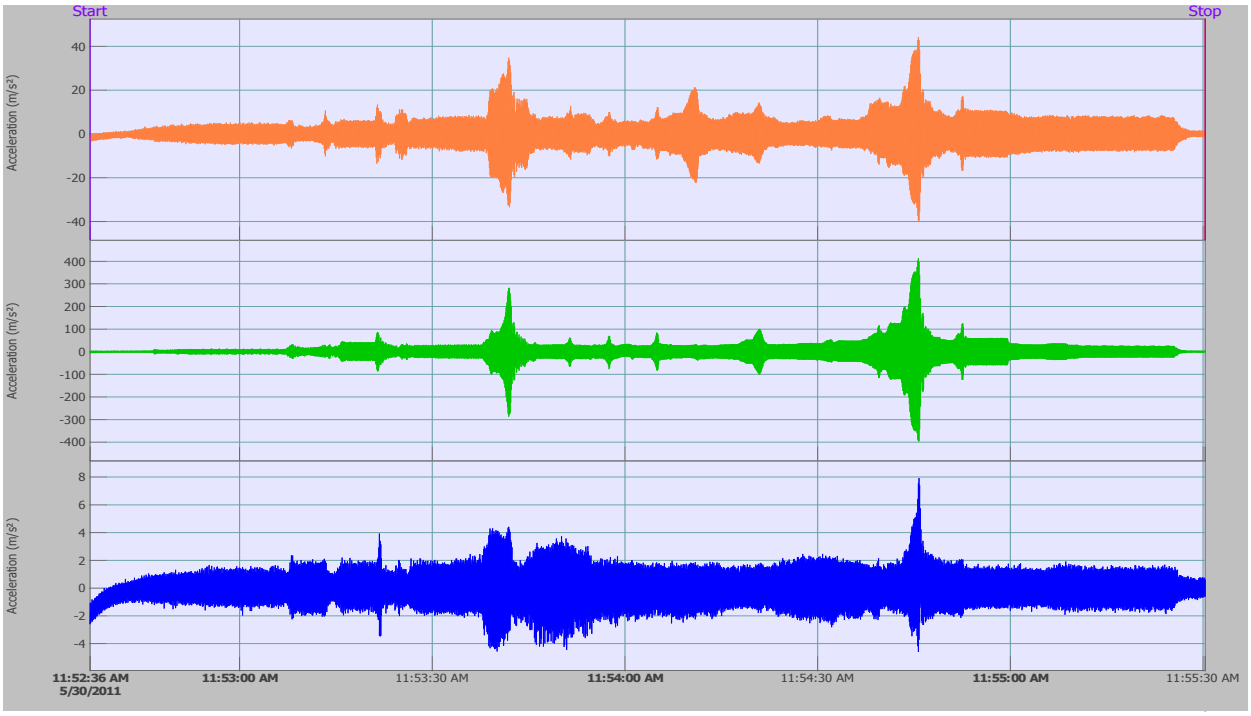

Figure 4.20 Time-response graph for mild steel beam of thickness 10 mm

Figure 4.20 shows that initial acceleration data is in the time domain, which is converted to the frequency domain via FFT (Fast Fourier Transform) so that the natural frequencies and damping can be identified

The three colours i.e. orange, green and blue represents the acceleration data in x, y, and z direction respectively in the time domain.

It can be observed from 4.20 that for constant excitation force, the maximum response (acceleration) occurred in x-direction as indicated by red spikes in the time domain plot.

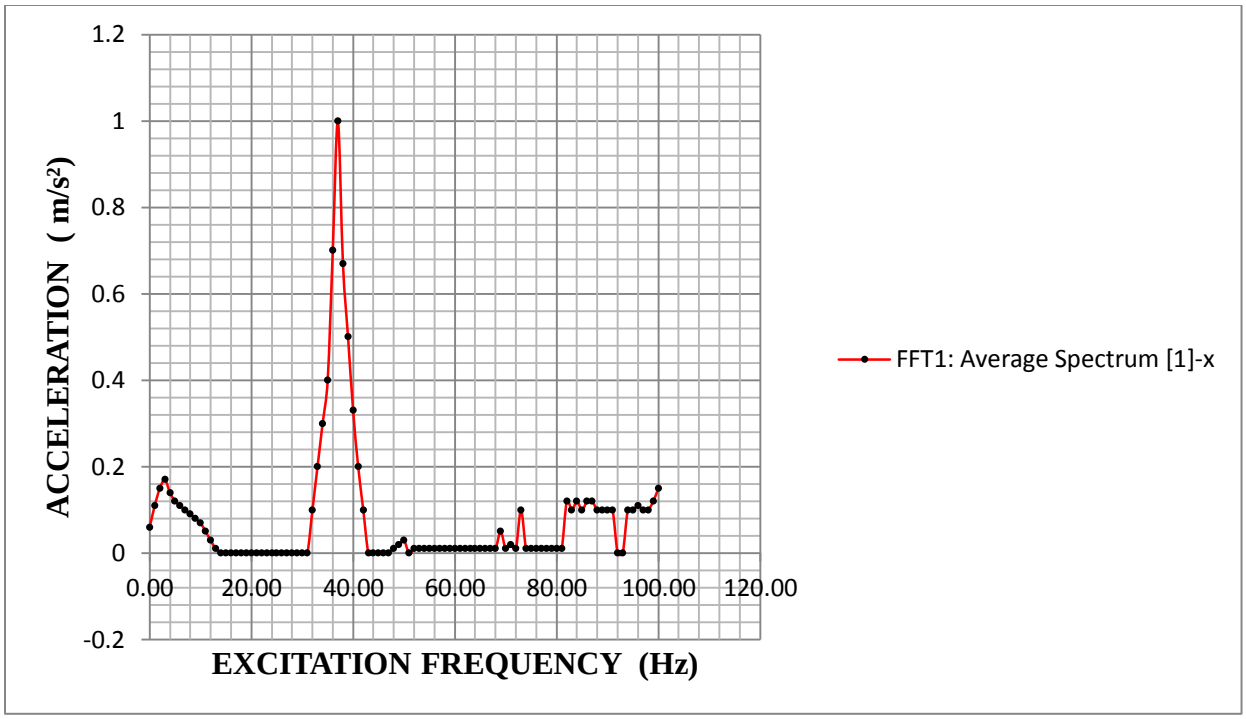

Figure 4.21 (a) Acceleration Vs excitation frequency graph for mild steel beam in x-direction (500mm X 25.4mm X 10mm)

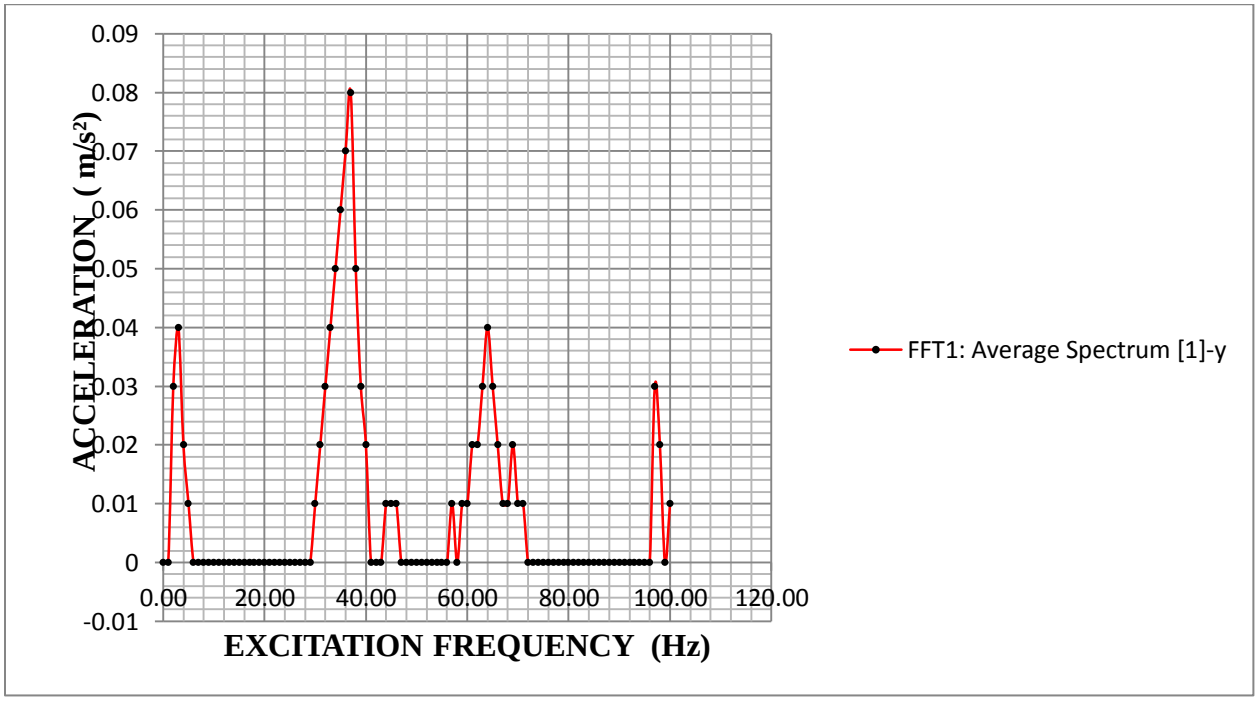

Figure 4.21 (b) Acceleration Vs excitation frequency graph for mild steel beam in y-direction (500mm X 25.4mm X 10mm)

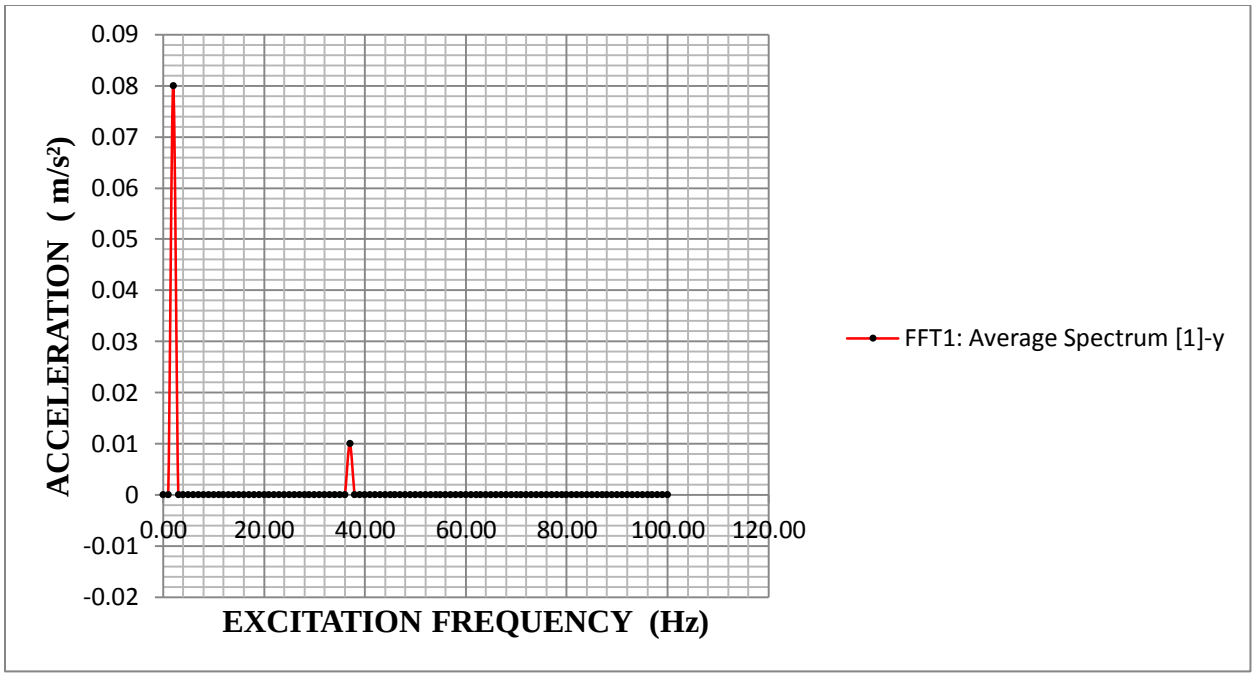

Figure 4.21 (c) Acceleration Vs excitation frequency graph for mild steel beam in z-direction (500mm X 25.4mm X 10mm)

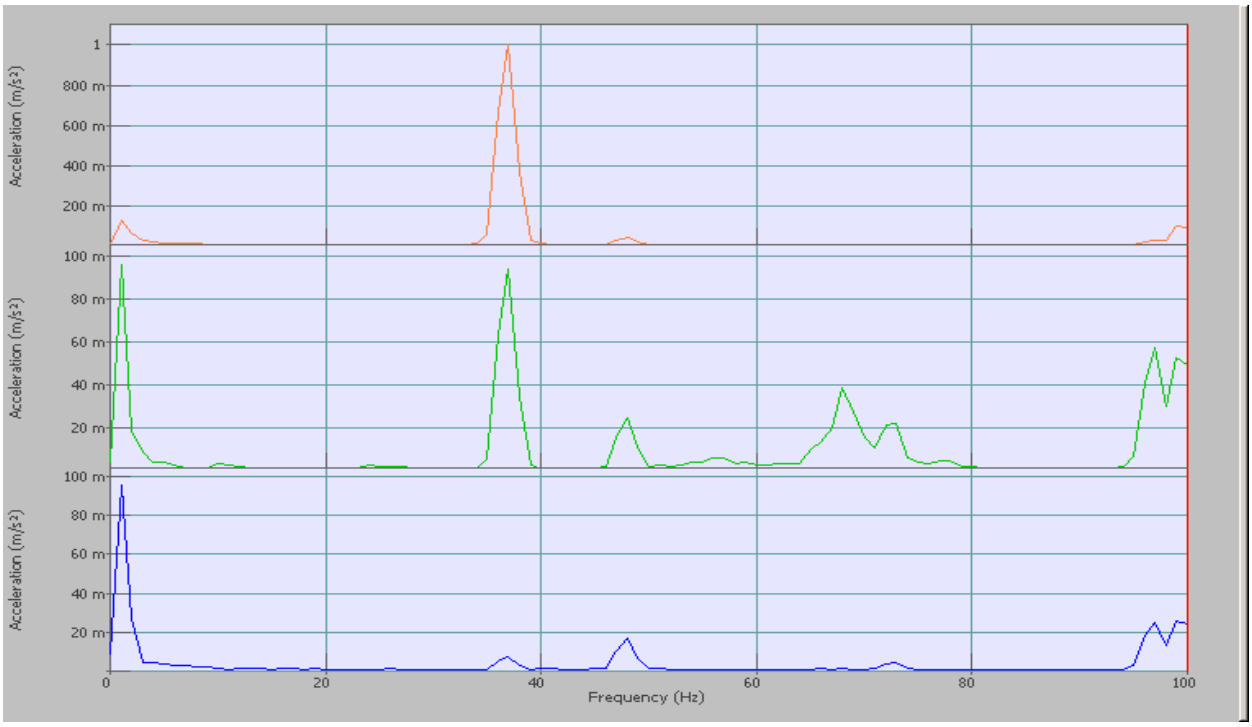

Figure 4.22 Average spectrums of FFT in x, y and z directions for mild steel beam of thickness 10 mm

The FRFs (i.e. FFT) obtained using OROS analyzer for mild steel of beam length 500 mm through sweep sine test has been shown in the figures 4.21(a) to 4.21(c)

This shows variation of amplitude in terms of acceleration (g) with respect to excitation frequency for mild steel beam in three directions by analyzing the acceleration signals from orthogonally aligned tri axial accelerometer.
The peak value shows maximum amplitude in terms of acceleration corresponding to fundamental natural frequency i.e. resonant frequency.

From figure 4.21(a) the natural frequency which corresponds to the peak response can be seen to be 36 Hz. The half power points where the response amplitude is equal to 0.707 times the peak response can be identified as $\omega_{1=}$ 35.60 Hz and ω_2 =38.10 Hz.

From analysis point of view resonant frequency response amplitude is very important. Since the input force is constant during excitation, the output can be viewed as frequency response function. Hence output response can be considered for analysis of damping for first mode in x-direction only. As shown in figure 4.21 (a) for constant force, it is seen that he maximum amplitude occurs not at the resonant frequency i.e. at frequency of 33.43 Hz but its right i.e. at frequency of 36 Hz. At first mode, ω_p =36 Hz is the frequency corresponding to peak amplitude i.e. 1 m/s2. Hence the damping ratio corresponding to natural frequency 36 Hz is 0.034722.
From figure 4.22 it has been observed from average spectrum of response that the maximum response occurs in the x-axis which is the dominant axis (i.e., transverse to the axis of beam) in which specimen vibrates (in the direction of moving shaker table) more as compared in other two axes.

As seen from the experiment results for the vibration characteristics of mild steel beam of thicknesses 10 mm and 6mm ,the natural frequency reduces in case of thickness 6 mm for the same span length and are in fair matching with theoretical. Hence the damping ratio in case of thickness 6 mm was found to be more as compared to thickness 10mm. The reason for

higher damping could be the gap between the frequency range of half power points and lower stiffness value i.e. 2231.87 N/m.

Figure 4.23-4.24 shows the comparison of natural frequencies and damping ratios for mild steel beams of different thickness (6mm and 10mm).

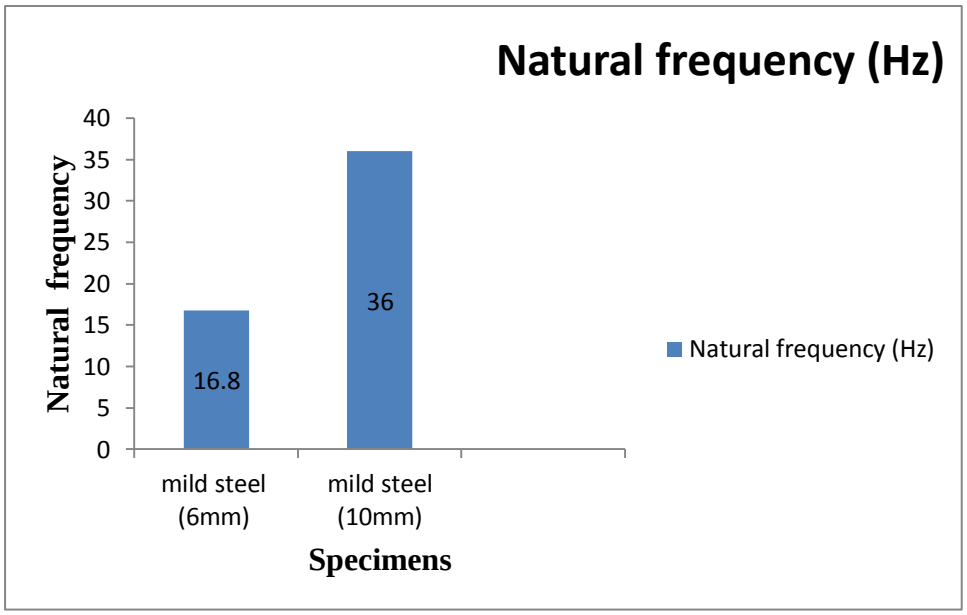

Figure 4.23 Comparison of natural frequencies for mild steel beam of thickness 6 and 10mm

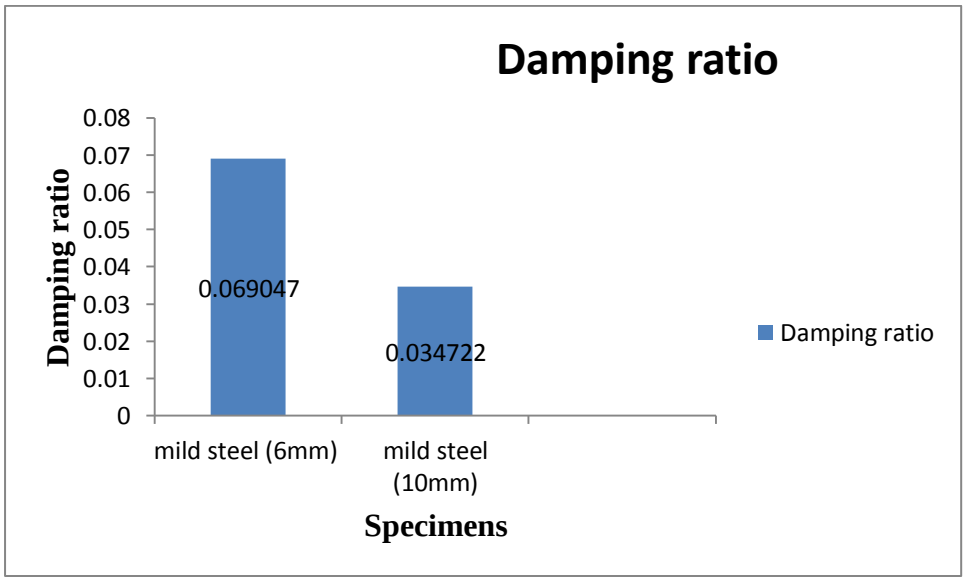

Figure 4.24 Comparison of damping ratios for mild steel beam of thickness 6 and 10mm

4.7 COMPARISON OF FREQUENCIES FOR DIFFERENT MATERIALS BEAMS OF DIFFERENT THICKNESS

The modal frequencies (Hz) for different beam specifications are compared as below:

Material	Beam dimensions	Mode	Frequency (by theoretical method)	Frequency (by experimental method)	Percentage of error
Aluminium	500 mm x 25.4 mm x 10 mm	1	32.90	37.00	11.08%
Brass	500 mm x 25.4 mm x 10 mm	1	24.73	15.50	37.32%
Mild steel	500 mm x 25.4 mm x 10 mm	1	33.43	36.00	7.13%

Table 4.1 Comparison of fundamental frequencies of beams of thickness 10mm

Material	Beam dimensions	Mode	Frequency (by theoretical method)	Frequency (by experimental method)	Percentage of error
Aluminium	500 mm x 25.4 mm x 6 mm	1	19.58	17.60	10.11%
Brass	500 mm x 25.4 mm x 6 mm	1	14.84	9.50	35.98%
Mild steel	500 mm x 25.4 mm x 6 mm	1	20.06	16.80	16.25%

Table 4.2 Comparison of fundamental frequencies of beams of thickness 6mm

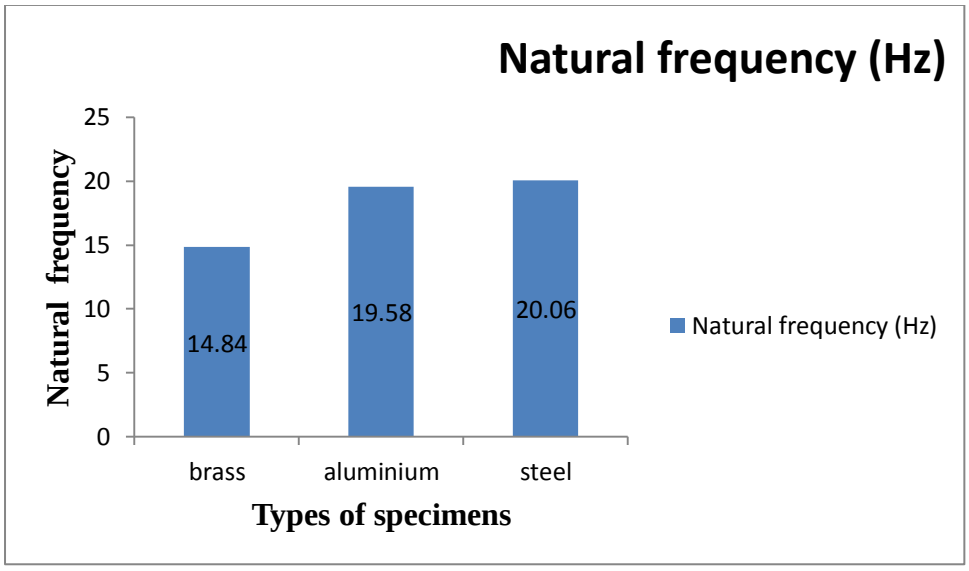

Figure 4.25 Comparison of theoretical determined natural frequencies of three specimens (500 mm x 25.4 mm x 6mm)

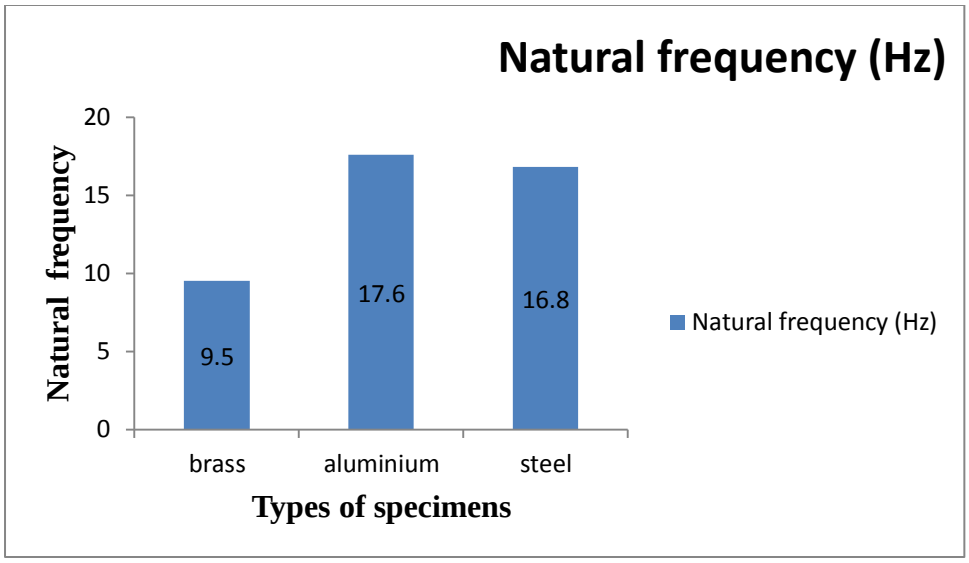

Figure 4.26 Comparison of experimentally determined natural frequencies of three specimens (500 mm x 25.4 mm x 6mm)

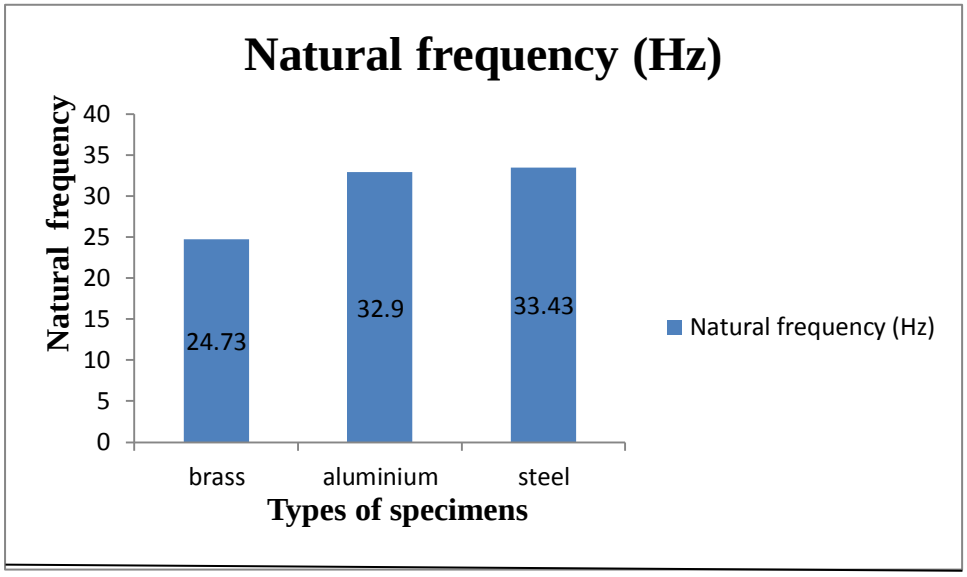

Figure 4.27 Comparison of theoretical determined natural frequencies of three specimens (500 mm x 25.4 mm x 10mm)

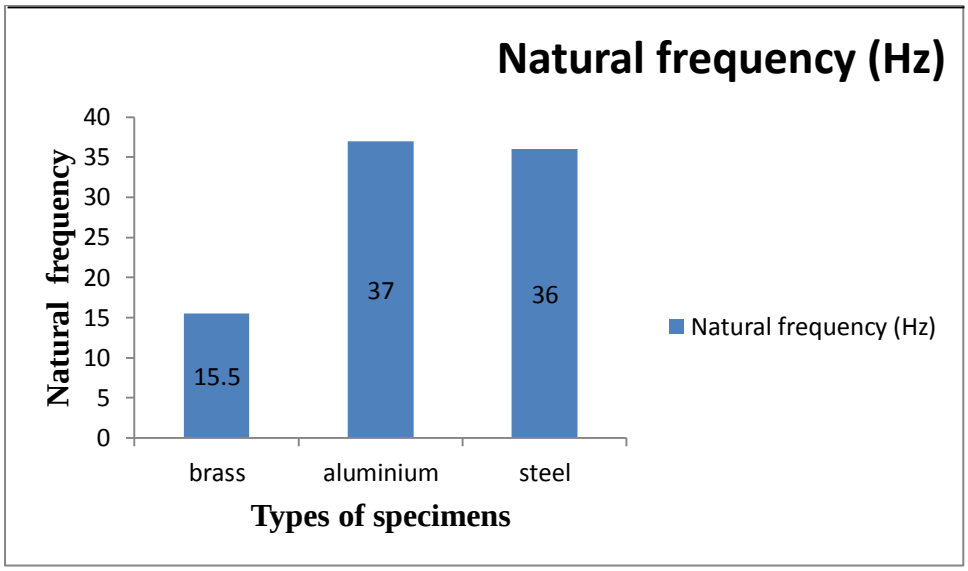

Figure 4.28 Comparison of experimentally determined natural frequencies of three specimens (500 mm x 25.4 mm x 10mm)

From Table 4.1-4.2 it can be seen from the experiment that steel and aluminium has higher natural frequency in comparison with brass. The reasons could be of higher stiffness hence in turn higher elastic modulus. Figure 4.25-4.28 compares natural frequency of three specimens of same length and same width but different thickness. As seen from the theoretical and experimental values of natural frequencies for the first fundamental mode in the above tables, the effect of thickness variates the natural frequency. In case of beam of thickness 6 mm, the natural frequency reduces for all the three material in comparison with beam of thickness 10 mm. This can be accounted to be lower moment of inertia which results in lower stiffness value.

4.8 COMPARISON OF DAMPING RATIOS FOR DIFFERENT MATERIALS BEAMS OF DIFFERENT THICKNESS

The damping ratios 'ζ 'are compared as below in tables (4.3-4.4):

Dimensions 500mm X 25.4mm X 10mm

Material	Fundamental mode(Hz)	Damping ratio(ζ)
Steel	36.00	0.034722
Brass	15.50	0.032259
Aluminium	37.00	0.02756

Table 4.3 Estimated damping ratio by half-power band width method (10mm)

Dimensions 500mm X 25.4mm X 6mm

Material	Fundamental mode(Hz)	Damping ratio(ζ)
Steel	16.80	0.069047
Brass	9.50	0.063157
Aluminium	17.60	0.03039

Table 4.4 Estimated damping ratio by half-power band width method (6mm)

From Tables 4.3-4.4., it is evident that damping ratio for the first mode is higher for steel in comparison with brass and aluminium of same span length and width. The reasons for higher damping could be of lower stiffness. Figure 4.29-4.30 compares damping ratios of three specimens of same length and same width but different thickness.

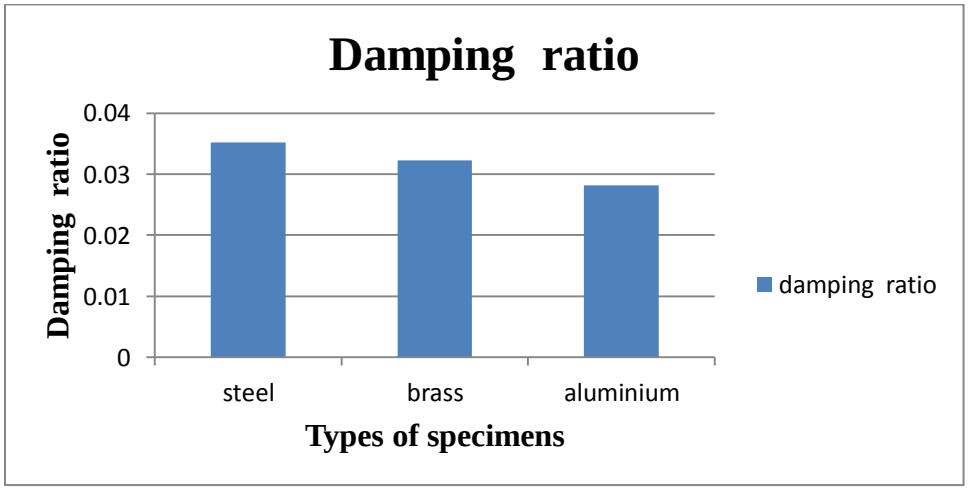

Figure 4.29 Comparison of damping ratios of three specimens of dimensions (500 mm x 25.4 mm x 10mm)

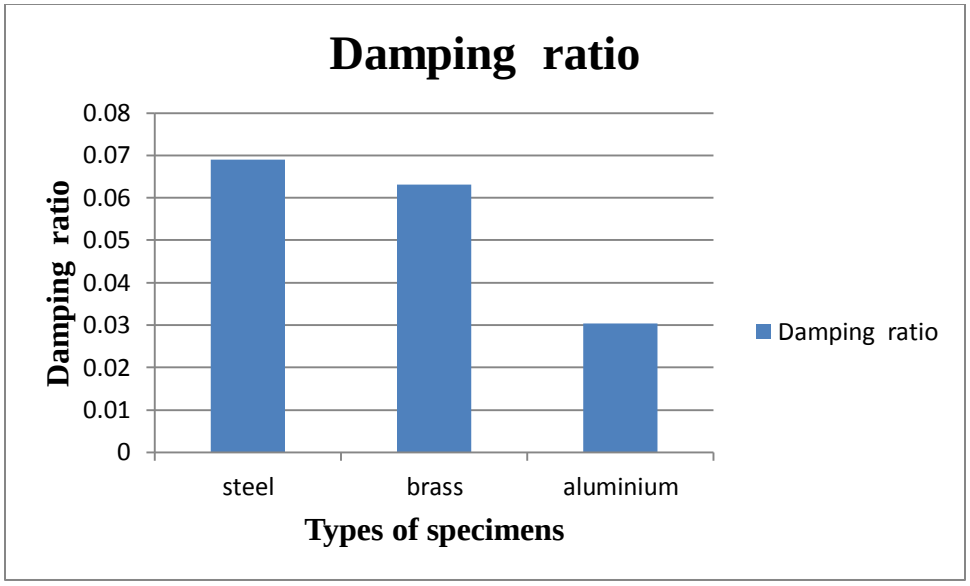

Figure 4.30 Comparison of damping ratios of three specimens of dimensions (500 mm x 25.4 mm x 6mm)

The effect of thickness also variates the damping. The different material beam of thickness 6 mm has found to be higher damping ratio as compared to thickness 10 mm and it has been found that in case of steel the damping value is around 0.034722 and 0.069047 for thickness 10mm and 6mm respectively. Brass has second highest damping value after steel. Aluminium damping was found to be lowest.

4.9 SUMMARIZED RESULTS AND DISCUSSIONS

1. The resonant frequencies obtained experimentally at the first mode of vibration of all the three specimens can be compared with theoretical results
2. There is good agreement of the theoretical calculated natural frequency with the experimental one.
3. Comparing theoretical results with experimental results at the first resonant point shows that the experimental results are somewhat lower than the theoretical results in case of thickness 6mm.

4. The slight discrepancy is due to the present theoretical calculation is based on the cantilever beam end conditions .The mass of the combo base slip table may also affect the natural frequency.
5. Noise in the measurement may give error in locating the amplitude and this may give deviation in experimentally estimated natural frequency and damping ratio.

CHAPTER 5

CONCLUSION AND SCOPE FOR FUTURE WORK

5.1. CONCLUSION

The main objective of the present work is to study the vibration damping characteristics of three materials i.e. aluminium, brass and steel. To collect the data based on two parameters i.e. excitation force and excitation frequency using forced vibration technique and compare it theoretical results. The cantilever beams have been subjected to sine sweep test and damping ratio has been computed using half power bandwidth method.

On the basis of present study following conclusions are drawn:

- From the experiments it is evident that damping is higher for steel in comparison with brass and aluminium.

  For steel beam of thickness 6mm it has been found to be 6.9% and for thickness 10mm is 3.4%.
- The brass damping is found very close to steel specimen i.e. 6.3% (6mm) and 3.2 %(10mm).
- The material damping decreases with increases in natural frequency of the cantilever specimens for each material.
- The Damping ratio increases with decrease in thickness for each material specimens.
- The damping of aluminium was found to be lowest than either steel or brass.
- The theoretical results obtained by the method proposed in this work and the experiments results vibration are in fair matching in terms of natural frequency.

5.2. SCOPE FOR FUTURE WORK

- The present work may be extended in one of the following ways. There are composite materials i.e. metal matrix composite (MMC) in the use today. Using different materials (metal and their alloys), one can study the damping results and choose the most appropriate structural material.
- Mode shapes can be studied and analyzed.
- Different boundary conditions can be analyzed

REFERENCES

1. **R. D. Adams, "***The damping characteristics of certain steels, cast irons and other metals***",** Journal of Sound and Vibration , Volume 23, Issue 2, Pages 199-216, 22 July 1972.
2. **J. M. Lee and K. G. McConnell, "***Experimental Cross Verification of Damping in Three Metals",* Journal of Sound and Vibration , Volume 15, Pages 347-353, 1975.
3. **R.F. Gibson et al , "***An improved Forced-vibration Technique for Measurement of Material Damping",* Journal of Sound and Vibration , Volume 6, Pages 10-14, April 1982.
4. **Y.Kume and F.Hashimoto, "***Material Damping of cantilever beams*", Journal of Composite Materials, Volume 80(1), Pages 1-10, 1982.
5. **Edward F. Crawley and Marthinus C. Van School, "***Material Damping in Aluminum and Metal Matrix Composites*", Journal of Composite Materials, Volume 21(6), Pages 553-568, 1987.
6. **Marek Pietrzakowski, "***Experiment on a cantilever beam control and theoretical approximation*", Jounal of theoretical and applied mechanics, Volume 40(3), 2002.
7. **A. Salzmann, S. Fragomeni, Y. C. Loo, "** *The Damping Analysis of Experimental Concrete Beams under Free-Vibration"* Journal Advances in Structural Engineering, Volume 6, Number 1 , Pages 53-64, January 2003.
8. **Jean-Luc Wojtowicki, Luc Jaouenb, Raymond Panneton**, "*New approach for the measurement of damping properties of materials using the Oberst beam*", Review of scientific instruments, Volume 75, Number 8, August 2004.
9. **R. F. Gibson and R. Plunkett: "***A forced-vibration technique for measurement of material damping*", Experimental Mechanics, Volume 17, Number 8, Pages 297–302, 2007
10. **Richard S. Norek** ," *Lateral forced vibration of beam with material damping*", ISCORMA-4, Calgary, Alberta, Canada, Inc. 86 Garrison Drive, Eliot, Maine 03903-1626 207-439-2821,27-31 August 2007**.**

11. **D. Ravi Prasad and D.R. Seshu,** "A *study on dynamic characteristics of structural materials using modal analysis",* Asian Journal Of Civil Engineering, Volume 9, Number 2, Pages 141–152, 2008.
12. **M. Chiba,** "*Influence of Horizontal Excitations on Dynamic Stability of a Slender Beam under Vertical Excitation",* Experimental Mechanics, Volume 49, Pages 541–549, 2009.
13. **Umashankar K.S., Abhinav Alva, Gangadharan K. V. and VijayDesai,**" *Damping behavior of cast and sintered aluminium*", ARPN Journal of Engineering and Applied Sciences , Volume 4(6), August 2009.
14. **David M. Beams**, "Natural Frequencies of a Cantilever Beam", ENGR 1200 Laboratory Procedure.
15. **Fabio Lo Castro and Paolo Bisegna, "***Forced Damping Vibration of a Cantilever Beam*", Sensors and microsystems, World Scientific Publishing, Pages 307-31, 2011.
16. **Shibabrat Naik and Wrik Mallik**, "*Experimental modal testing for estimating the dynamic properties of a cantilever beam*" Structural Dynamics.
17. **Richardson, M. M.**, "*Who needs lMAC?*" Preceedings of the Second International Modal Analysis Conference, Orland, Florida, Volume 1, Pages 9, 1984
18. **Staker,** Modal Analysis, Background and Application, Bruel, Kjaer, Instruments, Inc., January, 1987.
19. http://www.wikipedia.org
20. http://www.mfg.mtu.edu/cyberman/machtool/machtool/vibration/damping.html.
21. http://home.um.edu.mt/auxetic/properties.html.
22. S. P. Nigam, Mechanical Vibrations.
23. W. T. Thomson, Vibration Theory and Applications.
24. S. Timoshenko and D.H. Young, Vibration Problems in Engineering.
25. http://www.deicon.com/vib_categ.html.
26. Electrodynamic shaker manual
27. http://www.engr.iupui.edu/me/courses/me340lab/labexp8.pdf

APPENDIX A

Table 4.1 Variation of response with frequency of FFT record for aluminium beam of thickness 10mm

	FFT1: AvSpc [1]-x	FFT1: AvSpc [2]-Y	FFT1: AvSpc [3]-Z
Frequency Hz	Acceleration m/s²	Acceleration m/s²	Acceleration m/s²
0.00	0.27	0.03	0.03
1.00	0.21	0.03	0.06
2.00	0.03	0.01	0.02
3.00	0.02	0.00	0.01
4.00	0.02	0.00	0.00
5.00	0.04	0.00	0.00
6.00	0.50	0.04	0.01
7.00	2.32	0.19	0.05
8.00	2.68	0.22	0.06
9.00	2.59	0.27	0.05
10.00	3.66	0.37	0.08
11.00	2.64	0.13	0.03
12.00	4.49	0.29	0.05
13.00	2.23	0.14	0.02
14.00	0.35	0.02	0.02
15.00	0.10	0.02	0.03
16.00	0.05	0.01	0.01
17.00	0.08	0.01	0.00
18.00	0.16	0.01	0.01
19.00	0.22	0.01	0.03
20.00	0.25	0.02	0.03
21.00	0.92	0.04	0.01
22.00	2.13	0.07	0.02
23.00	2.76	0.21	0.04
24.00	1.47	0.22	0.06
25.00	0.87	0.13	0.03
26.00	0.43	0.06	0.01
27.00	0.24	0.05	0.02
28.00	2.17	0.31	0.16
29.00	6.75	1.03	0.48
30.00	4.94	0.76	0.35
31.00	0.54	0.07	0.04

32.00	1.25	0.10	0.04
33.00	2.75	0.24	0.05
34.00	4.71	0.48	0.08
35.00	18.14	2.42	0.54
36.00	*32.92	4.68	1.13
*37.00	66.00	10.34	2.52
38.00	*51.30	8.03	1.96
39.00	11.98	1.87	0.46
40.00	4.35	0.69	0.18
41.00	1.56	0.25	0.07
42.00	0.82	0.13	0.03
43.00	0.31	0.03	0.02
44.00	0.75	0.20	0.03
45.00	0.64	0.15	0.04
46.00	0.51	0.10	0.03
47.00	0.24	0.08	0.02
48.00	1.98	0.42	0.11
49.00	2.90	0.67	0.16
50.00	1.02	0.25	0.05
51.00	0.38	0.17	0.02
52.00	0.61	0.15	0.03
53.00	0.51	0.10	0.02
54.00	0.36	0.13	0.02
55.00	0.32	0.13	0.02
56.00	0.48	0.21	0.03
57.00	0.57	0.27	0.04
58.00	0.59	0.26	0.04
59.00	0.88	0.35	0.06
60.00	1.23	0.42	0.09
61.00	0.93	0.29	0.07
62.00	0.35	0.11	0.03
63.00	0.06	0.04	0.01
64.00	0.04	0.05	0.00
65.00	0.07	0.06	0.01
66.00	0.16	0.24	0.02
67.00	0.24	0.64	0.04
68.00	0.67	1.53	0.10
69.00	0.54	1.08	0.07
70.00	0.24	0.62	0.03
71.00	0.22	0.33	0.02
72.00	0.19	0.29	0.04

73.00	0.19	0.18	0.04
74.00	0.06	0.20	0.09
75.00	0.08	0.31	0.10
76.00	0.08	0.14	0.04
77.00	0.12	0.12	0.02
78.00	0.15	0.09	0.01
79.00	0.19	0.08	0.01
80.00	0.21	0.09	0.01
81.00	0.22	0.09	0.01
82.00	0.22	0.08	0.01
83.00	0.31	0.08	0.01
84.00	0.49	0.11	0.01
85.00	0.41	0.07	0.01
86.00	0.21	0.04	0.01
87.00	0.40	0.03	0.01
88.00	0.57	0.02	0.01
89.00	0.20	0.02	0.00
90.00	0.08	0.02	0.00
91.00	0.08	0.02	0.00
92.00	0.05	0.01	0.00
93.00	0.05	0.01	0.00
94.00	0.07	0.01	0.00
95.00	0.07	0.02	0.01
96.00	0.13	0.04	0.03
97.00	0.16	0.06	0.05
98.00	0.13	0.03	0.03
99.00	0.19	0.02	0.01
100.00	0.24	0.03	0.01

APPENDIX B

Table 4.2 Variation of response with frequency of FFT record for brass beam of thickness 10mm

	FFT1: AvSpc [1]-x	FFT1: AvSpc [2]-Y	FFT1: AvSpc [3]-Z
Frequency Hz	Acceleration m/s²	Acceleration m/s²	Acceleration m/s²
0.00	0.01	0.01	0.04
0.50	0.01	0.01	0.03
1.00	0.00	0.00	0.01
1.50	0.00	0.01	0.01
2.00	0.00	0.00	0.00
2.50	0.00	0.00	0.01
3.00	0.00	0.00	0.00
3.50	0.00	0.00	0.00
4.00	0.00	0.00	0.00
4.50	0.00	0.00	0.01
5.00	0.01	0.00	0.02
5.50	0.03	0.00	0.06
6.00	0.15	0.01	0.10
6.50	0.55	0.02	0.23
7.00	0.64	0.04	0.36
7.50	0.27	0.10	0.47
8.00	0.09	0.13	0.61
8.50	0.04	0.11	0.89
9.00	0.03	0.10	1.11
9.50	0.02	0.08	1.49
10.00	0.01	0.08	1.71
10.50	0.01	0.13	1.92
11.00	0.03	0.22	2.22
11.50	0.05	0.31	2.97
12.00	0.06	0.29	3.35
12.50	0.04	0.17	3.56
13.00	0.01	0.04	3.89
13.50	0.01	0.03	4.03
14.00	0.01	0.03	4.69
14.50	0.06	0.16	*5.95
15.00	0.14	0.36	6.08
*15.50	0.16	0.42	*6.95

16.00	0.09	0.25	*4.99
16.50	0.04	0.12	1.78
17.00	0.03	0.10	1.44
17.50	0.02	0.05	0.68
18.00	0.02	0.04	0.70
18.50	0.02	0.04	0.62
19.00	0.01	0.03	0.48
19.50	0.00	0.02	0.19
20.00	0.01	0.02	0.21
20.50	0.01	0.03	0.50
21.00	0.02	0.04	0.83
21.50	0.03	0.05	1.02
22.00	0.03	0.05	0.96
22.50	0.03	0.04	0.90
23.00	0.04	0.07	1.28
23.50	0.05	0.09	1.70
24.00	0.05	0.09	1.63
24.50	0.03	0.06	1.07
25.00	0.01	0.02	0.46
25.50	0.01	0.02	0.40
26.00	0.01	0.02	0.40
26.50	0.02	0.02	0.57
27.00	0.02	0.05	0.57
27.50	0.02	0.05	0.57
28.00	0.01	0.03	0.52
28.50	0.01	0.03	0.46
29.00	0.01	0.03	0.35
29.50	0.03	0.06	0.94
30.00	0.07	0.14	2.12
30.50	0.09	0.19	2.83
31.00	0.08	0.16	2.36
31.50	0.04	0.09	1.24
32.00	0.03	0.09	0.98
32.50	0.03	0.09	1.02
33.00	0.03	0.08	0.79
33.50	0.02	0.09	0.68
34.00	0.02	0.09	0.65
34.50	0.03	0.11	0.75
35.00	0.04	0.20	1.11
35.50	0.05	0.30	1.35
36.00	0.04	0.31	1.26

36.50	0.03	0.21	0.92
37.00	0.01	0.10	0.38
37.50	0.01	0.22	0.33
38.00	0.01	0.18	0.20
38.50	0.01	0.10	0.21
39.00	0.01	0.06	0.17
39.50	0.01	0.05	0.17
40.00	0.00	0.05	0.05
40.50	0.00	0.05	0.13
41.00	0.01	0.06	0.12
41.50	0.01	0.12	0.23
42.00	0.02	0.15	0.44
42.50	0.02	0.23	0.47
43.00	0.01	0.25	0.42
43.50	0.02	0.33	0.41
44.00	0.02	0.26	0.34
44.50	0.03	0.50	0.56
45.00	0.08	1.71	1.59
45.50	0.13	2.89	2.53
46.00	0.13	3.13	2.57
46.50	0.08	2.07	1.68
47.00	0.05	0.77	0.95
47.50	0.08	1.14	1.30
48.00	0.06	0.75	1.17
48.50	0.03	0.42	0.74
49.00	0.03	0.46	0.75
49.50	0.02	0.33	0.58
50.00	0.03	0.24	0.50

APPENDIX C

Table 4.3 Variation of response with frequency of FFT record for mild steel beam of thickness 10mm

	FFT1: AvSpc [1]-x	FFT1: AvSpc [2]-Y	FFT1: AvSpc [3]-Z
Frequency (Hz)	Acceleration (m/s²)	Acceleration (m/s²)	Acceleration (m/s²)
0.00	0.06	0.00	0.00
1.00	0.11	0.00	0.00
2.00	0.15	0.03	0.08
3.00	0.17	0.04	0.00
4.00	0.14	0.02	0.00
5.00	0.12	0.01	0.00
6.00	0.11	0.00	0.00
7.00	0.10	0.00	0.00
8.00	0.09	0.00	0.00
9.00	0.08	0.00	0.00
10.00	0.07	0.00	0.00
11.00	0.05	0.00	0.00
12.00	0.03	0.00	0.00
13.00	0.01	0.00	0.00
14.00	0.00	0.00	0.00
15.00	0.00	0.00	0.00
16.00	0.00	0.00	0.00
17.00	0.00	0.00	0.00
18.00	0.00	0.00	0.00
19.00	0.00	0.00	0.00
20.00	0.00	0.00	0.00
21.00	0.00	0.00	0.00
22.00	0.00	0.00	0.00
23.00	0.00	0.00	0.00
24.00	0.00	0.00	0.00
25.00	0.00	0.00	0.00
26.00	0.00	0.00	0.00
27.00	0.00	0.00	0.00
28.00	0.00	0.00	0.00
29.00	0.00	0.00	0.00
30.00	0.00	0.01	0.00
31.00	0.00	0.02	0.00

32.00	0.10	0.03	0.00
33.00	0.21	0.04	0.00
34.00	0.33	0.05	0.00
35.00	0.45	0.06	0.00
*36.00	1.00	0.07	0.00
*37.00	0.89	0.08	0.01
38.00	0.77	0.05	0.00
39.00	0.60	0.03	0.00
40.00	0.33	0.02	0.00
41.00	0.20	0.00	0.00
42.00	0.10	0.00	0.00
43.00	0.00	0.00	0.00
44.00	0.00	0.01	0.00
45.00	0.00	0.01	0.00
46.00	0.00	0.01	0.00
47.00	0.00	0.00	0.00
48.00	0.01	0.00	0.00
49.00	0.02	0.00	0.00
50.00	0.01	0.00	0.00
51.00	0.00	0.00	0.00
52.00	0.01	0.00	0.00
53.00	0.01	0.00	0.00
54.00	0.01	0.00	0.00
55.00	0.01	0.00	0.00
56.00	0.01	0.00	0.00
57.00	0.01	0.01	0.00
58.00	0.01	0.00	0.00
59.00	0.01	0.01	0.00
60.00	0.01	0.01	0.00
61.00	0.01	0.02	0.00
62.00	0.01	0.02	0.00
63.00	0.01	0.03	0.00
64.00	0.01	0.04	0.00
65.00	0.01	0.03	0.00
66.00	0.01	0.02	0.00
67.00	0.01	0.01	0.00
68.00	0.01	0.01	0.00
69.00	0.05	0.01	0.00
70.00	0.01	0.01	0.00
71.00	0.02	0.01	0.00
72.00	0.01	0.00	0.00

73.00	0.01	0.00	0.00
74.00	0.01	0.00	0.00
75.00	0.01	0.00	0.00
76.00	0.01	0.00	0.00
77.00	0.01	0.00	0.00
78.00	0.01	0.00	0.00
79.00	0.01	0.00	0.00
80.00	0.01	0.00	0.00
81.00	0.01	0.00	0.00
82.00	0.12	0.00	0.00
83.00	0.10	0.00	0.00
84.00	0.12	0.00	0.00
85.00	0.10	0.00	0.00
86.00	0.12	0.00	0.00
87.00	0.12	0.00	0.00
88.00	0.10	0.00	0.00
89.00	0.10	0.00	0.00
90.00	0.10	0.00	0.00
91.00	0.10	0.00	0.00
92.00	0.00	0.00	0.00
93.00	0.00	0.00	0.00
94.00	0.10	0.00	0.00
95.00	0.10	0.00	0.00
96.00	0.11	0.00	0.00
97.00	0.10	0.03	0.00
98.00	0.10	0.02	0.00
99.00	0.12	0.00	0.00
100.00	0.15	0.01	0.00

APPENDIX D

Table 4.4 Variation of response with frequency of FFT record for aluminium beam of thickness 6mm

	FFT1: AvSpc [1]-x	FFT1: AvSpc [2]-Y	FFT1: AvSpc [3]-Z
Frequency Hz	Acceleration m/s²	Acceleration m/s²	Acceleration m/s²
0.00	0.33	0.01	0.04
0.80	0.24	0.01	0.08
1.60	0.01	0.01	0.07
2.40	0.01	0.00	0.08
3.20	0.07	0.00	0.08
4.00	0.35	0.00	0.05
4.80	1.63	0.02	0.03
5.60	2.19	0.03	0.02
6.40	2.72	0.04	0.02
7.20	3.62	0.06	0.02
8.00	3.18	0.05	0.01
8.80	0.75	0.01	0.01
9.60	0.22	0.01	0.02
10.40	0.09	0.02	0.04
11.20	0.09	0.02	0.04
12.00	0.06	0.01	0.01
12.80	0.20	0.01	0.01
13.60	0.53	0.02	0.02
14.40	1.57	0.02	0.04
15.20	3.46	0.04	0.09
16.00	8.22	0.08	0.22
16.80	18.27	0.21	0.53
*17.60	41.02	0.47	1.20
18.40	21.60	0.25	0.63
19.20	2.63	0.03	0.09
20.00	4.64	0.06	0.17
20.80	6.64	0.09	0.24
21.60	4.67	0.07	0.17
22.40	4.56	0.06	0.14
23.20	3.24	0.11	0.12
24.00	1.67	0.08	0.07
24.80	0.70	0.05	0.03

25.60	0.80	0.05	0.04
26.40	0.80	0.04	0.04
27.20	0.71	0.04	0.03
28.00	0.70	0.04	0.02
28.80	0.53	0.06	0.06
29.60	0.25	0.08	0.07
30.40	0.23	0.06	0.03
31.20	0.09	0.04	0.02
32.00	0.24	0.05	0.03
32.80	0.36	0.06	0.04
33.60	0.50	0.08	0.04
34.40	0.59	0.11	0.12
35.20	0.79	0.16	0.24
36.00	0.69	0.14	0.13
36.80	0.70	0.15	0.07
37.60	0.67	0.05	0.04
38.40	0.53	0.04	0.07
39.20	0.44	0.06	0.04
40.00	0.26	0.04	0.04
40.80	0.13	0.03	0.02
41.60	0.09	0.03	0.01
42.40	0.07	0.04	0.02
43.20	0.07	0.05	0.01
44.00	0.09	0.07	0.02
44.80	0.10	0.05	0.01
45.60	0.13	0.06	0.01
46.40	0.14	0.07	0.01
47.20	0.16	0.07	0.02
48.00	0.19	0.04	0.02
48.80	0.20	0.08	0.02
49.60	0.27	0.08	0.03
50.40	0.26	0.06	0.03
51.20	0.21	0.08	0.03
52.00	0.23	0.05	0.02
52.80	0.20	0.04	0.01
53.60	0.21	0.04	0.02
54.40	0.21	0.03	0.02
55.20	0.17	0.03	0.01
56.00	0.12	0.03	0.02
56.80	0.09	0.04	0.01
57.60	0.09	0.05	0.01

58.40	0.11	0.07	0.01
59.20	0.12	0.05	0.01
60.00	0.14	0.06	0.01
60.80	0.13	0.09	0.01
61.60	0.16	0.11	0.01
62.40	0.16	0.13	0.01
63.20	0.18	0.16	0.01
64.00	0.27	0.42	0.03
64.80	0.24	0.77	0.04
65.60	0.24	0.70	0.04
66.40	0.24	0.35	0.03
67.20	0.21	0.18	0.02
68.00	0.21	0.09	0.02
68.80	0.22	0.08	0.02
69.60	0.21	0.10	0.02
70.40	0.21	0.11	0.02
71.20	0.16	0.08	0.01
72.00	0.19	0.08	0.02
72.80	0.15	0.08	0.02
73.60	0.12	0.04	0.01
74.40	0.18	0.05	0.01
75.20	0.11	0.02	0.01
76.00	0.13	0.03	0.01
76.80	0.15	0.03	0.01
77.60	0.17	0.02	0.01
78.40	0.18	0.02	0.02
79.20	0.18	0.02	0.02
80.00	0.19	0.02	0.01

APPENDIX E

Table 4.5 Variation of response with frequency of FFT record for brass beam of thickness 6mm

	FFT1: AvSpc [1]-x	FFT1: AvSpc [2]-Y	FFT1: AvSpc [3]-Z
Frequency	Acceleration	Acceleration	Acceleration
Hz	m/s²	m/s²	m/s²
0.00	0.24	0.01	0.01
0.50	0.17	0.01	0.01
1.00	0.01	0.00	0.00
1.50	0.00	0.00	0.00
2.00	0.00	0.00	0.00
2.50	0.00	0.00	0.00
3.00	0.01	0.00	0.00
3.50	0.01	0.00	0.00
4.00	0.01	0.00	0.00
4.50	0.04	0.01	0.00
5.00	0.10	0.01	0.00
5.50	0.27	0.03	0.01
6.00	0.53	0.05	0.01
6.50	3.39	0.32	0.03
7.00	4.70	0.45	0.05
7.50	2.05	0.19	0.04
8.00	6.36	0.61	0.12
8.50	7.08	0.51	0.10
9.00	8.20	0.82	0.20
*9.50	10.07	1.00	0.25
10.00	3.58	0.36	0.09
10.50	0.66	0.07	0.02
11.00	0.17	0.02	0.00
11.50	0.25	0.02	0.01
12.00	1.33	0.13	0.05
12.50	1.67	0.16	0.06
13.00	0.72	0.08	0.03
13.50	0.93	0.11	0.04
14.00	0.75	0.09	0.03
14.50	0.27	0.03	0.01
15.00	0.09	0.00	0.01
15.50	0.15	0.01	0.01

16.00	0.22	0.00	0.02
16.50	0.18	0.01	0.02
17.00	0.06	0.01	0.01
17.50	0.10	0.01	0.01
18.00	0.21	0.03	0.01
18.50	0.32	0.04	0.03
19.00	0.46	0.06	0.03
19.50	0.46	0.06	0.03
20.00	1.02	0.13	0.06
20.50	2.06	0.28	0.12
21.00	1.96	0.28	0.11
21.50	0.77	0.11	0.04
22.00	0.13	0.03	0.01
22.50	0.16	0.08	0.02
23.00	0.36	0.19	0.03
23.50	0.81	0.33	0.06
24.00	1.28	0.43	0.09
24.50	1.88	0.48	0.13
25.00	1.47	0.34	0.10
25.50	0.66	0.16	0.05
26.00	0.20	0.06	0.01
26.50	0.30	0.11	0.02
27.00	0.69	0.25	0.07
27.50	1.37	0.45	0.17
28.00	1.76	0.52	0.25
28.50	1.24	0.35	0.19
29.00	0.53	0.15	0.08
29.50	0.20	0.05	0.03
30.00	0.07	0.02	0.01
30.50	0.05	0.04	0.02
31.00	0.09	0.08	0.03
31.50	0.11	0.13	0.04
32.00	0.13	0.15	0.04
32.50	0.14	0.19	0.04
33.00	0.17	0.22	0.04
33.50	0.16	0.17	0.03
34.00	0.48	0.19	0.05
34.50	0.76	0.26	0.09
35.00	0.65	0.17	0.08
35.50	0.20	0.06	0.03
36.00	0.11	0.06	0.01

36.50	0.13	0.10	0.01
37.00	0.17	0.16	0.01
37.50	0.17	0.18	0.01
38.00	0.11	0.13	0.00
38.50	0.11	0.22	0.01
39.00	0.19	0.41	0.01
39.50	0.32	0.65	0.01
40.00	0.47	0.90	0.01
40.50	0.58	1.12	0.01
41.00	0.78	1.49	0.01
41.50	0.73	1.41	0.02
42.00	0.45	0.98	0.01
42.50	0.19	0.50	0.01
43.00	0.05	1.08	0.02
43.50	0.10	2.67	0.05
44.00	0.15	3.49	0.07
44.50	0.23	2.45	0.04
45.00	0.32	1.57	0.02
45.50	0.49	1.34	0.01
46.00	0.70	1.18	0.02
46.50	0.85	0.93	0.03
47.00	0.82	0.59	0.04
47.50	0.58	0.30	0.03
48.00	0.33	0.40	0.04
48.50	0.43	0.42	0.04
49.00	0.31	0.26	0.03
49.50	0.08	0.08	0.01
50.00	0.08	0.04	0.01

APPENDIX F

Table 4.6 Variation of response with frequency of FFT record for mild steel beam of thickness 6mm

	FFT1: AvSpc [1]-x	FFT1: AvSpc [2]-Y	FFT1: AvSpc [3]-Z
Frequency	Acceleration	Acceleration	Acceleration
Hz	m/s²	m/s²	m/s²
0.00	0.20	0.00	0.00
0.80	0.10	0.10	0.00
1.60	0.00	0.00	0.10
2.40	0.00	0.00	0.10
3.20	0.10	0.00	0.10
4.00	0.40	0.00	0.10
4.80	0.58	0.00	0.00
5.60	0.51	0.00	0.00
6.40	0.47	0.00	0.00
7.20	0.36	0.10	0.00
8.00	0.20	0.00	0.00
8.80	0.30	0.00	0.00
9.60	0.10	0.00	0.00
10.40	0.20	0.00	0.00
11.20	0.10	0.00	0.00
12.00	0.10	0.00	0.00
12.80	0.20	0.00	0.00
13.60	0.50	0.00	0.00
14.40	0.60	0.00	0.00
15.20	1.50	0.00	0.10
16.00	2.90	0.10	0.20
16.80	3.70	0.20	0.50
17.00	3.57	0.50	1.20
18.40	1.29	0.20	0.60
19.20	1.13	0.00	0.10
20.00	0.60	0.10	0.20
20.80	0.30	0.10	0.20
21.60	0.30	0.10	0.20
22.40	0.60	0.10	0.10
23.20	0.80	0.10	0.10

24.00	1.20	0.10	0.10
24.80	0.70	0.00	0.00
25.60	0.80	0.10	0.00
26.40	0.80	0.00	0.00
27.20	0.70	0.00	0.00
28.00	0.70	0.00	0.00
28.80	0.50	0.10	0.10
29.60	0.30	0.10	0.10
30.40	0.20	0.10	0.00
31.20	0.10	0.00	0.00
32.00	0.20	0.10	0.00
32.80	0.40	0.10	0.00
33.60	0.50	0.10	0.00
34.40	0.60	0.10	0.10
35.20	0.80	0.20	0.20
36.00	0.70	0.10	0.10
36.80	0.70	0.20	0.10
37.60	0.70	0.00	0.00
38.40	0.50	0.00	0.10
39.20	0.40	0.10	0.00
40.00	0.30	0.00	0.00
40.80	0.10	0.00	0.00
41.60	0.10	0.00	0.00
42.40	0.10	0.00	0.00
43.20	0.10	0.10	0.00
44.00	0.10	0.10	0.00
44.80	0.10	0.10	0.00
45.60	0.10	0.10	0.00
46.40	0.10	0.10	0.00
47.20	0.20	0.10	0.00
48.00	0.20	0.00	0.00
48.80	0.20	0.10	0.00
49.60	0.30	0.10	0.00
50.40	0.30	0.10	0.00
51.20	0.20	0.10	0.00
52.00	0.20	0.10	0.00
52.80	0.20	0.00	0.00
53.60	0.20	0.00	0.00

54.40	0.20	0.00	0.00
55.20	0.20	0.00	0.00
56.00	0.10	0.00	0.00
56.80	0.10	0.00	0.00
57.60	0.10	0.00	0.00
58.40	0.10	0.10	0.00
59.20	0.10	0.10	0.00
60.00	0.10	0.10	0.00
60.80	0.10	0.10	0.00
61.60	0.20	0.10	0.00
62.40	0.20	0.10	0.00
63.20	0.20	0.20	0.00
64.00	0.30	0.40	0.00
64.80	0.20	0.80	0.00
65.60	0.20	0.70	0.00
66.40	0.20	0.40	0.00
67.20	0.20	0.20	0.00
68.00	0.20	0.10	0.00
68.80	0.20	0.10	0.00
69.60	0.20	0.10	0.00
70.40	0.20	0.10	0.00
71.20	0.20	0.10	0.00
72.00	0.20	0.10	0.00
72.80	0.20	0.10	0.00
73.60	0.10	0.00	0.00
74.40	0.20	0.10	0.00
75.20	0.10	0.00	0.00
76.00	0.10	0.00	0.00
76.80	0.20	0.00	0.00
77.60	0.20	0.00	0.00
78.40	0.00	0.00	0.00
79.20	0.00	0.00	0.00
80.00	0.00	0.00	0.00